Refinement of LC-MS Methodology for the Analysis of Saponins

A thesis submitted in partial fulfilment

of the requirements for the degree

of

Masters of Science

in Chemistry

at

The University of Waikato

by

Dylan Ball

The University of Waikato

2010

THE UNIVERSITY OF

WAIKATO

Te Whare Wānanga o Waikato

Abstract

Systematic evaluation of the factors affecting LC-MS detection of some saponins and sapogenins associated with hepatogenous photo-sensitisation diseases in livestock, as determined using a Thermo Finnigan LCQ Advantage mass spectrometer, showed that ion responses could be substantially improved by careful selection of analysis parameters. Eluent composition, capillary temperatures and flow rate were found to significantly affect the ionisation of the target analytes.

Optimisation of ionisation conditions resulted in a more than 100 fold (2 orders of magnitude) improvement in the detection of the model sapogenins and sapogenin glycosides relative to conditions utilised in previous studies at the University of Waikato. Optimal ESI and APCI responses were achieved using formic acid buffered acetonitrile-water eluent mixtures which possessed 30-40% acetonitrile for sapogenin glycosides or 50-60% acetonitrile for sapogenins and capillary interface temperatures in the range 275-325°C. Lower eluent flow rates also results in increased detector responses. Optimised ESI responses were greater by *ca* 2-10 times when compared to optimised APCI responses.

Analyses of full scan and MS^n ESI and APCI mass spectral fragmentation data showed that the molecular weight of conjugated sapogenin glycosides could be readily determined from $[M+H]^+$ ions observed in full scan spectra. Under MS^2 conditions sapogenin glycosides $[M+H]^+$ ions fragmented to afford ions attributable to the protonated parent sapogenin and a series of other ions that were found to present in the ESI and APCI mass spectra of parent sapogenins, including *m/z* 399, *m/z* 273 and *m/z* 255 ions.

Detailed analysis of full scan, MS^2 and MS^3 ESI and APCI fragmentation and chromatographic data determined for sarsasapogenin, episarsasapogenin, smilagenin, 20,20,23-$^2H_3$-sarsasapogenin and 2,2,4,4-$^2H_4$–episarsasapogenin, tigogenin and diosgenin showed that, unlike previously reported EI-GC-MS data, neither LC-MS ion ratio data, or retention time data could not be used to distinguish isomeric 3α/β, 5 α/β, 25(*R/S*)-spirostanol sapogenins of the type known to be present in the rumen and other GI tracts samples recovered from livestock suffering hepatogenous photo-sensitisation diseases.

Based on the results reported in this thesis it is apparent that a combination of EI-GC-MS and LC-ESI-MS^n data will be required to identify conjugated sapogenins present in rumen and other GI tract samples recovered from livestock suffering from hepatogenous photo-sensitisation diseases since LC-MS^n data alone is not capable of distinguishing isomeric forms of free and conjugated sapogenins.

It has been hypothesised that genetic factors may influence the nature of conjugates in the rumen and their metabolism to alternate conjugated analogues. The availability of combination of EI-GC-MS and optimised LC-MS methods to probe the nature and distribution of free and conjugated sapogenins in rumen and GI tact samples may assist in the identification of susceptible and resistant animals.

Acknowledgements

I wish to thank my supervisor, Professor Alistair L. Wilkins from the Chemistry Department at the University of Waikato for providing me with the research topic and the guidance required for the completion of this thesis.

The following people have assisted in the preparation of this thesis;

Mrs Wendy Jackson assisted with training and guidance with the University of Waikato's LC-MS instrumentation.

Ms Maria Teresa Revell for her assistance with editing and proof reading of my thesis drafts.

Miss Michelle Clarke for her assistance with GC-MS and NMR data for quality control of the purity of the model compounds.

For encouraging and motivating me to return to study after years in the work force I would like to thank my former work colleagues at the National Institute of Water and Atmospheric Research, in particular my co-workers in the water quality laboratory.

I would also like to extend my thanks to the other post graduate chemistry students who provided the cynical observations and the much needed distractions from my research that were required to get through.

I would like to thank my friends and family, who have been supportive through my studies, especially my mother who may be the only woman who will ever care for me.

Table of Contents

Abstract ii
Acknowledgements iv
Table of Contents v
List of Figures x
List of Tables xv
List of Abbreviations xvi
Chapter1. Introduction 1
1.1 The Need for Techniques for Determining Saponins 1
1.1.1 Analysis of Steroids and Triterpenoids using GC-MS 2
1.1.1.1 Reactions used to Modify Structures for Analysis by GC-MS 3
1.1.1.2 GC-MS Ionisation 6
1.1.2 Analysis of Steroids and Triterpenoids using LC-MS 7
1.1.2.1 LC-MS Ionisation 8
1.2 Analysis of Conjugated Steroidal and Triterpenoidal Compounds 9
1.2.1 Identification of Saponins and Sapogenins by LC-MS 9
1.2.1.1 Saponins and Sapogenins Implicated in Hepatogenous Photo-Sensitisation Diseases 10
1.3 Research Aims and Objectives 11
Chapter 2. Analysis of Steroids and Triterpenoids via LC-MS 13
2.1 LC-MS Instrumentation 13
2.1.1 Liquid Chromatography 15
2.1.2 Mass Spectrometric Detection 15
2.1.3 Ionisation of Steroidal and Triterpenoidal Compounds and Their Conjugated Analogues 16
2.1.3.1 Electro-Spray Ionisation ESI 17
2.1.3.2 Atmospheric Pressure Chemical Ionisation (APCI) 18
2.1.3.3 Eluent 18
2.1.3.4 Ionisation Agents 20
2.1.3.5 Signal Suppression 21
2.1.4 Ionisation via Chemical Derivatisation 23

2.1.4.1 Pre-Analysis Chemical Derivatisation 23
2.1.4.2 Post Column Chemical Derivatisation 25
2.2 Target Compounds 26
Chapter 3. Optimising Ionisation of Saponins and Sapogenins 29
3.1 Saponins and Sapogenins Selected for Optimisation of Ionisation Parameters 29
3.1.1 Optimising Ionisation of the Model Compounds 29
3.2 Electro-Spray Ionisation Source (ESI) 30
3.2.1 Alignment of the Spray Nozzle in the ESI Source 30
3.2.2 Voltage Settings (ESI) 31
3.2.3 Ionisation Agents (ESI) 31
3.2.3.1 Sarsasapogenin 32
3.2.3.2 Diosgenin 33
3.2.3.3 Sarsasapogenin-β-D-glucoside 34
3.2.4 Eluent Composition (ESI) 35
3.2.4.1 Sarsasapognin 36
3.2.4.2 Diosgenin 38
3.2.4.3 Sarsasapogenin-β-D-glucoside 40
3.2.5 Capillary Temperature (ESI) 42
3.2.5.1 Sarsasapogenin 42
3.2.5.2 Diosgenin 43
3.2.5.3 Diosgenin, LTQ Comparison 44
3.2.5.4 Sarsasapogenin-β-D-glucoside 45
3.2.6 Effect of Eluent Flow Rate upon ESI 45
3.3 Atmospheric Pressure Chemical Ionisation Source (APCI) 47
3.3.1 Voltage Settings APCI 48
3.3.2 Ionisation Agents (APCI) 48
3.3.2.1 Sarsasapogenin 48
3.3.2.2 Diosgenin 49
3.3.2.3 Sarsasapogenin-β-D-glucoside 50
3.3.3 Eluent Composition (APCI) 51
3.3.3.1 Sarsasapogenin 52

3.3.4 Interface Temperatures (APCI) 52
3.3.4.1 Sarsasapogenin 53
3.3.4.2 Diosgenin 53
3.3.4.3 Sarsasapogenin-β-D-glucoside 54
3.3.5 Effect of Eluent Flow Rate upon APCI 55
Chapter 4. LC-MS^n Characteristics of Saponins and Sapogenins 57
4.1 Mass Spectral Identification 58
4.2 Confirmation of the Model Compound Integrity by NMR 59
4.3 Confirmation of Model Compound Integrity by GC-MS 60
4.4 MS^n Fragmentation of the Model Compounds 61
4.4.1 Fragmentation of Sarsasapogenin (ESI) 62
4.4.2 Fragmentation of 2,2,4,4-$^2H_4$-episarsasapogenin (ESI) 65
4.4.3 Fragmentation of 20,23,23-$^2H_3$-sarsasapogenin (ESI) 68
4.4.4 Plausible Structures for Major ESI Fragment Ions of Sarsasapogenin 70
4.4.5 Fragmentation of Sarsasapogenin (APCI) 73
4.4.6 Fragmentation of 2,2,4,4-$^2H_4$-episarsasapogenin (APCI) 75
4.4.7 Fragmentation of 20,23,23-$^2H_3$-sarsasapogenin (APCI) 75
4.4.8 Summary of APCI Fragmentation of Sarsasapogenin 76
4.4.9 Fragmentation of Diosgenin (ESI) 77
4.4.10 Fragmentation of Diosgenin (APCI) 80
4.4.11 Summary of Fragmentation of Diosgenin 81
4.4.12 Fragmentation of Sarsasapogenin-β-D-glucoside (ESI) 82
4.4.13 Fragmentation of Sarsasapogenin-β-D-glucoside (APCI) 84
4.4.14 Fragmentation of Sarsasapogenin-β-D-galactoside (ESI and APCI) 86
4.4.15 Fragmentation of Episarsasapogenin, Tigogenin and Smilagenin (ESI and APCI) 88
4.5 Mass Spectral Findings 92
4.5.1 Established Mass Spectral Techniques for Isomeric Identification of Sapogenins 92
4.5.2 Mass Spectral Techniques for Isomeric Identification by LC-MS^n 93
4.6 Chromatographic Properties 94

4.6.1 The Need for Adequate Chromatographic Separation 94
4.6.2 Liquid Chromatographic Separation 95
4.6.3 Summary of LC-MS^n Chromatographic Retention Findings 96
Chapter 5. Summary, Conclusions and Recommendations for Further Work 97
5.1 Overview of the Research 97
5.2 Significance of Ionisation Conditions, Eluent Composition and Flow Rate 98
5.3 Recommendations for Further Work 101
5.3.1 LC-MS Analysis 101
5.3.2 Reducing Flow Rates by Application of low flow Columns 102
5.3.3 SRM Detection 103
5.3.4 Superiority of ESI Detection 104
5.3.5 Compensating for Signal Suppression 104
5.3.6 Requirement for Complementary GC-MS analysis 105
5.3.7 Requirement for Isolation, and Structural Determination via NMR and HRMS 106
5.4 Conclusions 107

List of Figures

Chapter 1

Figure 1.1. Cyclisation of squalene epoxide to afford lanosterol 1
Figure 1.2. Structure of sarsasapogenin-β-D-glucoside 2
Figure 1.3. Acid hydrolysis of a saponin 5
Figure 1.4. Alkaline hydrolysis of a fatty acid ester analogue 5
Figure 1.5. Enzymatic hydrolysis of a glycoside 5
Figure 1.6. Enzymatic hydrolysis of a sulphate 5
Figure 1.7. Trimethylsilylation of the hydroxyl group of a steroid 6
Figure 1.8. Trimethylsilylation of the hydroxyl groups of a sugar 6
Figure 1.9. Methylation of an acid group to a COOMe group 6

Chapter 2

Figure 2.1. Schematic diagram of a LC-MS system 13
Figure 2.2. LC-MS system with post column infusion 25
Figure 2.3. Structure of sarsasapogenin 27
Figure 2.4. Structure of episarsasapogenin 27
Figure 2.5. Structure of smilagenin 27
Figure 2.6. Structure of diosgenin 28
Figure 2.7. Structure of tigogenin 28
Figure 2.8. Structure of sarsasapogenin-β-D-galactoside 28

Chapter 3

Figure 3.1. ESI responses for sarsasapogenin in three ionisation agents 32
Figure 3.2. Effect of formic acid concentration upon the ESI response of sarsasapogenin 33
Figure 3.3. ESI responses for diosgenin in three ionisation agents 33
Figure 3.4. Effect of formic acid concentration upon the ESI response of diosgenin 34
Figure 3.5. ESI responses for sarsasapogenin-β-D-glucoside in three ionisation agents 34
Figure 3.6. Effect of formic acid concentration upon the ESI reponse of sarsasapogenin-β-D-glucoside 35
Figure 3.7. Effect of eluent composition upon the ESI response of sarsasapogenin 36
Figure 3.8. Effect of eluent composition upon the ESI response of sarsasapogenin 37
Figure 3.9. The estimated effect post column infusion of water would have upon the ESI reponse of sarsasapogenin 38
Figure 3.10. Effect of eluent composition upon the ESI response of diosgenin 39
Figure 3.11. Effect of eluent composition upon the ESI peak area diosgenin 39

Figure 3.12. The estimated effect post column infusion of water would have upon ESI reponses of diosgenin 40
Figure 3.13. Effect of eluent composition upon the ESI response of sarsasapogenin-β-D-glucoside 40
Figure 3.14. Effect of eluent composition upon the peak area of sarsasapogenin-β-D-glucoside 41
Figure 3.15. The estimated effect post column infusion of water would have upon ESI reponses of sarsasapogenin-β-D-glucoside 42
Figure 3.16. Capillary temperature effect upon the ESI responses of sarsasapogenin 42
Figure 3.17. Effect of capillary temperature upon the LCQ ESI response of diosgenin 43
Figure 3.18. Effect of capillary temperature upon the LTQ ESI response of diosgenin 44
Figure 3.19. Effect of capillary temperature upon the ESI response of sarsasapogenin-β-D-glucoside 45
Figure 3.20. Effect of flow rate upon the ESI peak area of sarsasapogenin 46
Figure 3.21. Effect of flow rate upon the ESI peak area of diosgenin ESI peak area 46
Figure 3.22. Effect of flow rate upon the ESI peak area of sarsasapogenin-β-D-glucoside 47
Figure 3.23. APCI responses for sarsasapogenin in three ionisation agents 49
Figure 3.24. Effect of formic acid concentration upon APCI response of sarsasapogenin 49
Figure 3.25. APCI responses for diosgenin in three ionisation agents 50
Figure 3.26. Effect of formic acid concentration upon APCI response of diosgenin 50
Figure 3.27. APCI responses for sarsasapogenin-β-D-glucoside in three ionisation agents 51
Figure 3.28. Effect of formic acid concentration upon APCI response of sarsasapogenin-β-D-glucoside 51
Figure 3.29. Effect of eluent composition of upon the APCI response of sarsasapogenin 52
Figure 3.30. The effect source heater and capillary temperatures upon the APCI response of sarsasapogenin 53
Figure 3.31. Effect of source heater and capillary temperatures upon the APCI response of diosgenin 54
Figure 3.32. Effect of source heater and capillary temperatures upon the APCI response of sarsasapogenin-β-D-glucoside 55
Figure 3.33. Effect of flow rate of upon the APCI response of sarsasapogenin 56
Figure 3.34. Effect of flow rate upon APCI response of sarsasapogenin-β-D-glucoside 56

Chapter 4

Figure 4.1. Plausible structures for the m/z 139 ion and deuterated analogues of these ions observed in the EI-MS of sarsasapogenin 61
Figure 4.2. Plausible structures for the m/z 302, 273 and 255 ions, and deuterated analogues of these ions observed in EI-MS of sarsasapogenin 61
Figure 4.3. Full scan ESI mass spectrum of sarsasapogenin 62
Figure 4.4. ESI Fragmentation tree for sarsasapogenin 64
Figure 4.5. Structure of 2,2,4,4-2H_4-episarsasapogenin 65
Figure 4.6. Full mass spectrum of 2,2,4,4-2H4-episarsasapogenin 65
Figure 4.7. ESI fragmentation tree for 2,2,4,4-2H4-episarsasapogenin 67
Figure 4.8. Structure of 20,23,23-2H3-sarsasapogenin 68
Figure 4.9. Full ESI mass spectrum of 20,23,23-2H3-sarsasapogenin 68
Figure 4.10. ESI fragmentation tree of 20,23,23-2H3-sarsasapogenin 69
Figure 4.11. Plausible sarsasapogenin pseudo-molecular ion structures 70
Figure 4.12. Plausible C-3 dehydration structures 71
Figure 4.13. Plausible pathways to *m/z* 399, 273 and 255 ions observed for sarsasapogenin 72
Figure 4.14. Full scan APCI mass spectrum of sarsasapogenin 73
Figure 4.15. APCI fragmentation tree for sarsasapogenin 74
Figure 4.16. Full APCI mass spectrum of 20,23,23-2H3-sarsasapogenin 75
Figure 4.17. Full scan ESI mass spectrum for diosgenin 77
Figure 4.18. ESI fragmentation tree for diosgenin 79
Figure 4.19. APCI fragmentation tree for diosgenin 81
Figure 4.20. Plausible pathways to m/z 397, 271 and 253 ions for diosgenin 82
Figure 4.21. Full scan ESI mass spectrum of sarsasapogenin-β-D-glucoside 82
Figure 4.22. ESI fragmentation tree for sarsasapogenin-β-D-glucoside 84
Figure 4.23. Full scan APCI mass spectrum of sarsasapogenin-β-D-glucoside 85
Figure 4.24. APCI fragmentation tree for sarsasapogenin-β-D-glucoside 86
Figure 4.25. ESI fragmentation tree for sarsasapogenin-β-D-galactoside 87
Figure 4.26. APCI fragmentation tree for sarsasapogenin-β-D-galactoside 88
Figure 4.27. ESI fragmentation tree for episarsasapogenin 89
Figure 4.28. ESI fragmentation tree for tigogenin 89
Figure 4.29. ESI fragmentation tree for smilagenin 90
Figure 4.30. APCI fragmentation tree for episarsasapogenin 90
Figure 4.31. APCI fragmentation tree for tigogenin 91
Figure 4.32. APCI fragmentation tree for smilagenin 91

Chapter 5

Figure 5.1. Comparison of optimal ionisation conditions and those commonly used prior to this investigation 99
Figure 5.2. Comparison of optimal ionisation conditions and those commonly used prior to this investigation 100

List of Tables

Table 4.1. ^{1}H and ^{13}C NMR chemical shifts (δ ppm in $CDCl_3$) determined for some sapogenins 60

Table 4.2. GC-MS of sapogenin acetates..... 93

List of Abbreviations

ACN	Acetonitrile
APCI	Atmospheric Pressure Chemical Ionisation
ca	Circa
EI	Electron Impact
eg	For Example
ESI	Electro-Spray Ionisation
GC	Gas Chromatography
GC-MS	Gas Chromatography Mass Spectrometry
Gal	Galactoside
GI	Gastro-Intestinal
Glu	Glucoside
HPLC	High Performance Liquid Chromatography
HRMS	High Resolution Mass Spectrometry
id	Internal Diameter
IUPAC	International Union of pure and Applied Chemistry
LC	Liquid Chromatography
LC-MS	Liquid Chromatography Mass Spectrometry
$LC\text{-}MS^n$	Liquid Chromatography Multiple Mass Spectrometry
MS	Mass Spectrometry
MS^2	Secondary Sequential Mass Spectrometry
MS^3	Tertiary Sequential Mass Spectrometry
MS^n	Multiple Sequential Mass Spectrometry
NMR	Nuclear Magnetic Resonance
SIM	Single Ion Monitoring
SRM	Selected Reaction Monitoring
TIC	Total Ion Chromatogram
UPLC	Ultra Performance Liquid Chromatography
UV-vis	Ultra-Violet Visible Spectroscopy
v/v	Volume to Volume

1 Introduction

1.1 The Need for Techniques for Determining Saponins

Steroidal and triterpenoidal compounds and their conjugated analogues are a widely distributed group of naturally occurring compounds. The polycyclic ring structure of the aglycone part of these compounds are derived by cyclisation of squalene[1-3] (Figure 1.1), and (in the case of steroids) the subsequent loss of some of the angular methyl groups. In some cases (eg androstanes, pregnanes, etc) the shortening or the complete loss of the 8-carbon side chain attached to ring D occurs[4, 5]. Conjugated analogues of steroids and triterpenoids include compounds where a functional group, often a glycoside, is attached (conjugated) to the steroid or triterpenoid aglycone.

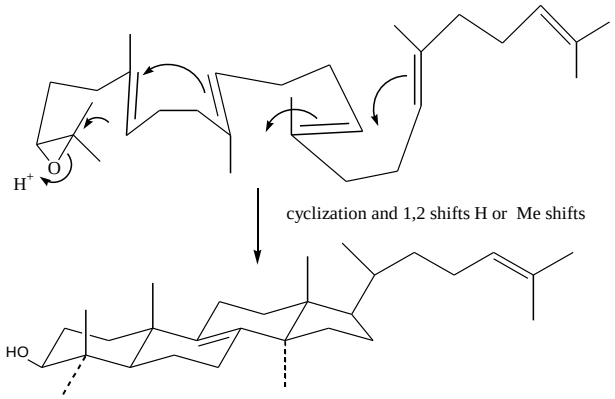

Figure 1.1. Cyclisation of squalene epoxide to afford lanosterol

Steroidal and triterpenoidal compounds frequently possess significant biological activity[6, 7]. Interest in detecting and quantifying these compounds include applications covering medicine, toxicology, environmental contaminant modelling[8], and organic geo-chronological dating[9, 10].

Asparagoside A or sarsasapogenin-β-D-glucoside (Figure 1.2) has been identified as a bioactive constituent of *Asparagus officinalis*[11]. More highly glycosylated sarsasapogenin-β-D-glucosides have been implicated as causative agents in the development of some livestock photo-sensitisation[12-15].

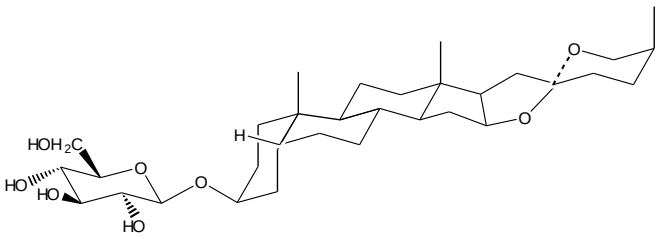

Figure 1.2. Structure of sarsasapogenin-β-D-glucoside

Many of the methodologies employed to detect conjugated steroidal and triterpenoidal compounds such sarsasapogenin analogues have significant limitations, particularly gas chromatography (GC) based methods. This is especially evident with conjugated analogues[8]. Some of these limitations can be mitigated using liquid chromatography mass spectrometry (LC-MS) based methodologies.

Steroids and triterpenoids are relatively non-polar compounds, so are not soluble in the polar aqueous mediums used by higher organisms to transport metabolites around the organism. The solubility of the relatively non-polar steroids and triterpenoids in these mediums are often improved by conjugation with a polar entity through metabolic processes. Functional groups typically conjugated to the steroids or triterpenoids are glycoside, sulfate, or fatty acid entities. Many biological processes involve attachment of conjugated groups to aid transportation of these compounds within the organism[8].

1.1.1 Analysis of Steroids and Triterpenoids using GC-MS

Commercial GC-MS instrumentation has been available for more than three decades during which time a variety of analytical procedures have been developed. Historically analytical methods for determining the levels of steroidal and triterpenoidal compounds (genins) and their conjugated analogues have generally relied on the use of GC-MS to determine the level of parent genins derived via hydrolysed of the conjugated analogues[8, 16]. The best attributes of GC-MS are the ability to allow;

(i) unequivocal identification of substances from a combination of retention time and mass spectral fragmentation pattern data.

(ii) quantitative determination of analytes due to proportionality between the fragment ion response and the quantity of analyte entering the mass spectrometer.

GC-MS has some significant limitations; the most important of which is the need for chemical derivatisation of polar genins to more volatile and thermally stable analogues prior to GC-MS analyses. Genins possessing relatively polar conjugate groups such as glycoside or sulfate residues are not volatile enough for direct analysis by GC-MS[8]. Another disadvantage of GC-MS analysis is that it involves exposing the analyte to elevated temperatures (typically 250-300^{o}C) for prolonged periods of time as the analyte is eluted through the GC column. This can result in thermally induced structural modifications to the analyte.

The derivatisation reactions used to remove conjugate groups are often incomplete and can result in underestimation of the concentration of the conjugated steroidal or triterpenoidal compounds[8]. Conjugate groups can be removed from steroids or triterpenes by either enzymatic or chemical reactions[8]. Chemical reactions used to remove conjugates groups include acid and base hydrolysis.

1.1.1.1 Reactions used to Modify Structures for Analysis by GC-MS

Acid Hydrolysis

Saponins (steroidal and triterpenoidal glycosides) can be converted to sapogenins by mild acid hydrolysis (Figure 1.3). GC-MS analysis of saponins or steroidal compounds are achieved by firstly hydrolysing the parent compound under mildly acidic conditions (0.5 molar HCl at 85-90°C, 30-60 min), followed by isolation of the parent sapogenin or steroidal compound(s) and hydrolysed sugar residues, followed by derivatisation of these compounds with reagents such as trimethylsilylchloride or trimethylsilylimdazole, acetic anhydride, or diazomethane[16]. This derivatisation converts hydroxyl and/or acid groups present

in the hydrolysed sapogenin, steroidal (Figure 1.7) and sugar (Figure 1.8) residues to non polar analogues which can be analysed using TIC or SIM GC-MS techniques.

Sulfate conjugated analogues are typically harder to cleave via hydrolysis than the glycosides. Strongly acidic conditions are required to remove conjugated sulphate groups by chemical hydrolysis (solvolysis) such as 4 molar H_2SO_4 heated to 53°C for 1 to 2 hours[17]. The free steroid or triterpene must then be derivatised to a more volatile and thermally labile analogue, analogous to the saponins (Figure 1.7).

Base Hydrolysis

In the case of conjugated ester analogues (e.g. steroidal fatty acid esters) the initial hydrolysis step is usually performed under alkaline conditions and affords the parent sterol or sapogenin and fatty acid[18] (hydrolysis in 90% methanol and 10% aqueous K_2CO_3 solution at 50°C for 18 hours) (Figure 1.4). Thereafter derivatisation with reagents such as trimethylsilylchloride or trimethylsilylimdazole, acetic anhydride, or diazomethane is required to afford GC volatile analogues of the hydrolysed products (Figure 1.7).

Methylation of Carboxylic Acids

Carboxylic acid analogues of steroids or triterpenes must be converted to a more volatile and thermally labile analogue prior to analysis by GC-MS. A common method for increasing the volatility and thermal labiality of carboxylic acid analogues is methylation[19] (Figure 1.9).

Enzymatic Hydrolysis

Enzymatic hydrolysis can achieve good efficiency without exposing the compound to the elevated temperatures associated with chemical hydrolysis. The choice of the enzyme and method is dependent upon the conjugate moiety and the steroid structure. Common sources of enzymes used for the cleavage of conjugate moieties are bacterial (*Escherichia coli*) and mollusc (*Helix pomatia* and *Patella*

vulgata). Bacterial sources of enzymes only contain β-glucoronidase activity (Figure 1.5), whilst mollusc sources contain both β-glucoronidase and sulfatase (Figure 1.6) activity. The sulfatase activity from the molluscs is weak and highly specific to the structure of the conjugated steroidal sulfate[8].

Reactions commonly used for removal of conjugated groups from steroidal or triterpenoidal compounds to aid analysis via GC-MS; (Figure 1.3-1.6)

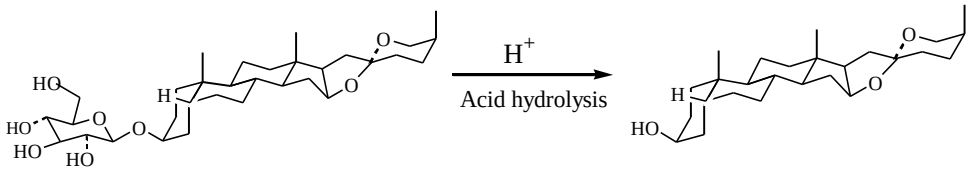

Figure 1.3. Acid hydrolysis of a saponin

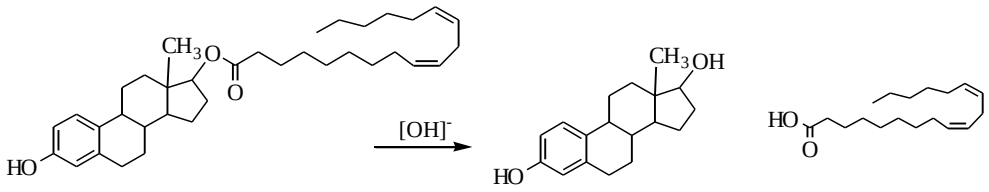

Figure 1.4. Alkaline hydrolysis of a fatty acid ester analogue

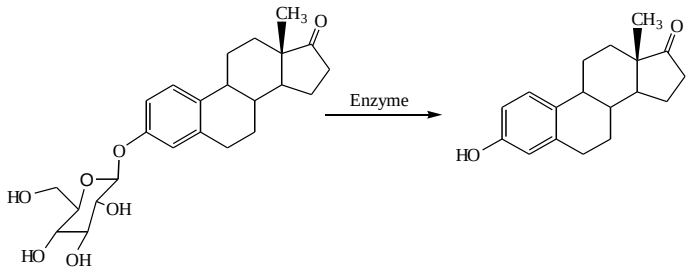

Figure 1.5. Enzymatic hydrolysis of a glycoside

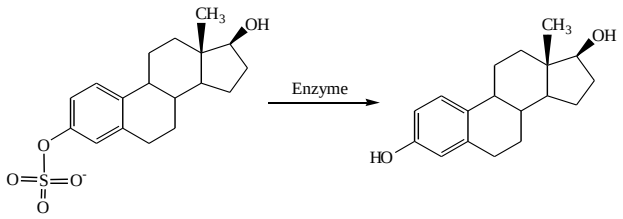

Figure 1.6. Enzymatic hydrolysis of a sulphate

Reactions commonly used for increasing the volatility and thermal labiality of steroids and triterpenes for analysis via GC-MS; (Figure 1.7-1.9)

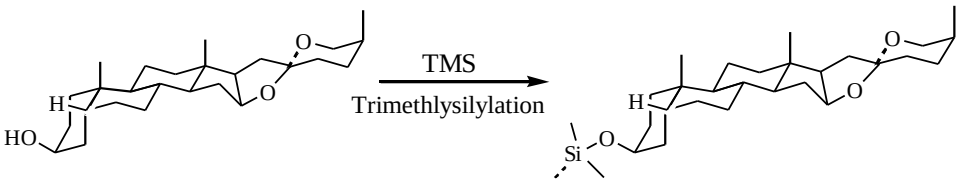

Figure 1.7. Trimethylsilylation of the hydroxyl group of a steroid

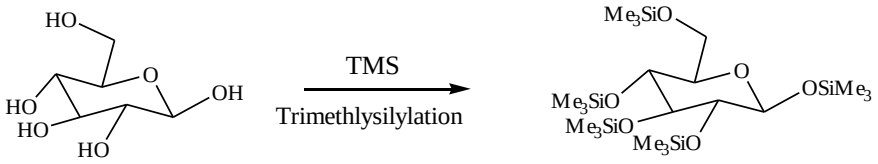

Figure 1.8. Trimethylsilylation of the hydroxyl groups of a sugar

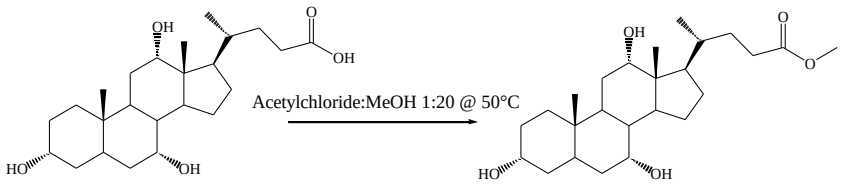

Figure 1.9. Methylation of an acid group to a COOMe group

While the fore mentioned procedures can be used to identify and quantify the aglycone component of conjugated genins, they do not identify the gross structure of the conjugated analogues. In particular, information concerning the point of attachment of gylcosyl residues to steroidal or sapogenin skeletons is lost, as is information concerning the nature of glycoside linkages (α- or β-) at anomeric carbons. The identity of the specific conjugated group attached to a specific steroid or triterpene is also lost upon removal of the conjugate group.

1.1.1.2 GC-MS Ionisation

GC-MS techniques generally use a ‘hard’ ionisation technique such as electron impact ionisation (EI). Hard ionisation techniques cause a larger degree of fragmentation than ‘soft’ ionisation techniques, resulting in less chance of seeing the molecular ion or pseudo-molecular ion. The application of hard MS ionisation techniques such as EI techniques on gas phase analytes tend to afford more

predictable and reproducible MS data than is the case with softer chemical ionisation techniques on liquid phase analytes typical of LC-MS[20].

Soft ionisation techniques such as atmospheric pressure chemical ionisation (APCI) techniques can be coupled to GC-MS instrumentation resulting in reduced fragmentation of the analyte[20]. The analyte, however, must still be volatile to allow it to be introduced via the GC column. The lack of volatility associated with many conjugated analogues of genins means these compounds still require pre-analysis structural modification before analysis by GC-MS.

1.1.2 Analysis of Steroids and Triterpenoids using LC-MS

Since LC-MS separates and detects analytes in the liquid phase it can detect polar compounds without prior structural modification, providing the compounds are soluble in the liquid phase. Therefore LC-MS, unlike GC-MS, can be performed on conjugated gennins without the requirement for acid or base hydrolysis of parent glycoside, sulfate, or fatty acid ester analogues[8].

Since the introduction of LC-MS instrumentation there has been a gradual shift to measuring some of the compounds more problematic under GC-MS techniques to LC-MS techniques. Like GC-MS, LC-MS has some significant limitations. The chromatographic resolution than can be achieved using a LC column packed with 5 µm stationary phase particles is much less than can be achieved using a capillary GC column. The reduced chromatographic separation of analyte peaks in LC-MS methodologies are frequently compensated for by utilising selective reaction monitoring (SRM), where a specific ion from the analyte is collected and fragmented to daughter ions that uniquely identify that analyte.

Another major limitation of LC-MS methodologies are the difficulties associated with ionising compounds of neutral or low polarity in liquid matrices. LC-MS techniques are more prone to ionisation difficulties than GC-MS, these are in part due to the liquid matrices[20]. The factors of significance in the ionisation of analytes in LC-MS are discussed below.

1.1.2.1 LC-MS Ionisation

LC-MS typically uses soft ionisation techniques and therefore causes much less fragmentation and is more likely to generate the pseudo-molecular ion. A significant disadvantage of soft ionisation techniques is that they do not induce ionisation of the analyte to the same extent achieved using hard ionisation techniques[20].

Generation of the pseudo-molecular ion can identify the molecular weight of an analyte, and opens up the possibility of progressive MS^2, MS^3, MS^n fragmentation of the pseudo-molecular ion under controlled conditions. The ability of the soft ionisation techniques to induce a charge on the analyte is highly dependent upon the structure of the analyte[20-22]. Steroidal and triterpenoidal compounds are typically thought of as difficult to ionise compounds using soft ionisation techniques[22].

Two major reasons exist for lack of reliability of soft ionisation techniques;

(i) Ionisation of the analyte is usually incomplete and many of the analyte molecules pass through the ionisation interface unionised.

(ii) The matrix that the analytes are analysed in changes as the compounds in that sample elute through the chromatographic column.

To minimise the effect matrix exerts upon the ionisation of the target analytes ionisation agents are added in to the eluent[20]. Ionisation agents function by buffering the eluent solution so the effective ionisation conditions are similar throughout the chromatogram, and to aid ionisation which increases the ion response seen at the detector.

1.2 Analysis of Conjugated Steroidal and Triterpenoidal Compounds

1.2.1 Identification of Saponins and Sapogenins by LC-MS

Saponins are naturally occurring surface-active glycosides possessing a steroidal or triterpenoid alycone component linked to one or more glycoside residue[23]. While saponins are predominantly produced by plants they also found in lower marine animals and synthesised by some bacteria[24, 23].

The identification of parent saponins using LC-MS techniques, as opposed to only the hydrolysed algycone using GC-MS techniques, is beneficial in that saponins containing the same algycone group may possess differing physiology activities and their metabolism (fate) in ovine or other environments often differ. Determining the specific pairing of genins and their conjugate glycoside groups are indiscernible with GC-MS methodologies as GC-MS is unable to detect the parent saponin[15, 25].

SRM can be applied to the analysis of both saponins and sapogenins, with good specificity based on knowledge of daughter ion fragmentation characteristics of a target analyte, however, SRM may not distinguish stereoisomeric forms of a particular saponin unless a significant difference in the fragmentation characteristics are present.

GC-MS can generally distinguish stereoisomeric forms of free sapogenins or acetylated analogues by comparing fragmentation pattern ion intensities and retention time data [16, 25, 26]. In some circumstances the levels of pairs of unresolved or only partially resolved peaks can be determined by comparing the ratio of selected pairs of fragment ions determined for the mixed peak, with those determined for pure specimens of the two contributing compounds. The same principles can be applied to LC-MS to see if similar correlations can be observed. This technique is covered in more detail in Section 4.5.1.

Various applications requiring the identification and quantification of saponins in their conjugated forms are currently of interest at the University of Waikato. The application to be investigated in this research involves the need for the identification and quantification of saponins implicated as possible causative agents in the development of hepatogenous photo-sensitisation diseases of sheep.

1.2.1.1 Saponins and Sapogenins Implicated in Hepatogenous Photo-Sensitisation Diseases

Episarsasapogenin and epismilagenin glucuronides have been implicated as possible causative or marker agents in several plant associated photo-sensitisation diseases of sheep, cattle and other ruminant animals[12-14, 27]. The current analytical methodology utilised in these studies has involved the isolation of extracts containing free and conjugated sapogenins (dichloromethane and methanol extracts respectively), followed by hydrolysis of the conjugated extracts and GC-MS analysis of acetylated genins present in these extracts[27, 28].

The structures of the saponins present in many of the plants implicated in the development of hepatogenous photo-sensitisation are known, as are aspects of the ruminal conversions of free genins and subsequent isomerisation to episapogenins (3α-OH analogues)[15, 28]. Little is known about the nature of conjugated genins present in post rumen gastrointestinal tract samples other than that the bile crystals recovered from animals exhibiting disease symptoms have been found to be calcium salts of epismilagenin and/or episarsasapogenin β-D-glucuronides[12-14]. Specifically it is not known if the conjugated saponins present in post-rumen samples are unhydrolysed or partly hydrolysed analogues of ingested plant saponins or other conjugated analogues (eg sulphates, phosphates).

It is anticipated that LC-MS^n analysis can be used to identify conjugated sapogenins present in gastrointestinal tract samples and to determine whether or not only epismilagenin or episarsasapogenin conjugates were selectively absorbed in the small intestine and transported to the liver where they appeared to be precipitated as the calcium salts of epismilagenin and/or episarsasapogenin β-D-

glucuronides. By having a more detailed understanding of these processes, including the total array of conjugated steroids (saponins) that are present in the bile crystals, gastrointestinal tract, and feed stock of animals suffering photo-sensitisation diseases, it can be anticipated that a better understanding of the processes involved in the development of disease symptoms will be derived.

Based on field observations that within a flock grazing the same pasture not all animals appear to be prone to the development of photo-sensitisation symptoms. It has been proposed that some animals may be more prone to the development of photo-sensitisation symptoms than others, and that this might be a genetically influenced characteristic[29]. Currently a Brazilian veterinary group is separating a flock of sheep grazing saponin containing plants over a four year trial period into susceptible and non-susceptible groups, in the expectation that resistance susceptibility night be an inheritable characteristic. Possibly genetic factors may influence the nature of conjugates in the rumen and their conversion to conjugate analogues including glycosides, sulfates, phosphates or the bile acid type analogues of taurine and/or glycine. If so the availability of LC-MS methods to probe the nature and distribution of conjugated sapogenins in rumen and GI tact samples may assist in the identification of susceptible and resistant animals.

The selective breeding approach has been successfully applied in the context to the identification of sheep that exhibit more or less susceptibility to sporidesmin toxicities in New Zealand[30]. Sporidesmin causes a primary photo-sensitisation disease in sheep grazing affected pastures.

1.3 Research Aims and Objectives

The principle objectives of the investigation reported in this thesis were to determine optimal LC-MS conditions for the analysis of saponins and sapogenins implicated in photo-sensitisation diseases of livestock, using the University of Waikato's Thermo Finnigan LCQ Advantage LC-MS system. Only limited sensitivity (much less than that which was considered acceptable) had been

obtained in previous investigations of a variety of free and conjugated steroidal and triterpene substrates, including estrogenic sterols[31].

In order to address the disappointing sensitivity of the University of Waikato's LC-MS system, and in the absence of a budget to purchase a higher performance mass spectrometry system (e.g. an updated Thermo Finnigan LTQ system, or a triple quad MS system) it was desirable that a systematic evaluation of instrument specific factors which influence the overall sensitivity for detecting free and conjugated sapogenins was undertaken. The research was undertaken with a view to the identification of conditions which could be applied to the analyses of free and conjugated sapogenins recovered from the rumen and GI tract of sheep in a breeding trial in Brazil. In order to address quarantine and bio security conditions, it is envisaged that when the samples become available (after two to three years of selective breeding) biological material (freeze dried rumen, GI tract, etc) will be processed and extracted and the resulting non-biological material would be forwarded to the collaborating groups with appropriate LC-MS expertise at the University of Waikato, or the National Veterinary Institute (Oslo).

To achieve the objectives required for LC-MS analysis of the sapogenins and their conjugated analogues it was determined there was a need to;

(i) Evaluate the factors that contribute to the ionisation efficiency and consequentially the sensitivity of LC-MS analyses of the saponins and sapogenins associated with hepatogenous photo-sensitisation diseases.

(ii) Determine the LC-MS fragmentation characteristics of model saponins and sapogenins associated with hepatogenous photo-sensitisation diseases with the intention of elucidating an LC-MS method for their identification and quantification. A supplementary objective of the sapogenin investigations was to determine whether not MS^n ion intensities could be used to define the C-3, C-5 and/or C-25 chemistry of genins in a manner analogous to that previously reported using GC-MS ion ratio data[16, 25, 26].

2 Analysis of Steroids and Triterpenoids via LC-MS

As discussed in Chapter 1 it was anticipated that a research programme, namely that directed towards the characterisation groups of plant saponins and sapogenins implicated in the development of hepatogenous photo-sensitisation diseases of livestock would benefit from the development on LC-MS methodologies which would supplement existing GC-MS methodologies. Prime objectives of the LC-MS investigations were the identification of conditions which overcome the sensitivity limitations encountered in earlier University of Waikato studies on steroidal or triterpenoidal compounds.

While literature information concerning acquisition conditions utilised in related studies by other workers is helpful, it does not of itself serve to define optimal conditions on the University of Waikato LC-MS system since it is well known that optimum conditions vary for system to system. These factors depend on a range of factors including subtle differences in interface design, such as heated capillary tube length and diameter, ionisation source layout and geometry, etc.

2.1 LC-MS Instrumentation

A simplistic description of a LC-MS system as a series of functional modules consists of an, Auto Sampler → Chromatographic Column → Ionisation Source → Mass Separation Device → Detector.

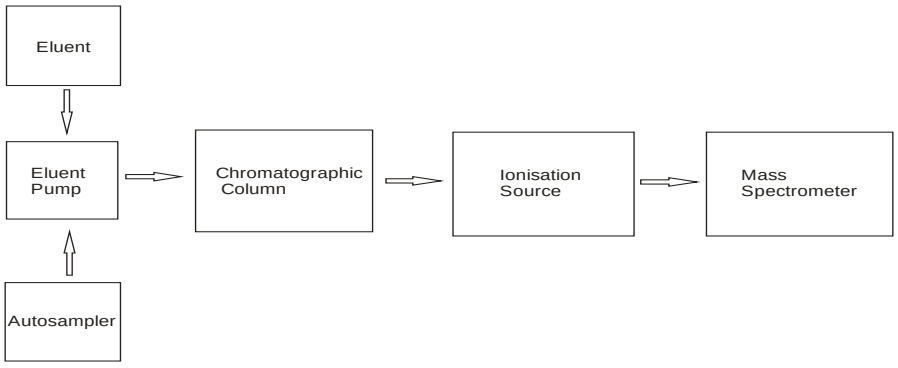

Figure 2.1. Schematic diagram of a LC-MS system

A typical LC-MS system consists of an auto-sampler that injects a liquid sample to a chromatographic column where it is eluted isocratically, or gradient-wise, with a suitable solvent or solvent mixture. Compounds with differing affinities for the column will get eluted off at different retention times.

Following separation, the analytes are then transported to the ionisation interface in the eluent flow, upon arrival the eluent and analytes are ionised by a complex process which involves creating charged droplets followed by removal of the solvent matrix from these droplets. This can lead to a variety of ions including $[M+H]^+$, $[M+Na]^+$, $[M+NH_4]^+$, $[M_2+H]^+$, and $[M_2+Na]^+$ ions, depending in part on ions intentionally added to eluent buffers (eg H^+ ions ex formic acid) or present in trace levels in the aqueous buffer solutions (eg Na^+ ions).

Once ionised, the mass spectrometer then separates the ions by their mass to charge ratio, using either a quadrupole stage or an ion trap cavity from which ions are expelled as a function of their mass, before sending them to the detector. Other non-destructive detectors (e.g. UV-vis, or refractive index detectors) may be connected inline into the eluent stream post chromatographic separation to detect analytes prior to the mass spectrometer.

The University of Waikato LC-MS instrumentation consists of a Thermo Finnigan Advantage LCQ instrument, comprising of a Surveyor auto-sampler, Surveyor LC pump, Surveyor diode array UV-vis detector, and a Thermo Finnigan Advantage LCQ mass spectrometer. The intention of this thesis is to optimise the instrument parameters affecting the detection of steroidal and triterpenoidal compounds and their conjugated analogues, allowing a wider variety of compounds to be measured by LC-MS at the University of Waikato.

2.1.1 Liquid Chromatography

The liquid chromatography system separates compounds in the liquid phase based on their relative affinities for the surface of the stationary phase of the column and eluent. Compounds that have a stronger affinity for the stationary phase will take longer to elute through the column than those with a weak affinity[32]. By using a column with an appropriately coated stationary phase and adjusting the eluent composition it is possible to achieve adequate separation of chromatographic peaks for most compounds using liquid chromatography, provided they are soluble in the mobile phase. Resolution using liquid chromatography is not as pronounced as can be achieved using gas chromatography, and peak overlap is often observed. To overcome the limitations of liquid chromatographic separation the mass spectrometer can be used to select parent → daughter ion combinations that are specific to that particular analyte (SRM).

Liquid chromatographic columns are available in differing dimensions and stationary phases. A liquid chromatographic column should be selected that enables adequate separation of analytes, is compatible with the liquid chromatographic systems flow requirements, and is inert to reaction with the eluent, analytes, or matrix of the samples.

2.1.2 Mass Spectrometric Detection

Mass spectrometry systems detect analytes by placing a charge on the analyte, followed by separation based upon the mass to charge ratio of the analyte, the charged analyte of specific mass to charge then reaches the detector where it is converted into a signal which is deciphered by a computer. Literature suggests that placing a charge on the analyte (ionisation) is usually the limiting factor in LC-MS detection of steroidal and triterpenoidal compounds[21, 22]. Further discussions into the factors affecting ionisation in LC-MS applications can be found from Sections 2.1.3, to 2.1.4.

The University of Waikato Thermo Finnigan Advantage LCQ instrument is an ion trap mass spectrometer. As eluded to in Sections 1.1.2 and 2.1.1, an ion trap mass spectrometer enables multiple fragmentations to be carried out in a sequence, allowing development and implementation of SRM methodologies. SRM methodologies require that the fragmentation patterns of specific analytes be investigated so a diagnostic parent to daughter ion fragmentation specific for the analyte can be selected. Upon generation of diagnostic fragmentation patterns specific to the analyte a SRM method that monitors that specific fragmentation during a chromatographic run can be developed. High sensitivity analysis utilising triple quadrupole MS technology requires knowledge of compound specific SRM transitions.

2.1.3 Ionisation of Steroidal and Triterpenoidal Compounds and Their Conjugated Analogues

It is well known that steroidal and/or triterpenoidal compounds can be hard to ionise in a mass spectrometer, and that the conditions required to achieve efficient ionisation can vary from molecule to molecule depending on the parent ring system, the substituent groups present in a molecule and the ionisation source used[22].

Ionisation of the analyte is considered to be the limiting step for the analysis of steroids by LC-MS[22]. By investigating the ionisation characteristics of a selection of genins that may be of interest to the University of Waikato Chemistry Department, it was anticipated that parameters which influenced the effective analysis of these steroids could identified and their contributions maximised.

The University of Waikato's LCQ Advantage instrument has two ionisation interfaces: electro-spray ionisation (ESI) and atmospheric pressure chemical ionisation (APCI). Variables that can be manipulated include the type of inlet, eluent, ionisation agent composition and concentrations can be manipulated to maximise the ion response seen for a particular analyte.

ESI and APCI ionisation sources have benefits and disadvantages with respect to each other. These benefits and disadvantages are often analyte, and sample matrix specific, so the most suitable interface for one compound may not be the most suitable for another compound. A general observation made by Gomes[8] on the topic of steroid analysis is that '*Though greater sensitivity is achievable by ESI, matrix effects are less for APCI*'.

2.1.3.1 Electro-Spray Ionisation ESI

ESI is the most widely used interface used in LC-MS applications[20], and is a 'soft' ionisation technique. ESI operates by exposing the analytes in the solvated matrix to a charge while it sprayed through a small capillary which induces ionisation of easily ionisable components of the eluent mixture (eg ionisation agents such as formic acid). Solvent is progressively removed via evaporation in the ESI and heated capillary interfaces resulting in charged analyte molecules. During these complex processes analyte species form ions such as $[M+H]^+$, $[M+Na]^+$, and $[M_2+H]^+$ which are detected at the mass spectrometer[20, 32, 33]. The ESI inlet allows the adjustment of capillary temperature, capillary and source voltages, along with physical alignment of the spray nozzle.

ESI is reported to show a correlation between ion intensity detected at the mass spectrometer and the concentration of the analyte in the eluent[20, 32, 33]. The correlation shows the larger the concentration of analyte in the eluent the larger the detected ion intensity. By reducing the flow of eluent through an ESI interface it may be possible to enhance the detection of the analyte. ESI should obtain better ionisation efficiencies at lower flow rates through the LC column. The optimal flow rate will be a compromise between, retention time, peak broadening, and analyte concentration in the eluent.

2.1.3.2 Atmospheric Pressure Chemical Ionisation (APCI)

APCI is a slightly harder ionisation technique than ESI, but still considered soft. APCI operates by exposing analytes in the solvated matrix to an elevated temperature in the source capillary to convert the analytes and solute to the gaseous phase before spraying the gas towards a charged 'probe' which ionises the analyte via complex mechanisms. The partially solvated analyte ions are then exposed to conditions to aid removal of the solvate and unionised molecules from the charged analytes, before guiding the de-solvated charged analytes into the mass spectrometer almost analogous to ESI.

APCI generally induces a larger degree of thermal decomposition of the analytes than the softer ESI. This is at least partially due to the increased exposure of the analyte to heat in the APCI source relative to the ESI source. APCI is particularly suited to analysis of volatile, thermally stable analytes and is ineffective at ionising compounds with low vapour pressures and are thermally labile such as sugars[20].

APCI is reported to show an ion intensity detected at the mass spectrometer that correlates with the quantity of the analyte in the eluent[20], thus the observed intensity should be proportional to the quantity of analyte in the detector. LC-MS analysis using an APCI interface should (reputably) exhibit a response that is relatively independent of flow rate.

2.1.3.3 Eluent

An ideal eluent would be capable of dissolving the analyte, cause analytes to elute with adequate peak separation, be inert to reacting with the analyte during the liquid chromatography separation, provide adequate ionisation of the analyte in the ionisation interface and be volatile. No one solvent can perform all these tasks, so a graidient of multiple solvents and ionisation agents are combined to approximate an ideal eluent.

In LC-MS most experiments are carried out on a reverse phase column, using an eluent gradient of water/acetonitrile (ACN) or water/methanol. The eluent gradient generally starts with a polar water biased solvent mixture and gradually becoming less polar. The polar compounds should elute of first in the water biased portion of the gradient followed progressively by the less polar compounds. Often methodologies employ an eluent gradient starting with polar solvents so that many interfering (ion suppressing) compounds can be eluted off first preventing them affecting the analysis for the target analyte.

Some concern exists that methanol may not be inert toward some of the analytes under acidic conditions, as would be present if an acidic ionisation agent was used with methanol as the organic component of the eluent[34]. The eluent cannot be too non-polar as some polarity is required for effective ionisation and the eluent must be miscible with water if a gradient is applied utilising water.

In LC-MS ionisation can be heavily influenced by the eluent composition. It has been reported that many compounds ionise more efficiently in the non-polar region of the eluent composition using ESI. Protriptyline[35] and cocaine[20] ionisation in LC-ESI-MS being specific examples where ionisation was much more efficient at higher organic (ACN) composition.

The effect eluent composition exerts upon ionisation will be investigated for a variety of model compounds, using both ESI and APCI interfaces. It is feasible that the optimal eluent composition may be different for the two ionisation interfaces as the mechanism of ionisation for each ionisation interface differs. The ability of the eluent to promote efficient ionisation may be of significance when an appropriate chromatographic column is selected for analysis of specific compounds. The investigation was restricted to ACN as the preferred organic eluent for its relative inertness and the favourable ionisation properties reported in literature[20, 22, 34].

2.1.3.4 Ionisation Agents

Ionisation agents are added to the eluent to act as an ionisation aid by increasing the efficiency of ionisation of the analyte, and act as an ionisation buffer by providing a matrix that is consistent between samples causing even ionisation of the analyte. The ionisation aid can have a large effect upon the efficiency of ionisation in the ionisation interface. Due to the large possibility of ionisation agents the number to be investigated will be limited to an acidic ionisation agent - formic acid, a weakly acidic ionisation agent - ammonium formate, and an alkaline ionisation agent - ammonium carbonate. A secondary benefit of many ionisation agents is the improvement many can make to the LC resolution and repeatablitiy.

In the positive ion spectrum, the acidic ionisation agent is expected to produce $[M+H]^+$ pseudo-molecular ions, the ammonium formate ionisation agent is expected to produce $[M+NH_4]^+$ pseudo-molecular ions and/or $[M+H]^+$ pseudo-molecular ions, and the ammonium carbonate ionisation agent is expected to produce $[M+NH_4]^+$. Cluster ions such as $[M_2H]^+$ and dehydration products such as $[M-H_2O+H]^+$ may also be formed.

In the negative ion spectrum, $[M-H]^-$ are commonly formed as pseudo-molecular ions. Cluster ions and dehydration products may also be formed in the negative ion spectrum. Under some circumstance $[M+X]^-$ ions may also be formed where X^- ions such as Cl^- or $COOH^-$ are present in a buffer. Alkaline ionisation agents are expected to be favourable to the generation of negative $[M-H]^-$ and $[M]^-$ pseudo-molecular ions.

2.1.3.5 Signal Suppression

Signal suppression the term applied to phenomena which cause attenuation of the ion current produced by a given amount of analyte in the sample. Such phenomena that cause attenuation of the ion current can result from both chemical and physical factors[20]. Signal suppression is a serious consideration for all LC-MS methodologies, and if not taken into account can result in detector response values that invalidate the quantification[36, 37].

Minimising signal suppression in the eluent system can be achieved by selecting appropriate eluent and ionisation agent combinations that promote ionisation of the analyte and buffer factors that affect ionisation such as solution pH and electrolyte concentration. Such appropriate combinations of eluent and ionisation agents are often specific to a class of compound, or even an individual analyte[22]. Many of the buffers used to obtain good resolution in high performance liquid chromatography (HPLC) can cause attenuation of the ion current for many compounds in LC-MS[20].

Buffers that result in generation of a mixture of ions (for example $[M+H]^+$ and $[M+NH_4]^+$) can reduce the effective intensity of the analyte ions and therefore reducing detection limits. Signal suppression can also be caused by the presence of signal suppressing compounds in sample matrices and cause signal suppression that fluctuates throughout a chromatographic run as the offending signal suppressing compounds elute through the ionisation interface[38]. Biological fluids such as urine[39] and plasma[40] can exhibit large effects upon the ion signal observed for an analyte. Several methods (processes) have been developed for dealing with the variable signal suppression that occurs throughout a chromatographic run due to interfering compounds in the matrix[41].

Internal standards are routinely used as a means of correcting for the effect of signal suppression. An internal standard of known concentration is added to the sample and standard matrices prior to analysis. By comparing the signal observed for the internal standards of each sample to those of the standards the effect signal suppression exerts upon every sample can be determined and compensated for.

This method is highly dependent on having matched the internal standards with the analytes for chromatographic and ionisation characteristics. Ideal internal standards possess the same chromatographic and ionisation characteristics but have differentiable fragmentation characteristics. For this reason stable isotope analogues of the analyte are often used as internal standards such as poly deuterated analogues. The need for matching of chromatographic characteristics can be overcome by post column infusing a suitable stable isotope analogue into the eluent allowing quantification of the target analytes at any retention time.

Another method involves manipulating the chromatographic conditions so the analyte elutes at a portion of the chromatogram where the signal suppression is weak. To achieve this experiments are carried out where the analyte/s are direct infused into the eluent steam as a blank sample matrix is injected onto the column. The signal for the direct infused analyte/s will reduce in the portions of the chromatogram where signal suppressing compounds elute[37]. The elution conditions are then manipulated so the analyte/s are not eluted during the same period as the offending signal suppressing compounds.

Alternatively the standard addition method can be employed. The standard addition method involves running each sample multiple times with known quantities of the analyte added. By subtracting the response of the sample with no standard added from the samples with standards added a calibration response curve can be generated which compensates for the matrix effects of that sample. The response of the sample with no sample added can then be quantified from the calibration response curve that was created for that sample. Standard addition methods are time consuming and laborious, therefore are not commonly applied in routine analysis. However, standard addition is a useful tool in method development for the quantifying the effect the matrix exerts (signal suppression).

2.1.4 Ionisation via Chemical Derivatisation

If adequate ionisation of the analytes cannot be achieved via the manipulation of ionisation parameters and eluent conditions it may be necessary to perform chemical derivatisation to convert the analyte to a form which is ionised prior to mass spectrometric separation[42]. Chemical derivatisation process can be carried out on samples prior to the analytes being analysed, or the chemical derivatisation process can be carried out in the eluent flow after separation by liquid chromatography and before the ionisation interface. Both methods have their benefits and limitations.

For either method to be suitable for the analysis of conjugated steroids or conjugated triterpenes, hydrolysis of the conjugated moiety must not occur during the derivatisation process. Some structural information will be lost during the derivatisation process, but critical information including the identity and point of attachment of the conjugate entity should be maintained, provided an appropriate derivatisation process is selected. Improving ionisation of analytes via chemical derivatisation can be used to produce either positive or negative ions, by careful selection of an appropriate derivatisation agent[42].

2.1.4.1 Pre-Analysis Chemical Derivatisation

Pre-analysis chemical derivatisation of analytes can improve the detection of problematic compounds significantly. For pre analysis chemical derivatisation to be suitable for liquid chromatography the derivatisation process must result in a compound that is able to be eluted off the chromatographic column. The derivatisation process consists of one or more easily ionised functional groups being attached to the target analyte. The easily ionised functional groups get ionised as the derivatised analyte passes through the ionisation interface.

Ideally the derivatised analyte will be a neutral compound that accepts a single charge over the molecule upon ionisation in the ionisation interface. Many derivatised products carry a permanent charge which causes the elution properties

to be vastly different to un-derivatised compounds. The different elution properties associated with permanently charged derivatives can be used to separate the analytes from possible matrix effects and interferences.

Pre-analysis chemically derivatised analytes elute through the liquid chromatographic column at retention times that are as a result of the derivitised analyte, so comparisons with liquid chromatographic data for the parent compound are not possible. Pre-analysis chemical derivatives that are suitable for the type of compounds investigated would selectively attach an easily ionised functional group or permanently ionised functional group to hydroxyl or ketone functionalities of the analyte.

Potentially suitable pre-analysis chemical derivatisation reagents include; ferrocene carbamate derivatisation of alcohols[42, 43], ferrocene boronate derivatisation of diols[42, 44], Girard's reagent P derivatisation of ketones , Girard's reagent T derivatisation of ketones, dansyl chloride derivatisation of hydroxyls attached to an aromatic ring, 1,2-dimethylimidazole-4-sulfonyl chloride derivatisation of hydroxyls attached to an aromatic ring (phenolic group), pyridine-3-sulfonyl chloride derivatisation of hydroxyls attached to an aromatic ring, and 4-(1H-pyrazol-1-yl) benzenesulfonyl chloride derivatisation of hydroxyls attached to an aromatic ring, mono-(dimethylaminoethyl) succinyl ester derivatisation of alcohols[42]. The ferrocene based derivatisation products rely upon a platinum capillary for effective ionisation of the derivitised analyte[43]. As the University of Waikato does not have a platinum capillary at its deposal, ferrocene based derivatisation is currently unsuitable.

2.1.4.2 Post Column Chemical Derivatisation

Post column chemical derivatisation of analytes can improve the detection of problematic compounds significantly. For post column chemical derivatisation to be suitable the analyte is eluted through the LC column as the parent compound before a chemical reagent is added to the eluent flow causing a reaction between the chemical reagent and the analyte. Ideally the derivatised product of the analyte will either be an ion that holds a singular charge, or a neutral compound that is easily ionised to a singularly charged ion in the ionisation interface. A benefit of post column derivatisation is the chromatographic data is that of the parent compound, causing chromatographic data collected under identical conditions where no derivatisation is present to be comparable. Post column chemical derivatives that are suitable for the type of compounds investigated would selectively and quickly attach an easily ionised functional group or permanently ionised functional group to hydroxyl or ketone functionalities of the analyte in the eluent prior to the ionisation source. A potentially suitable post column chemical derivatisation reagent includes fresh alkaline methanolic ammonia solution as used for the detection of oestrogenic sterols and their conjugates[45].

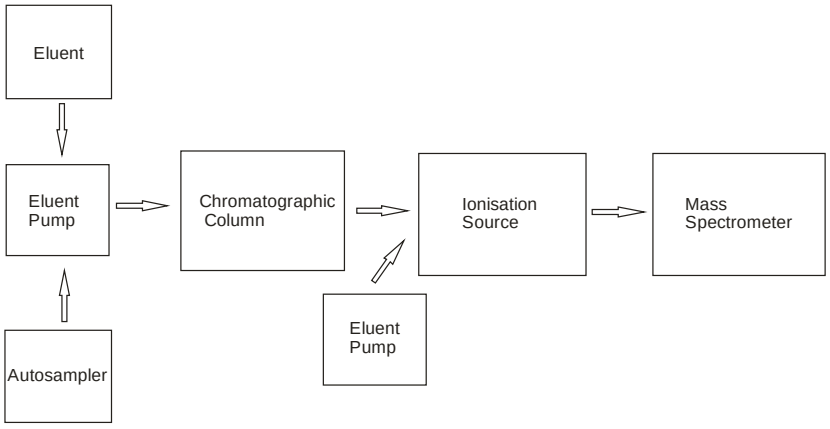

Figure 2.2. LC-MS system with post column infusion

2.2 Target Compounds

Model compounds investigated were chosen for a combination of their structural characteristics, and applications of relevance to curent or pending University of Waikato research interests. The model compounds chosen for investigation were saponins and sapogenins associated with hepatogenous photo-sensitisation diseases of livestock. Model compounds were chosen based upon their documented involvement in hepatogenous photo-sensitisation disease of livestock[28], and availability of the compounds. The relevance of developing methodology that can benefit the detection within the category is discussed in more detail in the following.

Saponins and sapogenins implicated in hepatogenous photo-sensitisation diseases of sheep and goats have been traditionally analysed by GC-MS methods[16]. It has been postulated that selected steroidal saponin glycosides are at least partially responsible for the bile crystals found in sheep suffering from photo-sensitisation diseases (aveld) associated with grazing *N. ossifragum*[15]. As LC-MS has significant advantages for the detection of saponins relative to GC-MS it has been hypothesised that detection by LC-MS could be a viable alternative method for analysis of the saponins implicated as possible causative agents for heptageneous photo-sensitisation diseases of sheep such as aveld. During the course of the topic an attempt will be made to develop parameters that aid the analysis of selected compounds implicated in the hepatogenous photo-sensitisation diseases of sheep and goats by LC-MS methodology.

Compounds of interest to the investigation of saponins and sapogenins implicated in hepatogenous photo-sensitisation diseases of sheep and goats include;

- Sarsasapogenin, a sapogenin implicated in the hepatogenous photo-sensitisation diseases in sheep[13, 14]. The IUPAC name for sarsasapogenin is (25*S*) 5β-spirostan-3β-ol. Molecular formula, $C_{27}H_{44}O_3$. Molecular mass, 416.64 amu

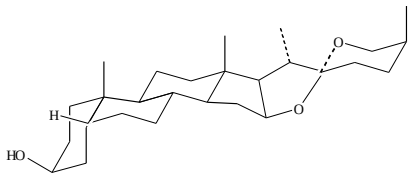

Figure 2.3. Structure of sarsasapogenin

A selection of deuterated analogues of sarsasapogenin and episarsasapogenin were made available for the investigation. 2,2,4,4-$^{2}H_4$-episarsasapogenin/2,2,4,4-$^{2}H_4$-sarsasapogenin (4:1) and 20,23,23-$^{2}H_3$-sarsasapogenin was synthesised during previous research into the implication of saponins as causative agents in the hepatogenous photo-sensitisation diseases of sheep[46]. The purity and site of dueteration of 2,2,4,4-$^{2}H_4$-episarsasapogenin/2,2,4,4-$^{2}H_4$-sarsasapogenin and 20,23,23-$^{2}H_3$-sarsasapogenin samples were established by NMR and GC-MS analysis (Sections 4.24.3).

- Episarsasapogenin, the C-3 isomer of sarsasapogenin. Episarsasapogenin conjugates are formed in-vitro by isomerisation of sarsasapogenin in the gastro-intestinal tract of sheep[28]. The IUPAC name for episarsasapogenin is (25*S*)-5β-spirostan-3α-ol. Molecular formula, $C_{27}H_{44}O_3$. Molecular mass, 416.64 amu

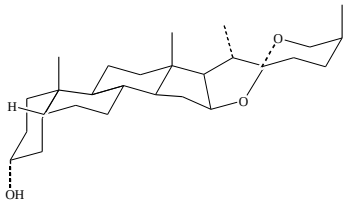

Figure 2.4. Structure of episarsasapogenin

- Smilagenin, a lithogenic sapogenin implicated in the photo-sensitisation diseases in sheep and goats[13, 14, 16, 47]. The 25*R* isomer of sarsasapogenin The IUPAC name for smilagenin is (25*R*)-5β-spirostan-3β-ol. Molecular formula, $C_{27}H_{44}O_3$. Molecular mass, 416.64 amu

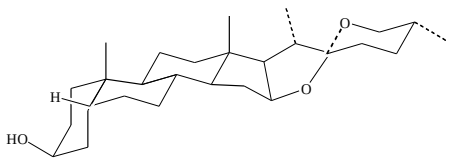

Figure 2.5. Structure of smilagenin

- Diosgen, C5(6) alkene analogue of sarsasapogenin. A lithogenic sapogenin implicated in the photo-sensitisation diseases in sheep and goats[16]. The IUPAC name for diosgenin is (25*R*)-5β-spirost-5-en-3β-ol. Molecular formula, $C_{27}H_{42}O_3$. Molecular mass, 414.63 amu

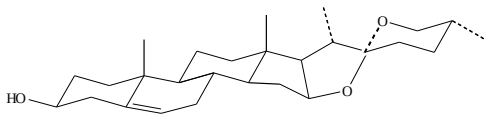

Figure 2.6. Structure of diosgenin

- Tigogenin, the C-5 (α-H) isomer of sarsasapogenin. A non-lithogenic sapognin that is not implicated in photo-sensitisation diseases of livestock[16, 47]. The IUPAC name for tigogenin is (25*R*)-5α-spirostan-3β-ol. Molecular formula, $C_{27}H_{44}O_3$. Molecular mass, 416.64 amu

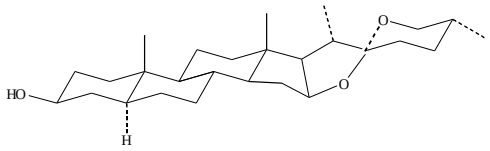

Figure 2.7. Structure of tigogenin

- Asparagoside A (Sarsasapogenin-β-D-glucoside), a saponin containing an aglycone implicated in the photo-sensitisation diseases in sheep and goats[13, 14].The IUPAC name for asparagoside A is (25*S*)-5β-spirostan-3β-*O*-β-D-glucoside. Molecular formula, $C_{33}H_{54}O_8$. Molecular mass, 578.77 amu. The chemical structure of asparagoside A is given in Figure 1.2

- Sarsasapogenin-β-D-galactoside, a saponin containing an aglycone implicated in the photo-sensitisation diseases in sheep and goats[13, 14]. The IUPAC name for sasasapogenin galactoside is (25*S*)-5β-spirostan-3β-*O*-β-D-galactoside. Molecular formula, $C_{33}H_{54}O_{8.}$ Molecular mass, 578.77 amu

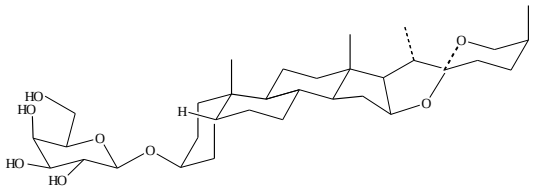

Figure 2.8. Structure of sarsasapogenin-β-D-galactoside.

3 Optimising Ionisation of Saponins and Sapogenins

3.1 Saponins and Sapogenins Selected for Optimisation of Ionisation Parameters

Two sapogenins and a saponin were selected as model compounds for the optimisation of LC-MS responses were compounds implicated in, or isomers of compounds implicated in heptageneous photo-sensitisation diseases such as Alveld and Geeldikkop[13].

The selected compounds were:

(i) sarsasapogenin and diosgenin - as model sapogenins.

(ii) sarsasapogenin-β-D-glucoside - as a model saponin.

These compounds were selected for the availability of sample and their close structural similarity (or identity) with compounds implicated in the development of photo-sensitisation diseases of sheep.

3.1.1 Optimising Ionisation of the Model Compounds

Two ionisation sources were used in the investigation into optimising ionisation of sarsasapogenin, diosgenin, and sarsasapogenin-β-D-glucoside. Both ionisation sources have benefits and disadvantages with respect to each other. Idealised (clean) matrices were used in the optimisation studies reported below. When ovine rumen and GI tract samples become available further optimisation studies will need to be performed in order to determine the extent to which actual sample matrices influence the respective detector responses since it is well known that sample matrices often suppress ionisation of real samples, relative to a clean standard matrix[48].

3.2 Electro-Spray Ionisation Source (ESI)

The application of genin analysis using the ESI inlet as the ionisation source was investigated by manipulating parameters affecting ionisation to maximise the ion responses of the model compounds. The parameters investigated include; alignment of the spray nozzle, cone voltages, ionisation agents, composition of the eluent, capillary temperature and eluent flow rate.

Initial investigations were performed in positive and negative ion modes by direct infusing the model compounds into the eluent flow (200 $\mu L min^{-1}$ 1:1 ACN:H_2O, capillary temperature 250°C, and 0.01% acetic acid buffer). During these investigations, sarsasapogenin gave disappointingly weak ion responses in the mass spectrometer. It was concluded poor ionisation was the most probable cause of the weak response.

The three model compounds formed identifiable ions in the positive ion mode, but in negative ion mode little if any compound related ion responses were observed. Due to the relative ease in which positive ions were generated, the investigation into the optimisation of ESI parameters centres on the generation of positive ions, in particular pseudo-molecular ions.

3.2.1 Alignment of the Spray Nozzle in the ESI Source

The alignment of the ionisation source spray jet was varied while sarsasapogenin was infused into the eluent flow via a syringe pump. The alignment of the spray jet was found to only exhibit a small effect upon the observed signal in the mass spectrometer and not be the cause of the low sensitivity observed. Since alignment of the spray nozzle was found not to be the source of the poor ionisation for sarsasapogenin the appropriate alignment position utilised for sarsasapogenin was used for all other compounds.

3.2.2 Voltage Settings (ESI)

The voltage settings of the ESI and mass spectrometer were optimised via the *Auto tune* function of the Thermo Finnigan software 'LCQ Tune'. Typically, a 0.01 $molL^{-1}$ solution of a model compound was direct infused into the eluent stream prior to the ESI inlet. The pseudo-molecular $[M+H]^+$ ions of the model compounds, sarsasapogenin (*m/z* 417), for diosgenin (*m/z* 415), and for sarsasapogenin-β-D-glucoside (*m/z* 579) were utilised when optimising the parameters.

3.2.3 Ionisation Agents (ESI)

The effect ionisation agents exert upon ionisation of the model compounds were investigated by direct infusing 0.001 $molL^{-1}$ of the model compounds into the eluent stream just prior to the ESI source and measuring the intensity of the model compounds specific ions in the spectra. By recording the ion intensities of the spectra during a period the ionisation agent composition had stabilised the effect the ionisation agent exerts upon the detected ion intensity can be measured.

Three ionisation agents were investigated on the model compounds; formic acid, ammonium formate, and ammonium carbonate. Experimental parameters for the collection of the data were 200 $\mu Lmin^{-1}$ 1:1 ACN: H_2O eluent, capillary temperature 300°C, 0.01% (v/v) formic acid, 0.01 $molL^{-1}$ ammonium formate, and 0.01 $molL^{-1}$ ammonium bicarbonate in the ACN. This produced eluent compositions of 0.005% (v/v) formic acid, 0.005 $molL^{-1}$ ammonium formate, and 0.005 $molL^{-1}$ ammonium bicarbonate respectively.

It was found that formic acid achieved the best ionisation of the three agents tested for positive ion spectra of all three model compounds (Figure 3.1, 3.3 and 3.5). As the most promising ionisation agent, the effect concentration of formic acid in the eluent was investigated on the model compounds (Figure 3.2, 3.4 and 3.6). Experimental conditions were as described previously (above) with the

exception that the eluent consisted of 1:1 ACN:H_2O with 0.1%, 0.05%, 0.024%, 0.005%, and 0% formic acid in the eluent. The ESI interface settings were optimised using sarsasapogenin-β-D-glucoside as described in Section 3.2.2.

The presence of formic acid in the eluent was found to be beneficial to the ionisation of the model compounds, with an observed general trend showing a reduction of ion intensity when no formic acid was present in the eluent for all three model compounds (Figure 3.2, 3.4 and 3.6).

3.2.3.1 Sarsasapogenin

Sarsasapogenin showed greater ionisation in the presence of formic acid than was the case for other ionisation agents investigated (Figure 3.1).

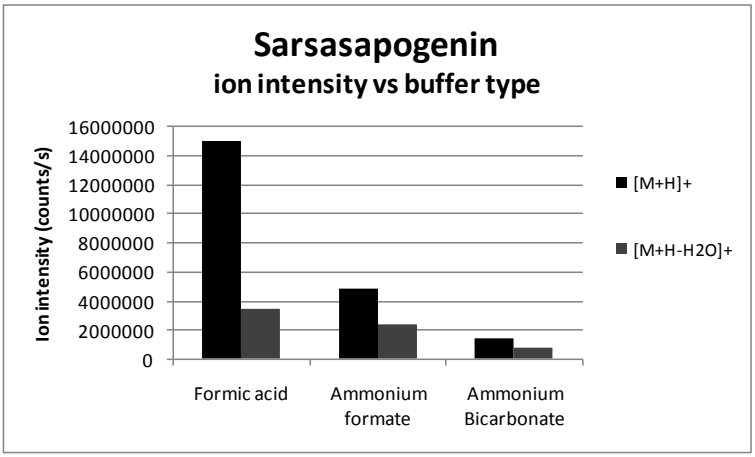

Figure 3.1. ESI responses for sarsasapogenin in three ionisation agents

The concentration of formic acid in the eluent was found to exhibit a small effect upon the ionisation of sarsasapogenin as can be seen in Figure 3.2. The intensity of the ion response with no formic acid present was approximately two thirds of that observed for 0.05% formic acid.

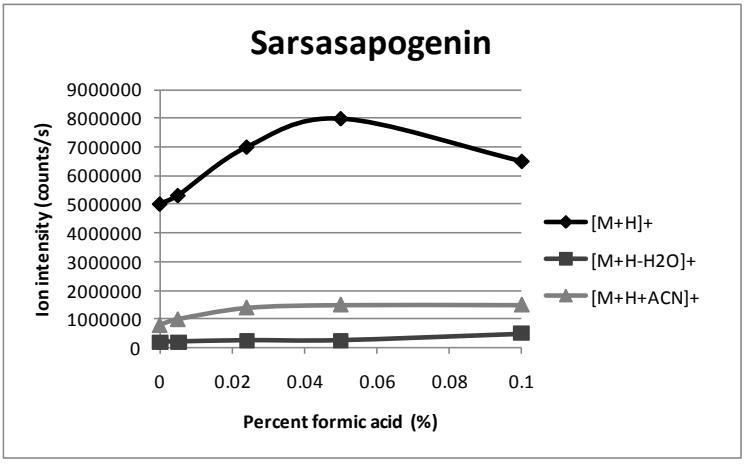

Figure 3.2. Effect of formic acid concentration upon the ESI response of sarsasapogenin

3.2.3.2 Diosgenin

Like sarsasapogenin, diosgenin showed preferential ionisation with formic acid as the ionisation agent (Figure 3.3).

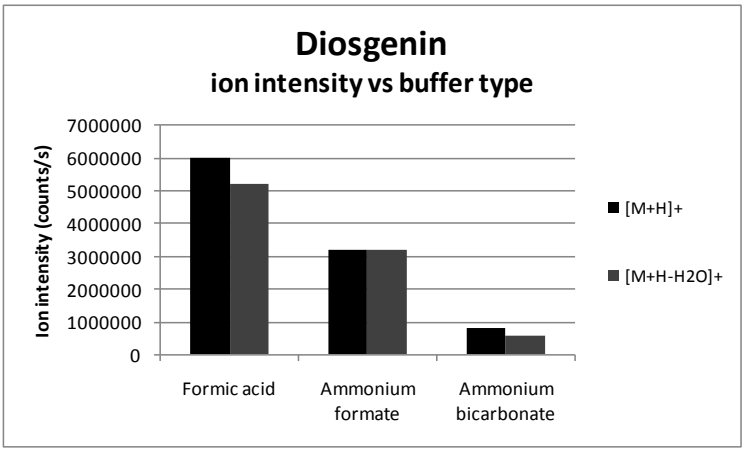

Figure 3.3. ESI responses for diosgenin in three ionisation agents

The concentration of formic acid in the eluent was found to exhibit a small effect upon the ionisation of diosgenin (Figure 3.4). The intensity of the ion response with no formic acid present was approximately half of that observed for 0.05 and 0.1% formic acid.

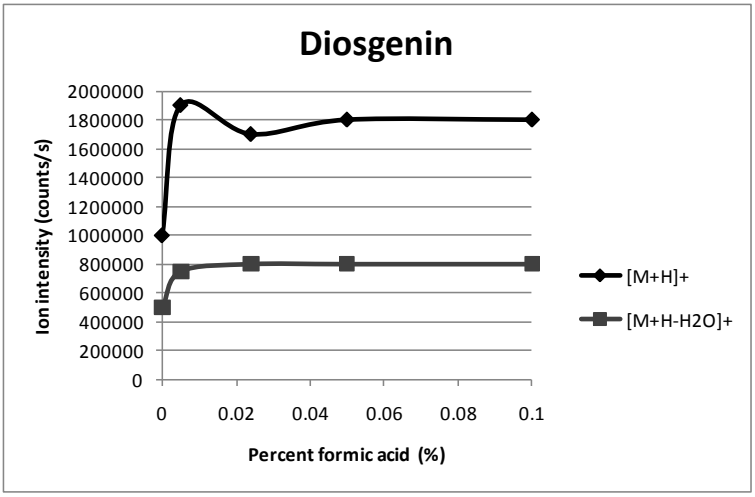

Figure 3.4. Effect of formic acid concentration upon the ESI response of diosgenin

3.2.3.3 Sarsasapogenin-β-D-glucoside

Like sarsasapogenin and diosgenin, sarsasapogenin-β-D-glucoside showed preferential ionisation with formic acid as the ionisation agent. A satisfactory response was also observed using ammonium formate (Figure 3.5).

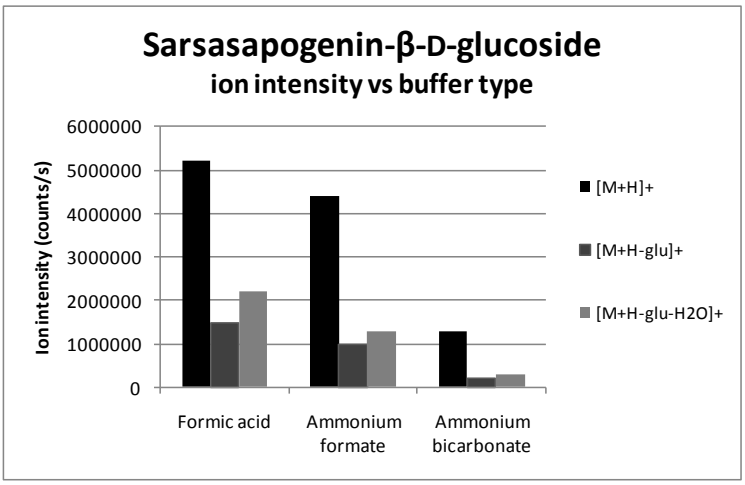

Figure 3.5. ESI responses for sarsasapogenin-β-D-glucoside in three ionisation agents

The concentration of formic acid in the eluent was found to exhibit a small effect upon the ionisation of sarsasapogenin-β-D-glucoside (Figure 3.6). The intensity of the ion response with no formic acid present was approximately half of that observed for 0.05 and 0.1% formic acid.

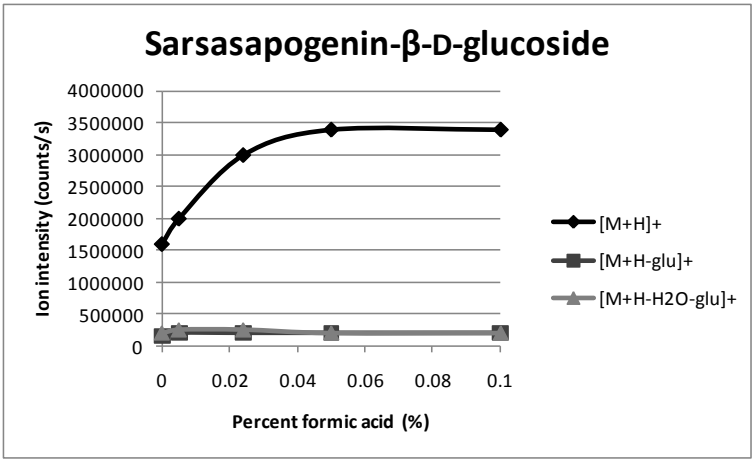

Figure 3.6. Effect of formic acid concentration upon the ESI reponse of sarsasapogenin-β-D-glucoside

3.2.4 Eluent Composition (ESI)

Direct infusion experiments. The composition of the eluent was varied from 0:100 (ACN-H_2O) to 100:0 (ACN-H_2O) as the model compounds were directly infused into the eluent stream just prior to the ESI source. Ion intensities were recorded during a period the eluent composition had stabilised A significant advantage of the direct infusion experiments was that the eluent composition was not limited by the composition of the solvent mixture required to elute a model compound through an LC column. Direct infusion enabled the influence solvent mixture comprised of 0-100% ACN to be determined (Sections 3.2.4.1-3.2.4.3).

Chromatographic experiments. Chromatographic experiments were undertaken to confirm or disprove the data trends observed in the direct infusion experiments. Chromatographic data was collected by eluting model compounds through a Phenomenex Prodigy 150 mm x 2.00 mm 5 µm C-18 LC column at various isocratic eluent compositions (ACN-H_2O, + 0.01% formic acid) and quantifying the peak areas (ion responses) observed for the corresponding pseudo-molecular ion. It was anticipated that chromatographic data should model the trends seen in the direct infusion experiments. Investigations were constrained to the range of solvent mixtures that could be employed to elute targets compounds for the C-18 LC column in a reasonable time.

3.2.4.1 Sarsasapognin

Direct infusion, ESI inlet; Sarsasapogenin was infused via a syringe pump just prior to the ionisation inlet into an ACN-H_2O eluent mixtures containing 0.01% formic acid. In all cases the eluent flow rate of 200 µLmin^{-1}. It was that the composition of the eluent had a large effect upon the intensity of the fragment ions observed (Figure 3.7). The maximum intensity of $[M+H]^+$ *m/z* 417 ion occurred at an eluent composition between 50 and 60% ACN.

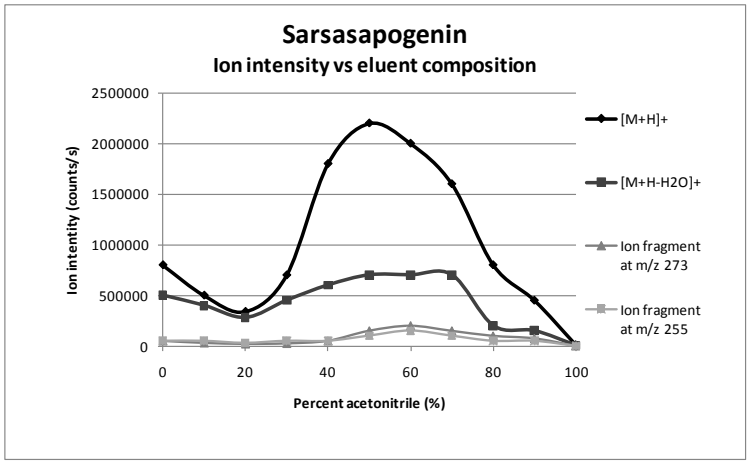

Figure 3.7. Effect of eluent composition upon the ESI response of sarsasapogenin

Using a C-18 LC column sarsasapogenin can be eluted using 80-100% ACN-H_20 mixtures either isocratically or as part of gradient elution programme before the retention time and flow rates become impractical. For this reason sarsasapogenin elutes from the C-18 column where the ionisation is unfavourable in the ACN-H_2O eluent composition. The ionisation current observed for *m/z* 417 $[M+H]^+$ of sarsasapogenin is 220 times higher in the presence of 1:1 ACN-H_2O than is the case for 100% ACN.

Chromatographic data, ESI inlet; Chromatographic experiments performed by injecting 10^{-9} mol of sarsasapogenin onto the C-18 column and eluting it using isocratic compositions of 100:0, 90:10, and 80:20 (ACN-H_2O, + 0.01% formic acid) verified the downward trend seen in the direct infusion experiments as the percent ACN was increased. Peak areas for TIC, $[M+H]^+$, and MS^2 on $[M+H]^+$ ions are shown in Figure 3.8. Chromatographic experiments were performed using a capillary temperature of 300°C and a flow rate 400 µLmin^{-1}. The extent to

which the ionisation decreased as the percent ACN increased was were slightly lower than that observed in direct infusion. This reduction may, at least in part, be attributed to the higher flow rates used in the chromatographic experiment relative to those used in the direct infusion experiment.

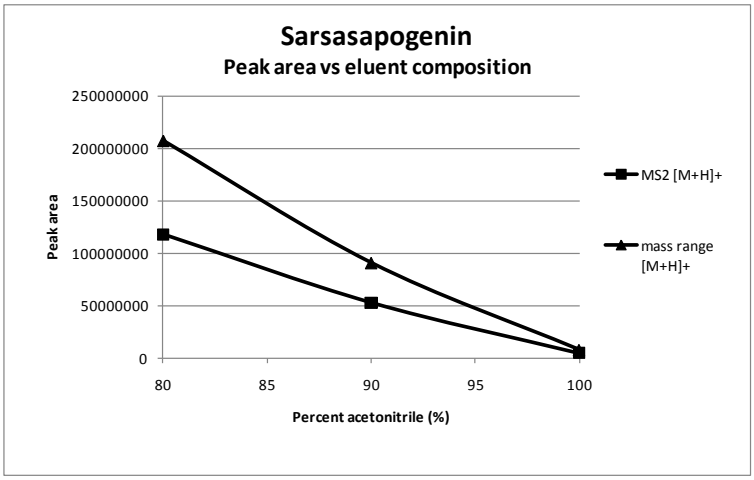

Figure 3.8. Effect of eluent composition upon the ESI response of sarsasapogenin

Several methods of manipulating the eluent composition exist so sarsasapogenin elutes from an LC column at a composition that is beneficial to its ionisation. Options include changing the LC column to one that allows sarsasapogenin to elute using a solvent mixture containing higher percent of water. For example a C-8, rather than C-18 column could be used. It is appears from the data represented in Figures 3.7 and 3.8 that it would be beneficial to add water post column to the eluent flow. The increase in ion intensity seen for the eluent composition would be much greater than the decrease in intensity due to dilution.

Assuming the ionisation is approximately proportional to the concentration of analyte for the ESI interface[20] the expected ion intensity can be calculated. The direct infusion data presented in (Figure 3.7) was utilised to estimate ion current intensities that would be observed with appropriate dilution from post column addition of water using 100% ACN as the LC eluent (Figure 3.9).

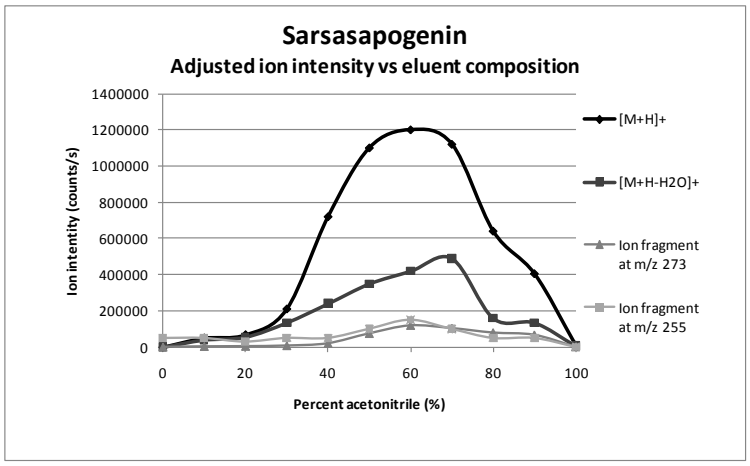

Figure 3.9. The estimated effect post column infusion of water would have upon the ESI reponse of sarsasapogenin

Unexpectedly however an experiment using 100% ACN (+0.01% formic acid) as the LC column eluent and infusing water (+0.01% formic acid) post column into the eluent flow did not result in a significant increase in intensity relative to the use of 100% ACN as eluent. It is hypothesised that the non-observation of an increase of ionisation intensity during the post column infusion experiments may be due to the eluent being heterogenous as it enters the ESI interface due to the inadequate mixing of the infused water with the LC eluent If so, the heterogeneous eluent formed as a result of inadequate mixing of the eluents may be able to be minimised by infusing the water further 'upstream' in the eluent flow and (or) extending the length of the capillary tube between the point of infusion and the ESI inlet.

3.2.4.2 Diosgenin

Eluent composition was varied as 0.01 $molL^{-1}$ diosgenin was directly infused via a syringe pump immediately prior to the ESI source into ACN-H_2O eluent mixtures contained 0.01% formic acid (flow rate 200 $\mu Lmin^{-1}$). Ion responses were determined when the eluent had stabilised. It was found that the composition of the eluent had a large effect upon the intensity of $[M-H]^+$ and fragment ions that were observed (Figure 3.10).

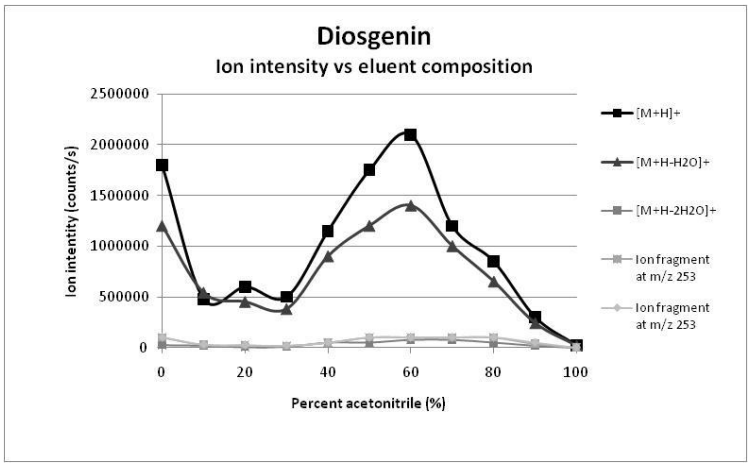

Figure 3.10. Effect of eluent composition upon the ESI response of diosgenin

The maximum intensity of $[M+H]^+$ *m/z* 415 ion response occurred at an eluent composition of *ca* 60% ACN. Diosgenin can be eluted in the 100% to 70% ACN portion of the elution gradient using the available C-18 column before the retention time and flow rates become impractical. Thus when using a C-18 column diosgenin elutes where the eluent composition greatly suppresses ionisation (Figure 3.10). The intensity observed for *m/z* 415 $[M+H]^+$ ion is 105 times higher at 60% ACN than it is using 100% ACN.

Direct infusion data and chromatographic runs at isocratic eluent compositions of 100%, 90%, 80% and 70% ACN showed at similar downward trend in ionisation responses as thepercentof ACN increased from 70 to 100% (Figure 3.11).

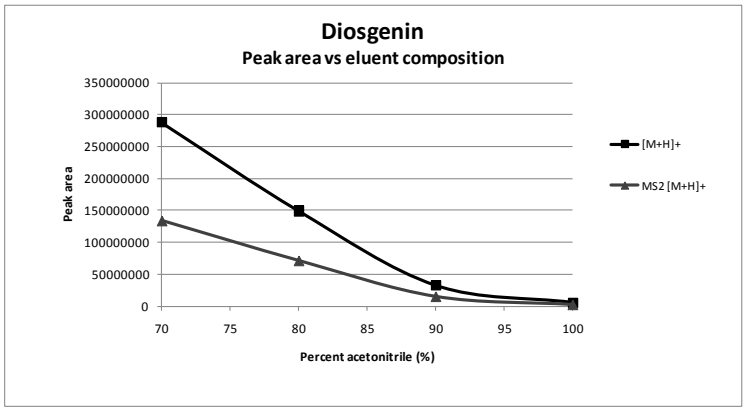

Figure 3.11. Effect of eluent composition upon the ESI peak area diosgenin

Post column infusion of water into the eluent as desricribed above for sarsasapogenin was investigated. The theoretical increase in sensitivity expected

for this experiment is depicted in Figure 3.12. As was the case for sarsasapogenin, no significant increase in ionisation was observed for diosgenin when water was infused into the eluent stream post column.

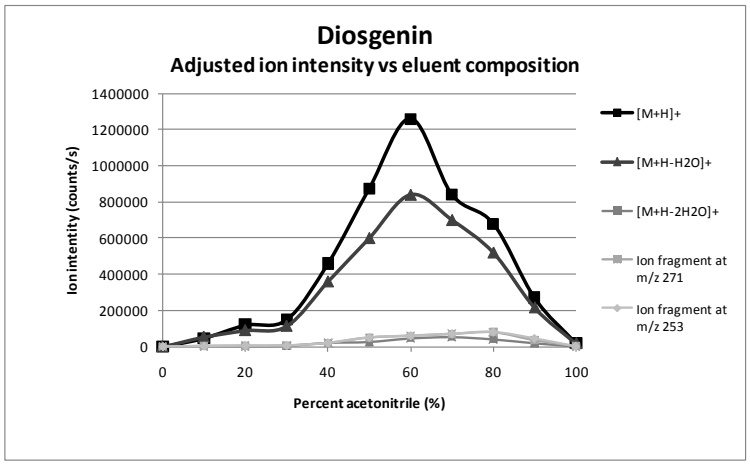

Figure 3.12. The estimated effect post column infusion of water would have upon ESI reponses of diosgenin

3.2.4.3 Sarsasapogenin-β-D-glucoside

Sarsasapogenin-β-D-glucoside 0.01 $molL^{-1}$ was directly infused via a syringe pump immediately prior to the ESI source into ACN-H_2O eluent mixtures contained 0.01% formic acid (flow rate 200 $\mu Lmin^{-1}$). The ESI inlet was maintained at 250°C. Ion responses were determined when the eluent had stabilised. It was found that the composition of the eluent had a large effect upon the intensity of the fragment ions observed (Figure 3.13).

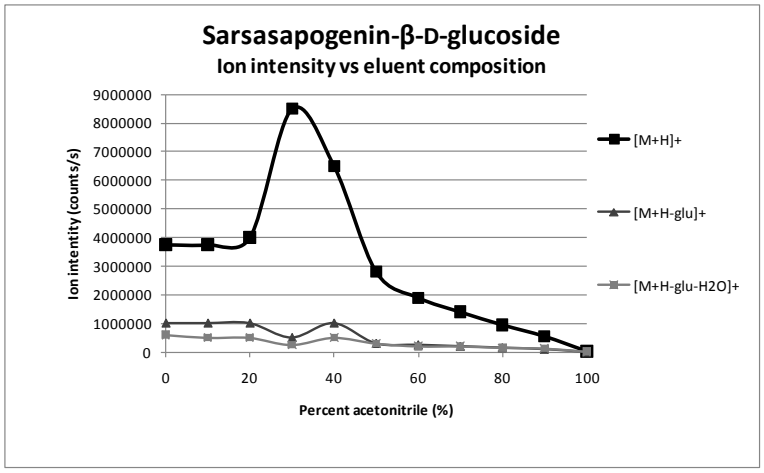

Figure 3.13. Effect of eluent composition upon the ESI response of sarsasapogenin-β-D-glucoside

The maximum intensity of $[M+H]^+$ *m/z* 579 occurred at an eluent composition of 30% ACN. Sarsasapogenin-β-D-glucoside was found to elute in the 60-100% ACN portion of the elution gradient when using the 150 x 2.00 mm id, 5 µm, C-18 reverse phase column. This eluent mixture has an appreciably higher ACN proportion than that which would be expected to afford the greatest response. The intensity of the *m/z* 579 $[M+H]^+$ ion is *ca* 280 times higher using 30:70 ACN-H_2O as eluent than is the case for 100% ACN.

Direct infusion chromatographic runs at isocratic eluent compositions of 100, 90, 80, 70, and 60% ACN showed similar trends in ion responses (Figure 3.14).

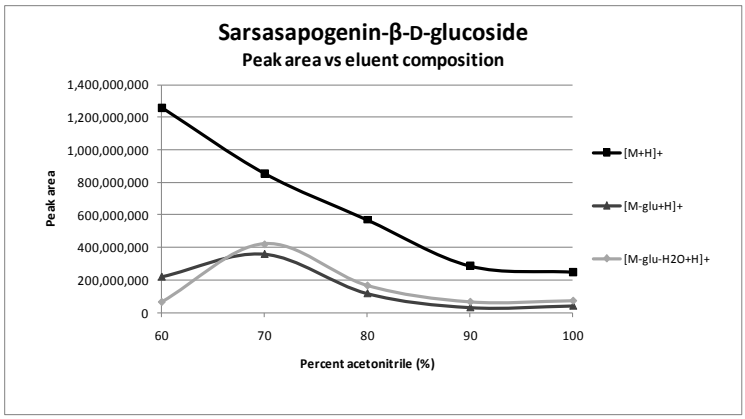

Figure 3.14. Effect of eluent composition upon the peak area of sarsasapogenin-β-D-glucoside

A theorectical depiction of the estimated increase ionisation that might be observed if water was infused post column, prior to the ESI inlet, is depicted in Figure 3.15. Disappointing, as was also the case for sarsasapogenin and diosgenin (see above), a significant increase in ionisation was not observed for sarsasapogenin-β-D-glucoside.

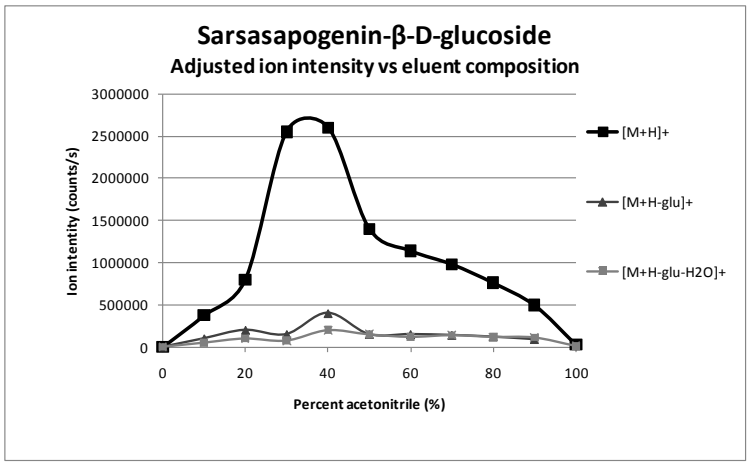

Figure 3.15. The estimated effect post column infusion of water would have upon ESI reponses of sarsasapogenin-β-D-glucoside

3.2.5 Capillary Temperature (ESI)

The capillary temperature was varied as the model compounds were directly infused into the eluent stream.

3.2.5.1 Sarsasapogenin

The greatest ion current responses for sarsasapogenin when the capillary interface was maintained at 300°C Figure 3.16. Data was collected while infusing 0.01 $molL^{-1}$ sarsasapogenin into an eluent stream of 1:1 ACN-H_2O containing 0.01% formic acid flowing at 200 $\mu Lmin^{-1}$.

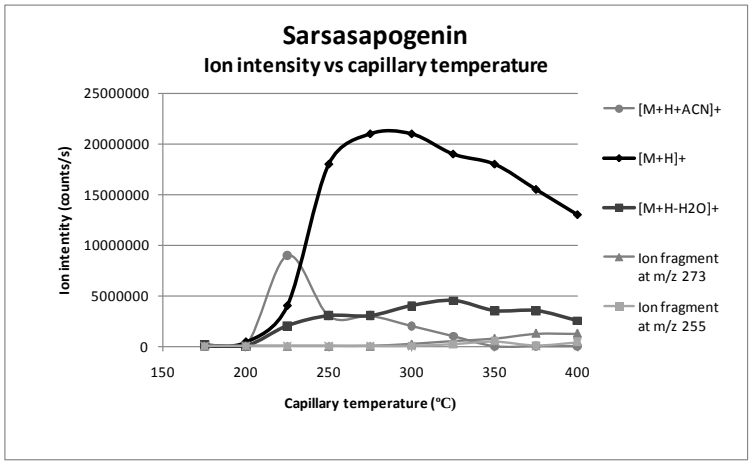

Figure 3.16. Capillary temperature effect upon the ESI responses of sarsasapogenin

Capillary temperatures below 200-225°C resulted much reduced ion ions, presumably due to condensation of sarsasapogenin on the capillary tube. Higher temperatures (>300°C) are thought to induce more fragmentation of the analytes ions.

3.2.5.2 Diosgenin

The ESI capillary temperature was varied as diosgenin was direct infused into the eluent stream just prior to the ESI source. The data obtained showed diosgenin, like sarsasapogenin, exhibit highest ion currents when the capillary was maintained in the vicinity of 300°C (Figure 3.17). Data was collected while infusing 0.01 $molL^{-1}$ diosgenin into an eluent stream of 1:1 ACN-H_2O containing 0.01% formic acid flowing at 200 $\mu Lmin^{-1}$.

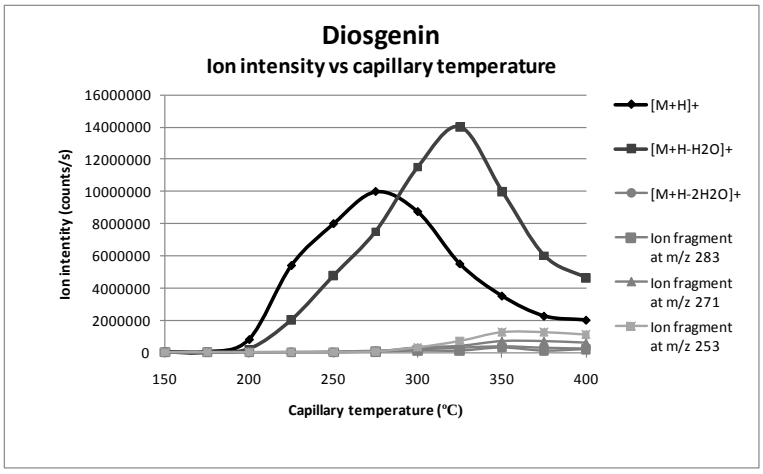

Figure 3.17. Effect of capillary temperature upon the LCQ ESI response of diosgenin

Lower capillary temperatures result in reduced ion intensity presumably due to condensation of diosgenin on the capillary tube while higher temperatures are thought to induce more fragmentation of the analyte. Dehydration of the $[M+H]^+$ ion to afford an $[M+H-H_2O]^+$ ion was more pronounced at 250-275°C than was the case for sarsasapogenin, presumably because of the stability of the conjugated 3,5-diene derivable from diosgenin. A similar tendency towards 3,5-diene formation is also observed in GC-MS analyses[25, 49].

3.2.5.3 Diosgenin, LTQ Comparison

The unexpectably high optimium capillary temperatures (275-325°C) found for diosgenin and sarsasapogenin (temperatures in the range 200-250°C are often selected as default set-up temperatures) prompted a comparison of the situation found for Waikato's LCQ system with that for an LTQ system avaliable at the National Veterinary Institute, Oslo. The comparative study was carried out by Professor Wilkins during a three month secondment.

Remarkably (against expectations of the National Veterinary Institute staff) it was found that the ion response continued to rise (appreciably so) until the maximium capillary temperature of 400°C was reached. At this temperature ion responses were an order of magnetude greater (10 times) than those determined at 250°C (Figure 3.18).

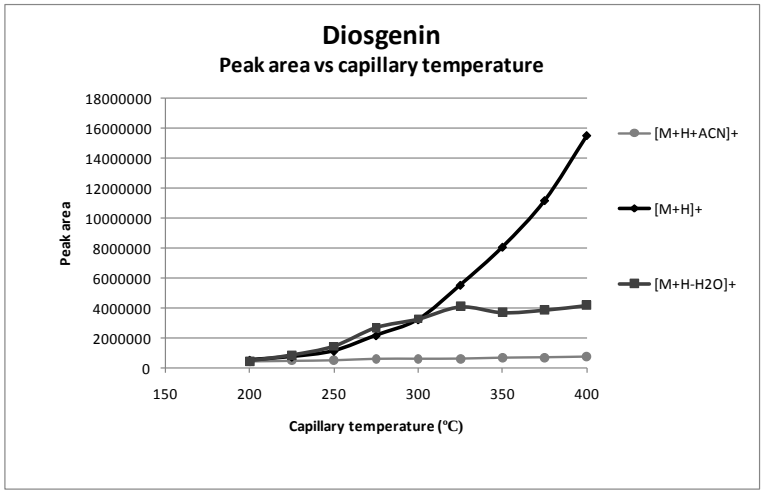

Figure 3.18. Effect of capillary temperature upon the LTQ ESI response of diosgenin

It is clear from the data presented in Figure 3.17 and Figure 3.18, that the optimum capillary temperature is an instrument dependent value, and that the use of moderate capillary temperatures in the range 200-250°C will, at least in the case of steroidal sapogenins, reduces the maximum sensitivity of analyses by an order of magnitude (10 fold) or more.

3.2.5.4 Sarsasapogenin-β-D-glucoside

The ESI capillary temperature was varied as sarsasapogenin-β-D-glucoside was direct infused into the eluent stream just prior to the ESI source. The data obtained showed sarsasapogenin-β-D-glucoside was best analysed at capillary temperatures around 300°C (Figure 3.19). Data was collected while direct infusing 0.01 $molL^{-1}$ sarsasapogenin-β-D-glucoside into an eluent stream of 1:1 ACN-H_2O containing 0.01% formic acid flowing at 200 $\mu Lmin^{-1}$.

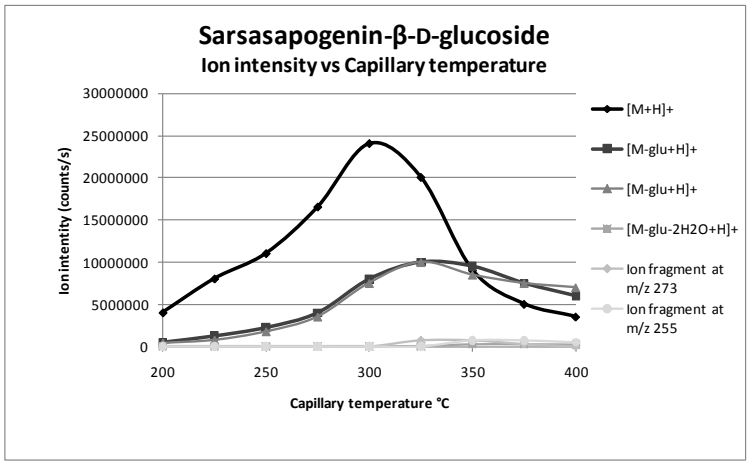

Figure 3.19. Effect of capillary temperature upon the ESI response of sarsasapogenin-β-D-glucoside

3.2.6 Effect of Eluent Flow Rate upon ESI

ESI interfaces are reported to show a correlation between the concentration of the analyte being sprayed through the interface and the ion intensity observed at the detector. Lower detection limits should be obtained at lower flow rates for applications utilising an ESI interface. The practical lower limit of the flow rate will be constrained by instrument factors (eg minimum stable flow rate, chromatographic column requirements, and analysis time).

The effect flow rate has upon ionisation response using the C-18 column that was available in the Chemistry Department at the time this investigation was performed by determining the pseudo-molecular ion peak areas at various eluent flow rates Figure 3.20-3.21. Analysis was carried out using, 9:1 ACN-H_2O

containing 0.01% formic acid as eluent, a capillary temperature of 300°C, and at flow rates of 200, 300, 400, and 500 μLmin^{-1} respectively.

In accord with expectations ion responses determined for sarsasapogenin, diosgenin and sarsasapogenin-β-D-glucoside reduced as the flow rate was increased. An essentially linear decrease in response was observed as the flow rates were increased (Figures 3.20-3.22).

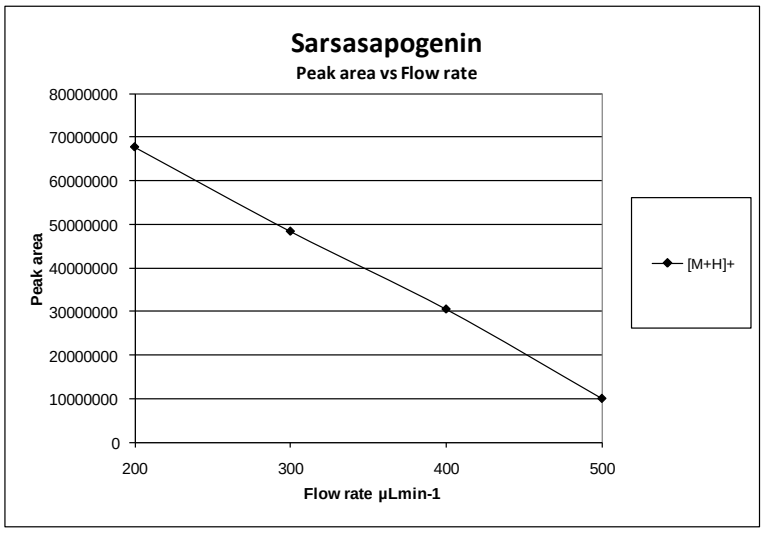

Figure 3.20. Effect of flow rate upon the ESI peak area of sarsasapogenin

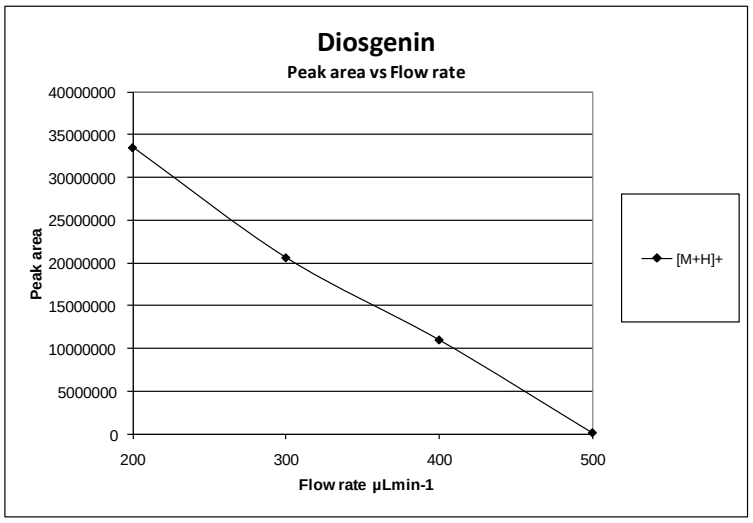

Figure 3.21. Effect of flow rate upon the ESI peak area of diosgenin ESI peak area

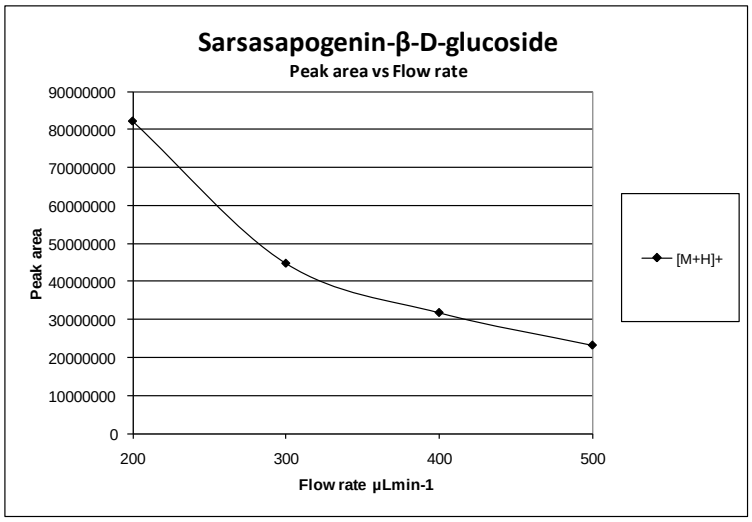

Figure 3.22. Effect of flow rate upon the ESI peak area of sarsasapogenin-β-D-glucoside

The data obtained for the model compounds confirmed the tendency of LC-ESI-MS to achieve better ionisation efficiency at low flow rates. The increase of ionisation at low flow rates would be complemented by the use of (micro or nano) columns that operate effectively at low flow rates.

The modern generation of low flow rate compatible ultra performance liquid chromatography (UPLC) columns (as opposed to conventional HPLC columns) typically afford good performance at low flow rates due to the effect of having small stationary phase particle size. Provided the solvent system can operate satisfactorily at the required flow rate and pressures, the use of low flow rate UPLC columns can lead to a substantial increase in sensitivity and chromatographic resolution[50, 51].

3.3 Atmospheric Pressure Chemical Ionisation Source (APCI)

APCI is an alternative ionisation technique to ESI that can give significantly better detection for particular compounds. APCI is reported to be less influenced by matrix effects than ESI, which will benefit the application of APCI in real samples[8].

The application of LC-MS analysis of the model compounds using the APCI interface as the ionisation source were investigated by manipulating ionisation

variables to maximise the detected ion responses for the model compounds. Initial investigations were performed in both positive and negative modes with direct infusion the model compounds into the eluent flow.

The three model compounds afforded readily identifiable ions in the positive ion spectrum, but the negative ion spectrum showed little if any analyte related ion responses which were not further investigated.

3.3.1 Voltage Settings APCI

The *auto tune* function of the Thermo Finnigan software 'LCQ Tune' was used to optimise the ionisation and cone voltages of the APCI inlet and mass spectrometer while 0.01 $molL^{-1}$ the model compounds were direct infused into the eluent stream prior to the APCI inlet.

3.3.2 Ionisation Agents (APCI)

The effect ionisation agents exert upon ionisation of the model compounds were investigated by direct infusing 0.001 $molL^{-1}$ of the model compounds into the eluent stream just prior to the APCI source analogous to the method used for determining the ionisation agents effect in ESI. Three ionisation agents were investigated; formic acid, ammonium formate, and ammonium carbonate.

The APCI source temperature was set to 150°C. Other experimental parameters for the collection of the data were as described in (Section 3.2.3) for ESI.

3.3.2.1 Sarsasapogenin

Under the chosen APCI condition the sarsasapogenin ionized to a greater extent using formic acid or NH_4COOH buffers (Figure 3.23). Generally similar ion responses were observed when the concentration of formic acid was varied (Figure 3.24).

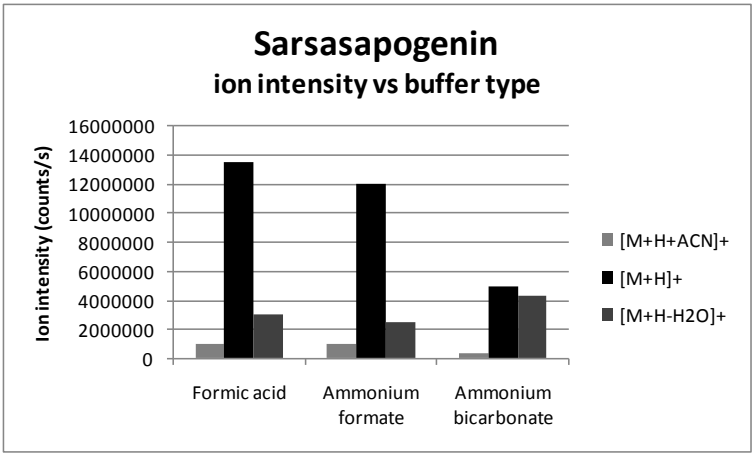

Figure 3.23. APCI responses for sarsasapogenin in three ionisation agents

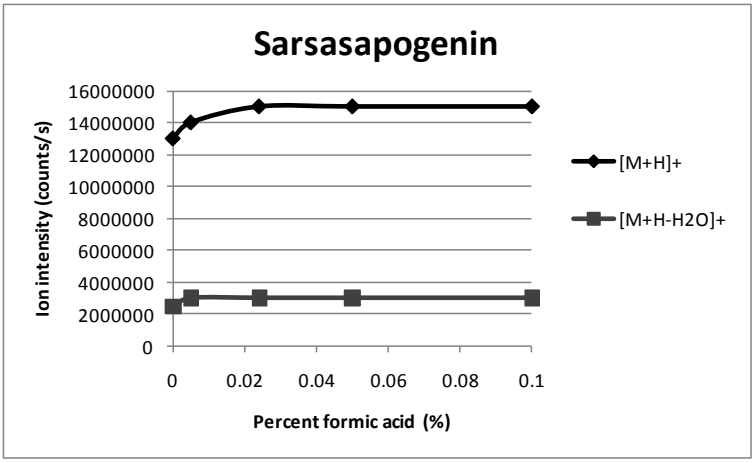

Figure 3.24. Effect of formic acid concentration upon APCI response of sarsasapogenin

3.3.2.2 Diosgenin

APCI data was collected via direct infusion methods using 1:1 ACN:H_2O as the eluent at a flow rate of 200 µLmin^{-1} Irrespective of the buffer used diosgenin exhibited an appreciable $[M+H-H_2O]^+$ ion in addition to the desired $[M+H]^+$ ion. As noted in Section 3.2.5.2 this characteristic can be attributed to the tendency of diosgenin to afford a conjugated 3,5-diene via either acid facilitated or thermally induced loss of water.

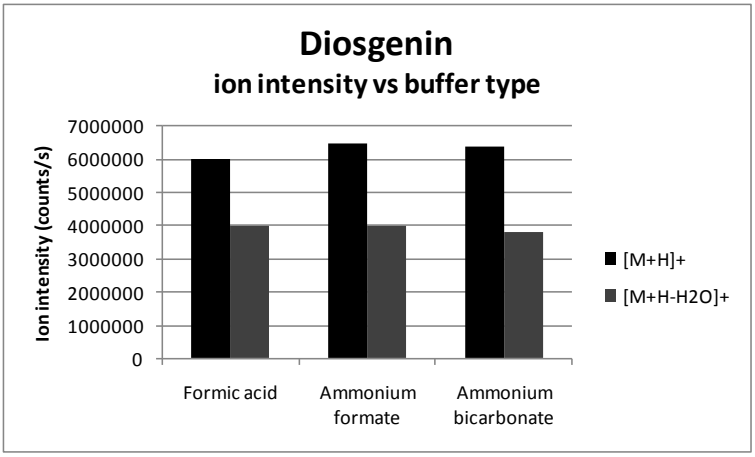

Figure 3.25. APCI responses for diosgenin in three ionisation agents

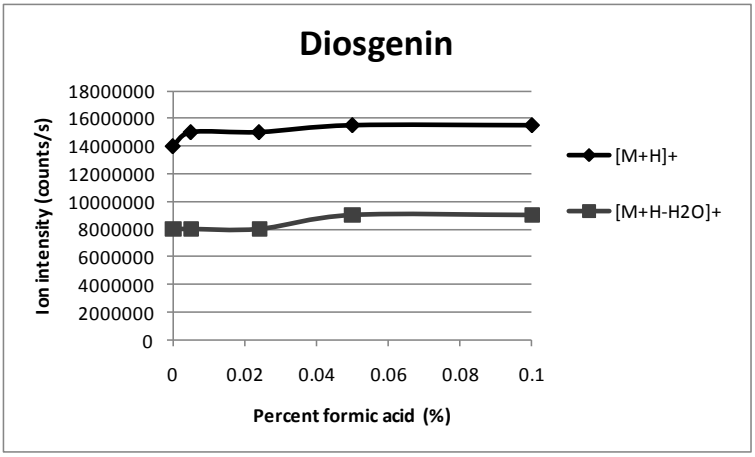

Figure 3.26. Effect of formic acid concentration upon APCI response of diosgenin

3.3.2.3 Sarsasapogenin-β-D-glucoside

Under the chosen APCI conditions sarsasapogenin-β-D-glucoside showed appreciable loss of dehydrated glucose, irrespective of the buffer used (Figure 3.27). Generally similar total ion currents were observed when the percent of formic acid was varied. Some minor variations in the relative contributions of the $[M+H]^+$, $[M+H\text{-}glu]^+$ and $[M+H\text{-}glu\text{-}H_2O]^+$ ions were noted as the concentration of formic acid was varied (Figure 3.28). It was uncertain if these minor variations observed were as a result of a trend or inconsistent ionisation currents.

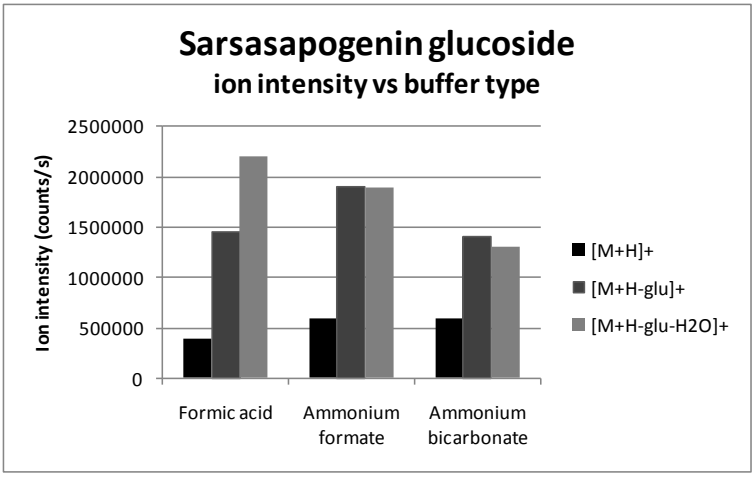

Figure 3.27. APCI responses for sarsasapogenin-β-D-glucoside in three ionisation agents

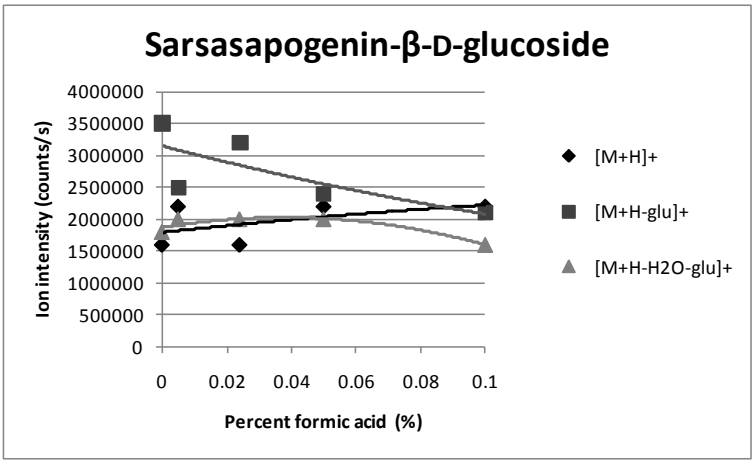

Figure 3.28. Effect of formic acid concentration upon APCI response of sarsasapogenin-β-D-glucoside

3.3.3 Eluent Composition (APCI)

Eluent composition was varied from 0:100 ACN-H_2O to 100:0 ACN- H_2O as model compounds were directly infused into the eluent stream just prior to the APCI source. ACN-H_2O eluent containing 0.01% formic acid was used at a flow rate of 200 $\mu Lmin^{-1}$ while 0.01 $molL^{-1}$ while sarsasapogenin was infused into the eluent via a syringe pump.

3.3.3.1 Sarsasapogenin

The highest $[M+H]^+$ ion current was observed for sarsasapogenin when the eluent contained 60% ACN (Figure 3.29). This finding parallels that observed using the ESI source (Section 3.2.4.1), namely the highest ion current is observed when the eluent contains an appreciable percent of water.

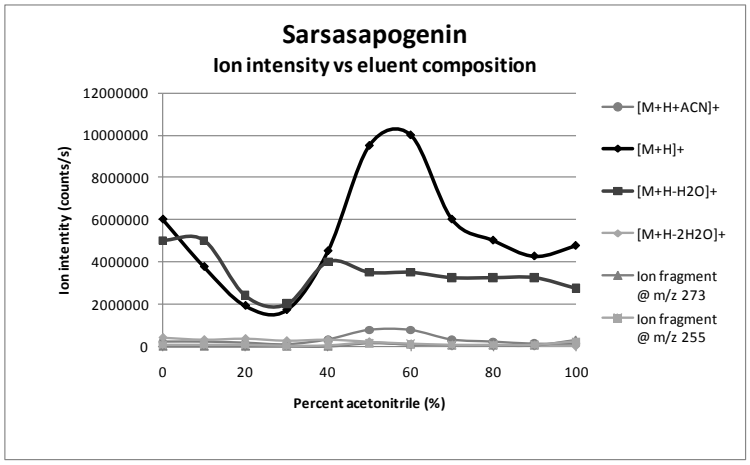

Figure 3.29. Effect of eluent composition of upon the APCI response of sarsasapogenin

As noted in Section 3.2.4.1, various options of manipulating the eluent composition exist such that sarsasapogenin can be eluted at an eluent composition that is beneficial to its ionisation. Options for increasing ionisation include changing the chromatographic column to one that causes the target compounds to elute in an eluent composition which is beneficial to their ionisation, or post column addition of water to the eluent flow. For post column infusion of water the consequential increase in ion intensity should be much greater than the decrease due to dilution.

3.3.4 Interface Temperatures (APCI)

The influence capillary temperature and source heater temperature exerts upon ionisation of the model compounds were investigated by directly infusing the model compounds into the eluent flow just prior to the APCI interface. Full scan mass spectra were acquired when capillary and source temperatures had equilibrated at chosen temperatures. Source and capillary temperatures were

adjusted between 150-400°C in 50°C increments. Source heater and capillary temperatures dependent ion currents are depicted below in three dimensional plots. In all cases data was collected under eluent conditions of 200 µLmin^{-1} of 1:1 ACN-H_2O containing 0.01% formic acid as an ionisation agent.

3.3.4.1 Sarsasapogenin

Maximum ionisation of sarsasapogenin occurred with a source heater temperature around 150°C and capillary temperature in the vicinity of 300-350°C (Figure 3.30)

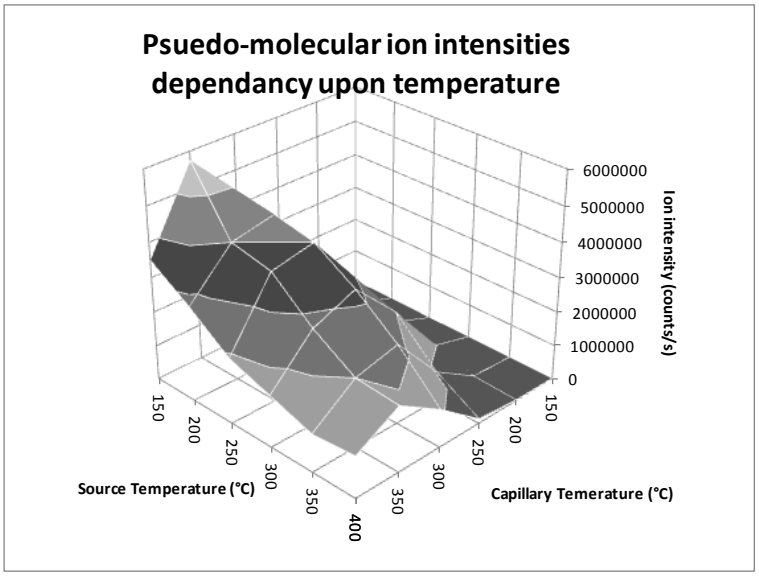

Figure 3.30. The effect source heater and capillary temperatures upon the APCI response of sarsasapogenin

The capillary tube is shared by APCI and ESI interfaces and in both cases gave optimal pseudo-molecular ion signal intensity at capillary temperatures of ~300°C for sarsasapogenin.

3.3.4.2 Diosgenin

Maximum ionisation of diosgenin occurred with a source heater temperature around 150-200°C and capillary temperature in the vicinity of 200-350°C (Figure 3.31). Acceptable ionisation currents for diosgenin were observed over a greater

range of capillary temperatures (200-350°C) than the case for sarsasapogenin (300-350°C).

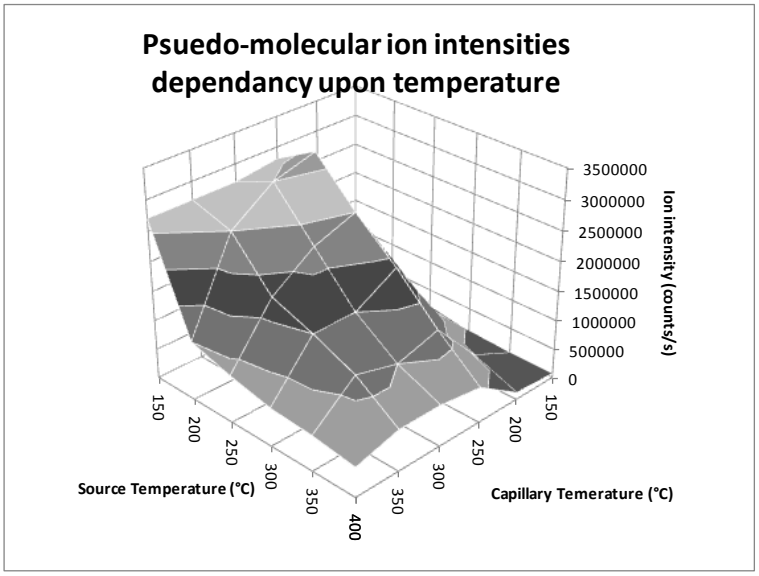

Figure 3.31. Effect of source heater and capillary temperatures upon the APCI response of diosgenin

3.3.4.3 Sarsasapogenin-β-D-glucoside

Maximum ionisation of sarsasapogenin-β-D-glucoside occurred with a source temperature in the range 200-300°C and capillary temperature in the vicinity of 250°C (Figure 3.32).

The source heater temperatures required to achieve maximum sensitivity of sarsasapogenin-β-D-glucoside were higher than those observed for either of the sapogenins investigated. This can be attributed to the lack of volatility that is associated with the glycoside functionality of the saponins.

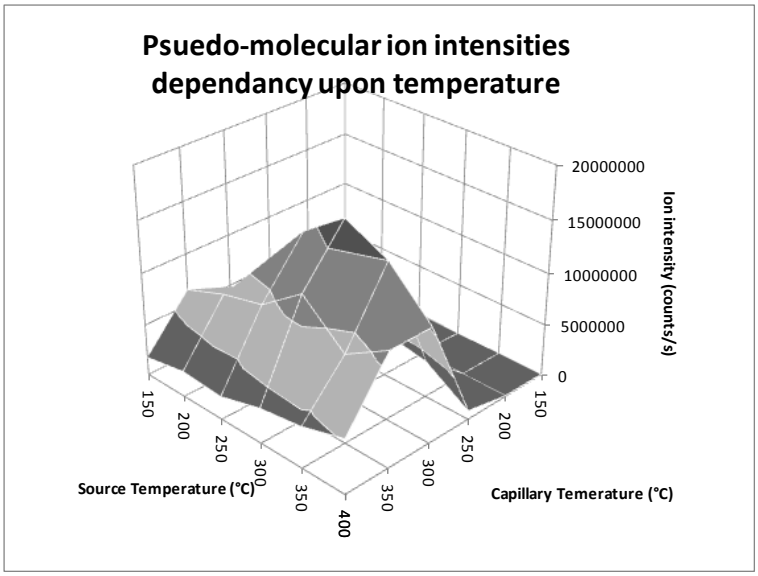

Figure 3.32. Effect of source heater and capillary temperatures upon the APCI response of sarsasapogenin-β-D-glucoside

3.3.5 Effect of Eluent Flow Rate upon APCI

APCI interfaces are reported to show a correlation between the quantity of the analyte being sprayed through the interface and the ion intensity observed at the detector. This correlation implies the ion intensity observed will not vary significantly as the flow rate of the eluent is varied.

Contrary to this expectation both sarsasapogenin and its glucoside showed essentially linear down trends in their $[M+H]^+$ peak area ion responses as the flow rate was decreased (Figures 3.33 and 3.34).

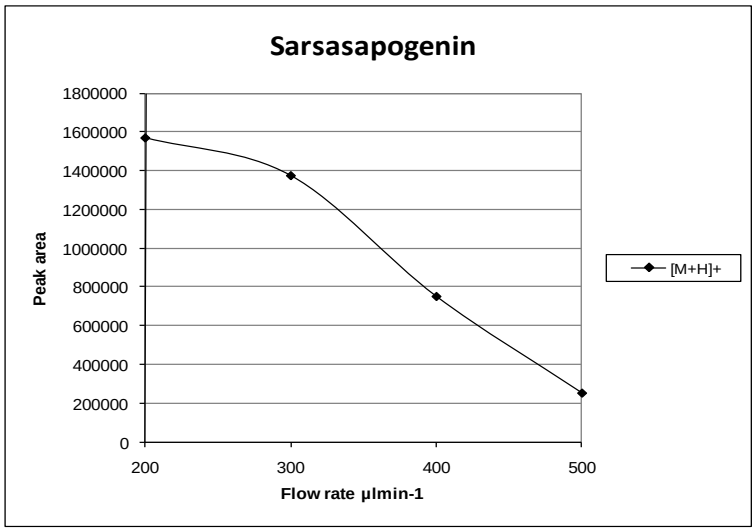

Figure 3.33. Effect of flow rate of upon the APCI response of sarsasapogenin

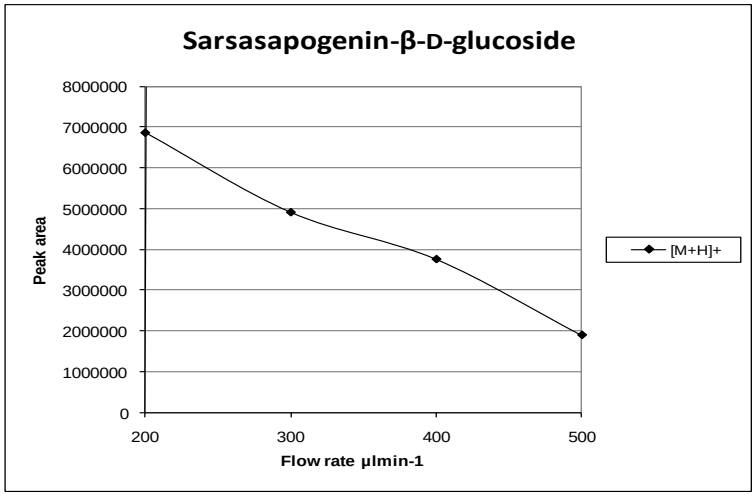

Figure 3.34. Effect of flow rate upon APCI response of sarsasapogenin-β-D-glucoside

4 LC-MS^n Characteristics of Saponins and Sapogenins

An objective of the investigation reported in this chapter was the identification of ESI and APCI mass spectral characteristics, including MS^2, and MS^3 parameters, that can be applied for the identification of sapogenins, and conjugated analogues of these compounds which have an association with hepatogenous photo-sensitisation diseases of livestock. Ideally, identified parameters should contribute to the unequivocal identification of the structures of free and conjugated analogues of sapogenins including analogues which have not hitherto been reported in the literature.

To achieve unequivocal identification of analytes the parameters LC-MS^n utilises for identification including; retention characteristics, MS^n fragmentation pathways and required collision energies must be investigated. Specifically knowledge of MS^n fragmentation pattern and appropriate collision energies for an analyte are required prior to the implementation of targeted SRM methods utilising either an ion trap MS^n system, or a triple quad mass spectrometer. LC-MS^n utilises retention time (chromatographic) data as well as mass spectrometric data for the identification of analytes. By chromatographically separating compounds that exhibit similar mass spectral characteristics it is possible to achieve unequivocal identification of an individual compound.

GC-MS methods have been used to characterise sapogenins recovered from rumen and other GI samples recovered from livestock exhibiting hepatogenous photo-sensitisation disease symptoms. GC-MS techniques can be used to distinguish the various isomers of sapogenins based on knowledge of the relative intensity of selected fragment ions and retention data[16, 26]. These techniques cannot be applied to identification of non-volatile conjugated analogues which must be hydrolysed to the parent sapogenin prior to GC-MS analyses.

Since LC-MS analyses are not subject to the requirement requiring hydrolysis of the glycoside entity, it was anticipated that it might be possible to define the

general structures, if not specific isomeric structural forms, of conjugated analogues present rumen and other GI tract samples.

Once the fragmentation pathways have been mapped variations in MS^n fragmentation characteristics were evaluated in the expectation that, as in GC-MS analyses, subtle variations in fragment characteristics and ion intensity ratio may serve to distinguish isomeric forms of specific compounds. When selecting possible distinguishing ions for use in SRM methods consideration needs to be given to their the relative intensity under chosen ESI or APCI conditions since the selection of low intensity ions will result in reduced detection limits.

4.1 Mass Spectral Identification

For differentiation based upon MS^n fragmentation, major fragmentation ions that were suitable for SRM analysis were elucidated by mapping the mass fragmentation pathways of selected compounds, including, sarsasapogenin, diosgenin, episarsasapogenin, smilagenin, tigogenin, and the saponins, sarsasapogenin-β-D-glucoside, and sarsasapogenin-β-D-galactoside. Fragmentation was mapped for both ESI and APCI inlets, with secondary and tertiary fragmentation occurring in the ion trap mass spectrometer (Section 4.4).

Some deuterated analogues of the sarsasapogenin and episarsasapogenin that had been synthesised during previous research were also utilised in the MS^n fragmentation investigations. One such sample was believed to be 20,23,23-$^2H_3$-sarsasapogenin while another was believed to be a mixture of 2,2,4,4-$^2H_4$-episarsasapogenin and 2,2,4,4-$^2H_4$-sarsasapogenin mixture. It was not however apparent from the information recorded on the historic sample vials if the deuterium atoms that were originally introduced at the 20- and 23-positions, or 2- and 4- positions respectively, were still present in the historic specimens.

A particular concern was that loss of one or more of the deuterium atoms at the 20- and 23-positions may have occurred post synthesis, given the well established tendency of at least the 20,23,23-$^2H_3$ deuterium atoms to back exchange with

water or exchangeable protons in solvents such as methanol[52]. The integrity of the historic deuterated samples was therefore established by ^{1}H and ^{13}C NMR analyses prior to the use of these samples in the LC-MS investigations.

4.2 Confirmation of the Model Compound Integrity by NMR

^{1}H and ^{13}C NMR assignments established for the dominant components of the deuterated samples deuterated samples are presented in Table 4.1. This data showed the 20,23,23-$^{2}H_3$-sarsasapogenin specimen to be a *ca* 19:1 mixture of 20,23,23-$^{2}H_3$-sarsasapogenin (25*S*) and 20,23,23-$^{2}H_3$-smilagenin (25*R*) based upon the relative intensities (integration) of the H-26 proton signals. It was also determined via the reduced intensities of the C-20 and C-23 signals that the 20,23,23-$^{2}H_3$-sarsasapogenin sample had retained greater than 95% of the three 20,23,23-deuterium atoms.

The NMR data also showed that the $^{2}H_4$-sararsapogenin sample was in fact a *ca* 4:1 mixture of 2,2,4,4-$^{2}H_4$ episarsasapogenin and 2,2,4,4-$^{2}H_4$ sarsasapogenin, as determined via integration of the respective H-3 proton signals. Low levels ($\leq$ 5%) of some other unidentified sapogenin analogues were detected in each of the samples.

The ^{1}H and ^{13}C NMR shifts determined for the commercial specimens of sarsasapogenin and episarsasapogenin used in the LC-MS investigations (Table 4.1) corresponded closely to those reported elsewhere for these compounds [52-54]. The commercial sarsasapogenin sample was found to consist of *ca* 95% sarsasapogenin and *ca* 5% smilagenin, based upon the relative intensities of the H-26 proton signals.

Table 4.1. ^{1}H and ^{13}C NMR chemical shifts (δ ppm in $CDCl_3$) determined for some sapogenins

	Sarsasapogenin		20,23,23-$^{2}H_3$-Sarsasapogenin		Episarsasapogenin		2,2,4,4-$^{2}H_4$-Episarsasapogenin	
Carbon	^{13}C	^{1}H	^{13}C	^{1}H	^{13}C	^{1}H	^{13}C	^{1}H
C_1	30.0	1.39, 1.50	30.0	1.41, 1.50	35.4	0.94, 1.77	35.2	0.95, 1.78
C_2	27.8	1.45, 1.60	27.9	1.42, 1.47	30.5	1.30, 1.65	**	**
C_3	67.1	4.10	67.1	4.11	71.7	3.60	71.6	3.62
C_4	33.6	1.32, 1.97	33.6	1.32, 1.98	36.5	1.50, 1.75	**	**
C_5	36.6	1.72	36.6	1.73	42.1	1.38	41.9	1.38
C_6	26.6	1.16, 1.90	26.6	1.14, 1.91	26.7	1.09, 1.43	27.1	1.27, 1.89
C_7	26.6	1.07, 1.40	26.6	1.04, 1.39	27.1	1.24, 1.85	26.6	1.32, 1.45
C_8	35.3	1.59	35.2	1.80	35.5	1.56	35.5	1.59
C_9	39.9	1.32	39.9	1.32	40.6	1.40	40.6	1.42
C_{10}	35.3	*	35.2	*	34.7	*	34.7	*
C_{11}	20.9	1.30,1.38	20.9	1.25, 1.39	20.6	1.24, 1.38	20.6	1.25, 1.38
C_{12}	40.3	1.15, 1.71	40.4	1.15, 1.72	40.3	1.14, 1.71	40.3	
C_{13}	40.7	*	40.7	*	40.7	*	40.7	*
C_{14}	56.5	1.16	56.5	1.17	56.4	1.14	56.4	1.16
C_{15}	31.8	1.23, 1.94	31.8	1.23, 1.98	31.8	1.23, 1.97	31.8	1.21, 1.99
C_{16}	81.0	4.40	81.1	4.40	81.0	4.39	81.0	4.40
C_{17}	62.1	1.76	62.0	1.77	62.1	1.75	62.0	1.75
C_{18}	16.5	0.76	16.5	0.76	16.5	0.74	16.5	0.77
C_{19}	23.9	0.97	24.0	0.98	23.4	0.92	23.4	0.94
C_{20}	42.2	1.81	42.1	**	42.1	1.79	42.1	1.82
C_{21}	14.4	0.99	14.2	0.98	14.3	0.97	14.4	0.99
C_{22}	109.8	*	109.7	*	109.7	*	109.8	*
C_{23}	26.0	1.39, 1.87	25.7	**	26.0	1.38, 1.86	26.0	1.40, 1.85
C_{24}	25.8	1.39, 2.02	25.6	1.39, 2.01	25.8	1.38, 2.02	25.8	1.40, 2.04
C_{25}	27.1	1.69	27.1	1.68	27.1	1.67	27.1	1.71
C_{26}	65.2	3.3, 3.96	65.2	3.29, 3.95	65.1	3.28, 3.73	65.1	3.35, 3.95
C_{27}	16.1	1.07	16.1	1.08	16.1	1.07	16.1	1.07

4.3 Confirmation of Model Compound Integrity by GC-MS

EI-GC-MS also confirmed the presence of 3 deuteriums in the ring E/F fragment ions of 20,23,23-$^{2}H_3$-sarsasapogenin which occurred at *m/z* 141 and 142 compared to *m/z* 139 in sarsasapogenin (Figure 4.1). Similarly the presence of four deuterium atoms in the ring A portion of 2,2,4,4-$^{2}H_4$-episarsasapogenin and 2,2,4,4-$^{2}H_4$-sarsasapogenin was consistent with the occurrence of fragment ions at *m/z* 259, 277 and 306, compared to *m/z* 255, 273 and 302 in EI-MS of sarsasapogenin and episarsasapogenin (Figure 4.2).

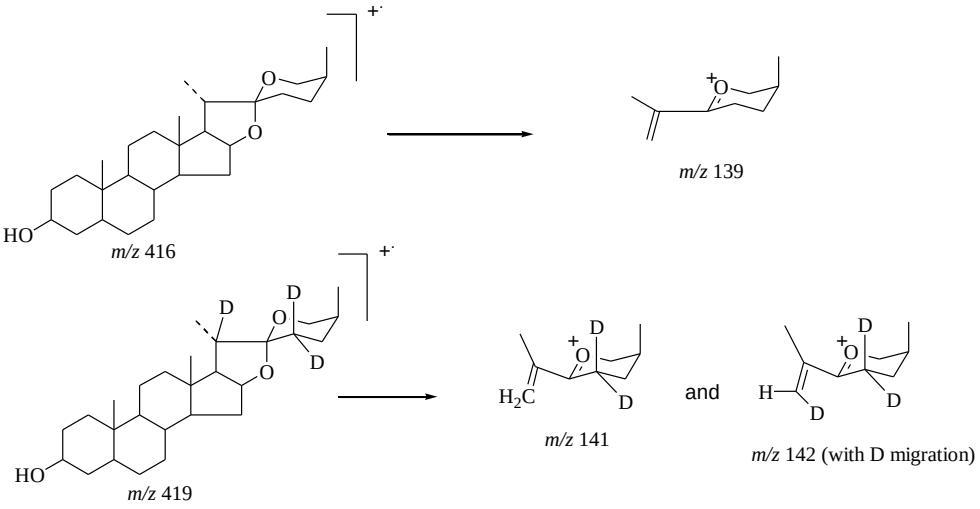

Figure 4.1. Plausible structures for the *m/z* 139 ion and deuterated analogues of these ions observed in the EI-MS of sarsasapogenin

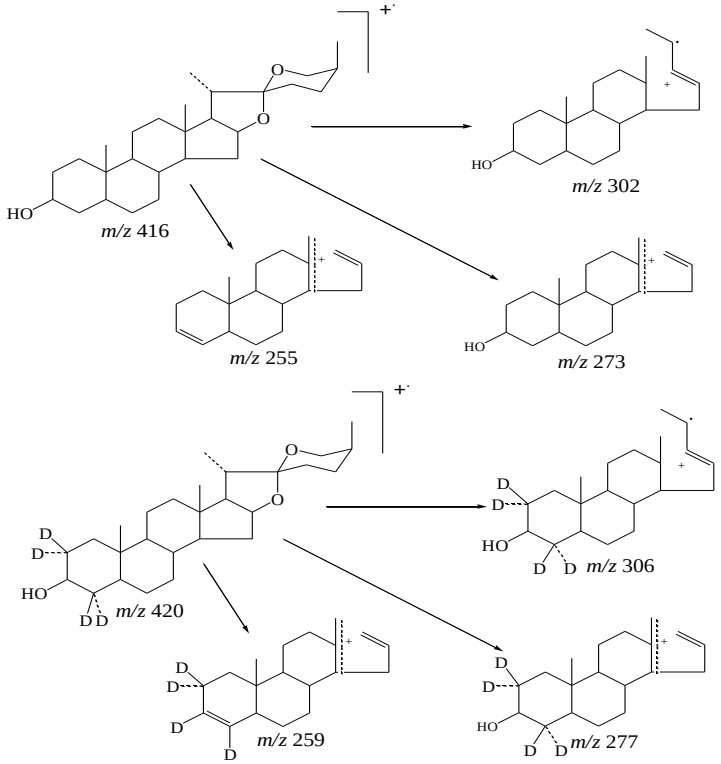

Figure 4.2. Plausible structures for the *m/z* 302, 273 and 255 ions, and deuterated analogues of these ions observed in the EI-MS of sarsasapogenin

4.4 MS^n Fragmentation of the Model Compounds

By comparing the spectra of sarsasapogenin and episarsasapogenin with the available deuterated analogues, 20,23,23-$^2H_3$-sarsasapogenin and 2,2,4,4-$^2H_4$-episarsasapogenin/2,2,4,4-$^2H_4$-sarsasapogenin (80:20), the region of the parent

compound that ion fragments originated from could be elucidated based upon the observation of a mass increase or no mass increase for the fragment ions of the deuterated analogues. An attempt was made to propose structures of the major fragment ions which are consistent with the data observed (Sections 4.4.4 and 4.4.11).

The effect collision energy in the ion trap had upon the fragmentation of various sapogenins was investigated prior to obtaining the mass spectral fragmentation pathways. It was found using collision energies of approximately 30% gave complete fragmentation of the parent ion in the ion trap without causing excessive fragmentation.

To improve the ease of following the fragmentation processes, a convention has been adopted where by ions originating in the full scan mass spectrum are indicated in bold in the description of the fragmentation processes.

4.4.1 Fragmentation of Sarsasapogenin (ESI)

The fragmentation of sarsasapogenin was investigated by direct infusion of 0.001 $molL^{-1}$ solution of sarsasapogenin solution into the eluent flow via a syringe pump. The following ionisation conditions were used: capillary temperature of 250°C, 1:1 ACN-H_2O eluent containing 0.01% formic acid as an ionisation buffer/aid was eluted at a flow rate of 200 $\mu Lmin^{-1}$.

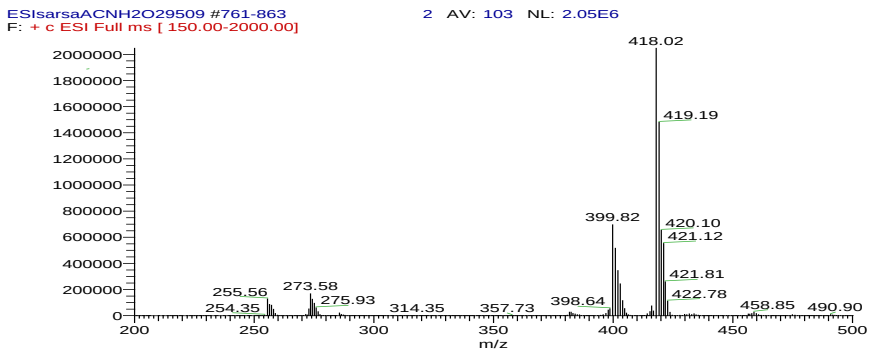

Figure 4.3. Full scan ESI mass spectrum of sarsasapogenin

The full scan mass spectrum of sarsasapogenin showed ions at *m/z* **458** (weak), **417**, **399**, **381** (weak), **273**, and **255**. No high mass $[M_2+H]^+$or $[M_3+H]^+$ cluster

ions were observed. Secondary fragmentation of ions seen in the full scan MS were investigated using a collision energy of 30% to determine MS^2 and MS^3 spectra.

The weak *m/z* **458** ion is attributed to the mono solvated $[M+ACN+H]^+$ pseudo-molecular ion. The intensity of this ion was too low to permit its MS^2 spectrum to be determined.

The *m/z* **417** ion is attributable to the $[M+H]^+$ pseudo-molecular ion of sarsasapogenin. MS^2 fragmentation of this ion afforded *m/z* 399, 381, 273, and 255 ions. The *m/z* 399 ion can be attributed to the loss of water (dehydration) from the pseudo-molecular ion. MS^3 (*m/z* **417** → *m/z* **399**) fragmentation of this ion predominantly afforded an afforded *m/z* 273 ion and to a lesser extent an *m/z* 381 ion. MS^3 (*m/z* **417** → *m/z* 273) fragmentation of the *m/z* 273 ion afforded an *m/z* 255 ion as a result of the loss of water (dehydration) and low intensities fragment ions at *m/z* 227, 213, 199, 173, 159, 147, 145, 133 and 121. MS^3 (*m/z* **417** → *m/z* 255) fragmentation of the *m/z* 255 ion also afforded *m/z* 227, 213, 199, 173, 159, 147, 145, 133 and 121 fragment ions.

MS^2 fragmentation of the *m/z* **399** observed in the full scan MS of sarsasapogenin afforded ions at *m/z* 381, 285, and 255. MS^2 fragmentation of the *m/z* **381** ion observed in the full scan MS of sarsasapogenin predominantly fragmented to afford an *m/z* 255 ion together with a low intensity *m/z* 363 ion.

MS^2 fragmentation of the *m/z* **273** ion observed in the full scan MS of sarsasapogenin predominantly fragmented to afford an *m/z* 255 ion together with lower intensity *m/z* 199 and 159 ions. The loss of 18 amu from *m/z* 273 →*m/z* 255 can be attributed to dehydration (water loss) occurring. The MS^3 (*m/z* **273** → *m/z* 255) afforded *m/z* 227, 213, 199, 173, 159, 147, 145, 133, and 121 ions analogous to those observed via the MS^3 (*m/z* **417** → *m/z* 273) pathway.

The fragmentation pathways observed for sarsasapogenin using an ESI inlet coupled to an advantage LCQ (ion trap) mass spectrometer are summarised in Figure 4.4.

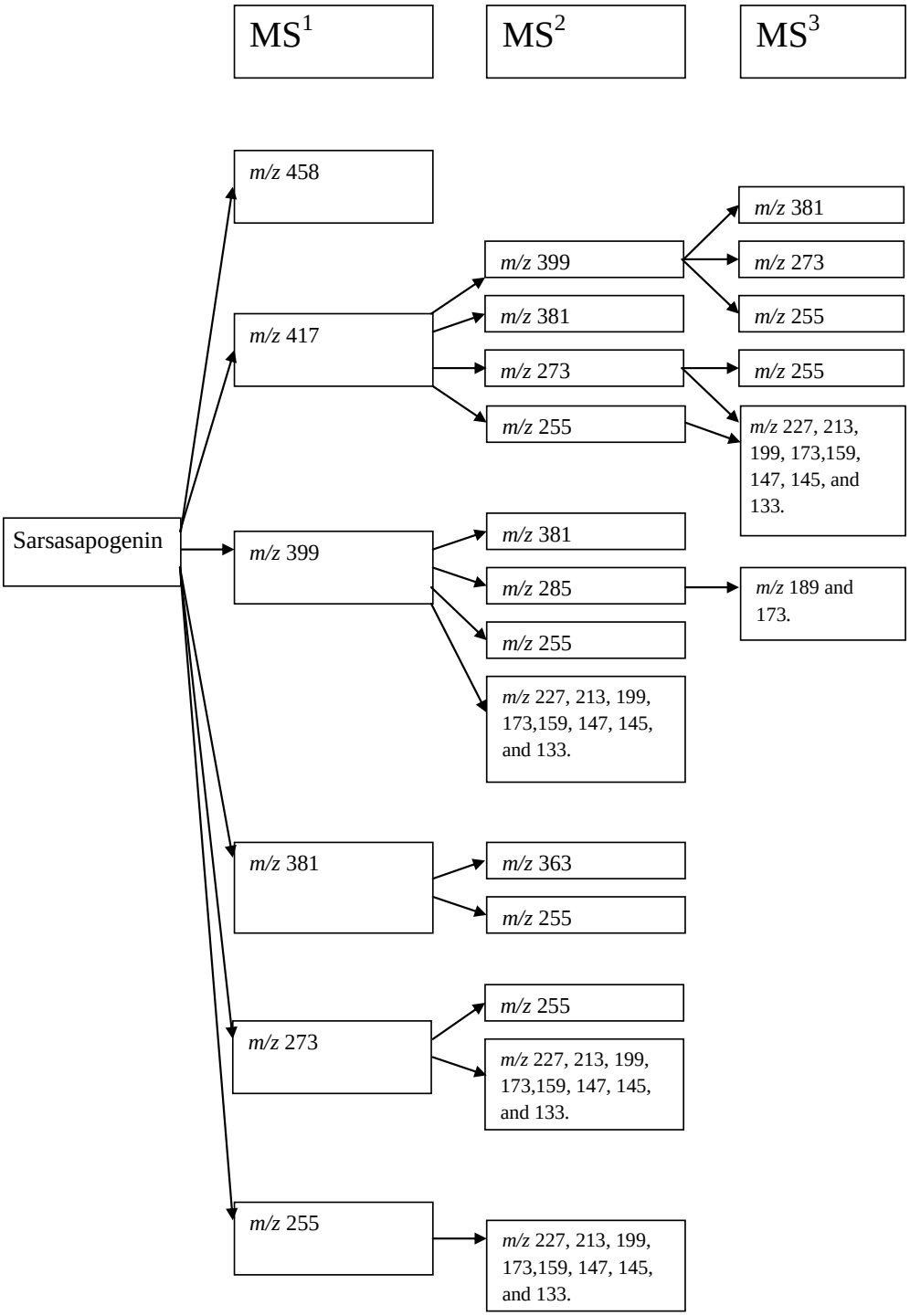

Figure 4.4. ESI Fragmentation tree for sarsasapogenin

4.4.2 Fragmentation of 2,2,4,4-$^{2}H_4$-episarsasapogenin (ESI)

The MS^n fragmentation of an 80:20 mixture of 2,2,4,4-$^{2}H_4$-episarsasapogenin and 2,2,4,4-$^{2}H_4$-sarsasapogenin was determined using the direct infusion conditions described above for sarsasapogenin.

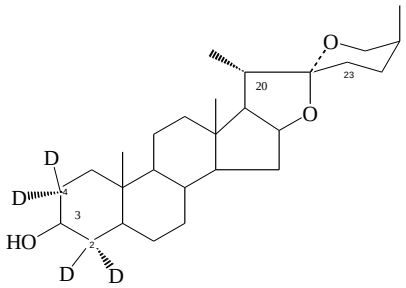

Figure 4.5. Structure of 2,2,4,4-$^{2}H^{4}$-episarsasapogenin

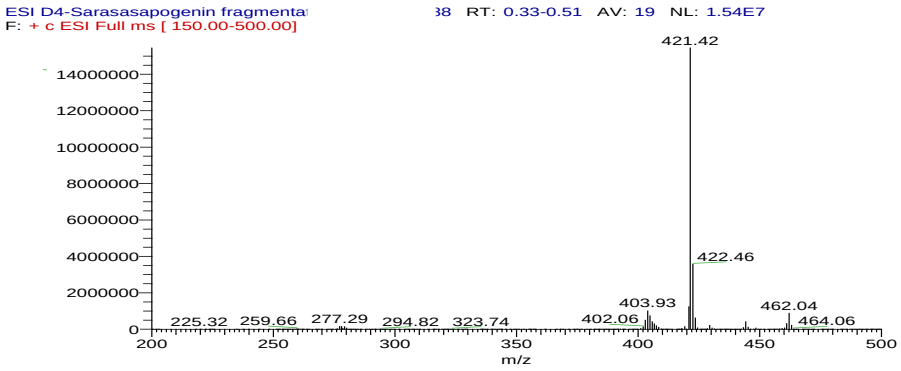

Figure 4.6. Full mass spectrum of 2,2,4,4-$^{2}H_4$-episarsasapogenin

The full scan MS of the 80:20 mixture of 2,2,4,4-$^{2}H_4$-episarsasapogenin and 2,2,4,4-$^{2}H_4$-episarsasapogenin, recorded in direct infusion mode, showed a strong *m/z* **421** ion and lower intensity **422**, **404**, **403**, **385**, **289**, **278**, **277** and **259** ions.

A complicating factor, often encountered with ion trap MS systems is that when high concentrations of ions are present in the trap, space charging effects arising from mutual charge repulsion effects between ions become significant. This results in the need for higher than expected potential (voltage) is required to expel the entire population of target ion from the trap. Thus a $[M+H]^+$ ion which, at low concentration, appears (say) at *m/z* 421.5, will occur at progressively higher and higher nominal mass (eg *m/z* 421.7, 421.9, 422.1, etc) as the concentration of ions in the trap is increased. Notwithstanding this issue MS^2, MS^3, MS^n spectra of an

ion that was initially subject to a modest space charging effect affords the correct nominally masses for it daughter ions since only a low level of ions are retained in the trap during MS^n steps and space charging effects are not significant.

The apparent presence of an *m/z* 421.42 ion in the full scan MS of 2,2,4,4-$^2H_4$-episarsasapogenin presented in Figure 4.6, as opposed to an expected *m/z* 421 ion, can be attributed to the high concentration of ions present in the trap when the direct infusion full scan MS spectrum was recorded. Quadrupole EI-MS spectra are not prone to space charging effects, since this type of MS system generates ions on the fly and does not trap a high concentration of ions in its source area. The correct $[M+H]^+$ ion mass (*m/z* 420) was observed for the 2,2,4,4-$^2H_4$-episarsasapogenin sample when it was examined using EI-GC-MS.

Since the mass of these ions (excluding isotope ions and ions whose masses appear to have been inflated by space charging effects: see above) are four amu greater than the *m/z* **417**, **381**, **285**, **273**, and **255** ions observed for sarsasapogenin or episarsasapogenin ions it can be reasoned they all contain the ring-A portion of the genin structure.

The *m/z* **421** ion is attributable to the pseudo-molecular $[M+H]^+$ ions of 2,2,4,4-$^2H_4$-episarsasapogenin and 2,2,4,4-$^2H_4$-episarsasapogenin. MS^2 fragmentation of this ion afforded ions at *m/z* 403 (water loss), 385, 277, and 259. MS^3 (*m/z* **421** → *m/z* 277) fragmentation afforded to an *m/z* 259 ion attributable to the loss of a water molecule. The *m/z* **403** ion observed in the full scan MS spectrum fragmented under MS^2 conditions to afford *m/z* 385, 367, 329, 289, 259, and 221 ions while the *m/z* **277** ion observed in the full scan MS spectrum fragmented to predominantly afford *m/z* 259 ions. MS^3 (*m/z* **277** → *m/z* 259) fragmentation afforded ions at *m/z* 231, 203, 174, 173, 159, and 157 ions.

The *m/z* **259** ion observed in the full scan fragmented to afford *m/z* 231, 217, 203, 189, 187, 173, 163, 159, 147, and 145 ions. The MS^2 (*m/z* **259**) and MS^3 (*m/z* **277** → *m/z* 259) fragmentation patterns of the deuterated *m/z* 259 ion appears to be more complex than that observed corresponding non-deuterated *m/z* 255 ion of sarsasapogenin.

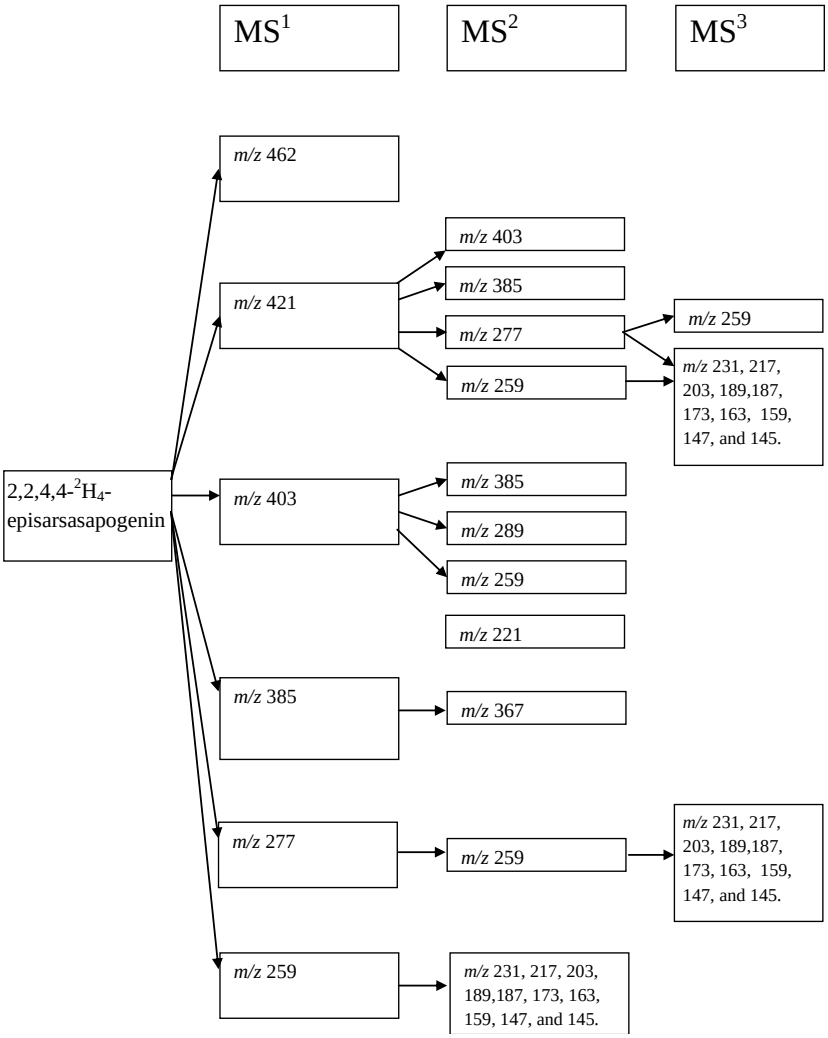

Figure 4.7. ESI fragmentation tree for 2,2,4,4-$^{2}H_4$-episarsasapogenin

4.4.3 Fragmentation of 20,23,23-$^{2}H_3$-sarsasapogenin (ESI)

The fragmentation of 20,23,23-$^{2}H_3$-sarsasapogenin was investigation in direct infusion mode under the same conditions as those described above for sarsasapogenin.

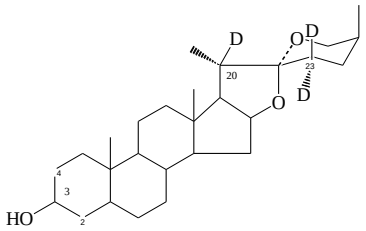

Figure 4.8. Structure of 20,23,23-$^{2}H_3$-sarsasapogenin

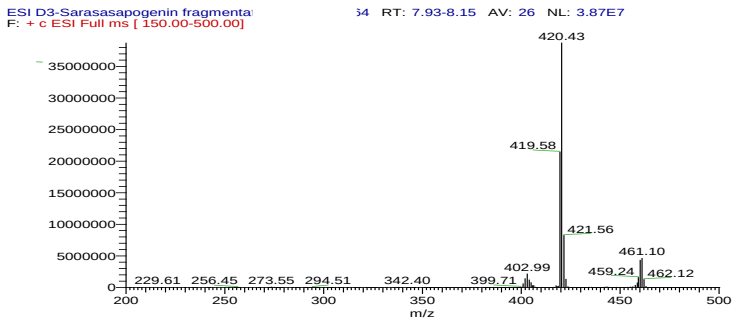

Figure 4.9. Full ESI mass spectrum of 20,23,23-$^{2}H_3$-sarsasapogenin

The full scan mass spectrum was dominated by ion clusters centred at *m/z* **461**, **421** and **403** together with low intensity *m/z* **274**, **273**, and **255 ions**.

The apparent presence of an *m/z* 420.43 ion in the full scan MS of 20,23,23-$^{2}H_3$-sarsasapogenin presented in Figure 4.9, as opposed to an expected *m/z* 420 ion, can be attributed to the high concentration of ions present in the trap when the direct infusion full scan MS spectrum was recorded (space charging). The correct $[M+H]^+$ ion mass (*m/z* 419) was observed for the 20,23,23-$^{2}H_3$-sarsasapogenin sample when it was examined using EI-GC-MS.

MS^2 fragmentation of the space charged *m/z* **418-422** ion cluster predominately afforded an *m/z* 403 ion and a less intense *m/z* 273 ion. MS^2 fragmentation of the *m/z* 273 ion observed in the full scan MS spectrum predominantly an *m/z* 255 ion attributable to water loss. MS^3 (*m/z* **420** → *m/z* 255) fragmentation afforded *m/z*

199, 173, 159, 145, and 131 ions analogous to those observed in the MS^2 (*m/z* **255**) spectrum. The space charged *m/z* **459-461** ion cluster can be attributed to formation of a solvated $[M+ACN+H]^+$ pseudo-molecular ion.

The MS^2 fragmentation of the *m/z* **402** ion cluster to predominately afforded an *m/z* 255 ion together, with lesser intensity ion fragments at *m/z* 384, 383, 382, 285, and 218. MS^2 fragmentation of the *m/z* **273** ion predominantly afforded an *m/z* 255 (water loss) ion. MS^2 fragmentation of the *m/z* **255** ion afforded ions at *m/z* 227, 213, 199, 187, 185, 173, 171, and 159. It is apparent from the MS^n data determined for sarsasapogenin, and its 20,23,23-deuterated analogue, that none of foregoing ions with exception of the *m/z* 402 ion are deuterated, and that they appear to include the ring A/B portion, but not the ring D/F portion of 20,23,23-$^2H_3$-sarsasapogenin. The *m/z* 402 ion was observed to afford an *m/z* 383 ion as a result of the loss of HOD (19 amu).

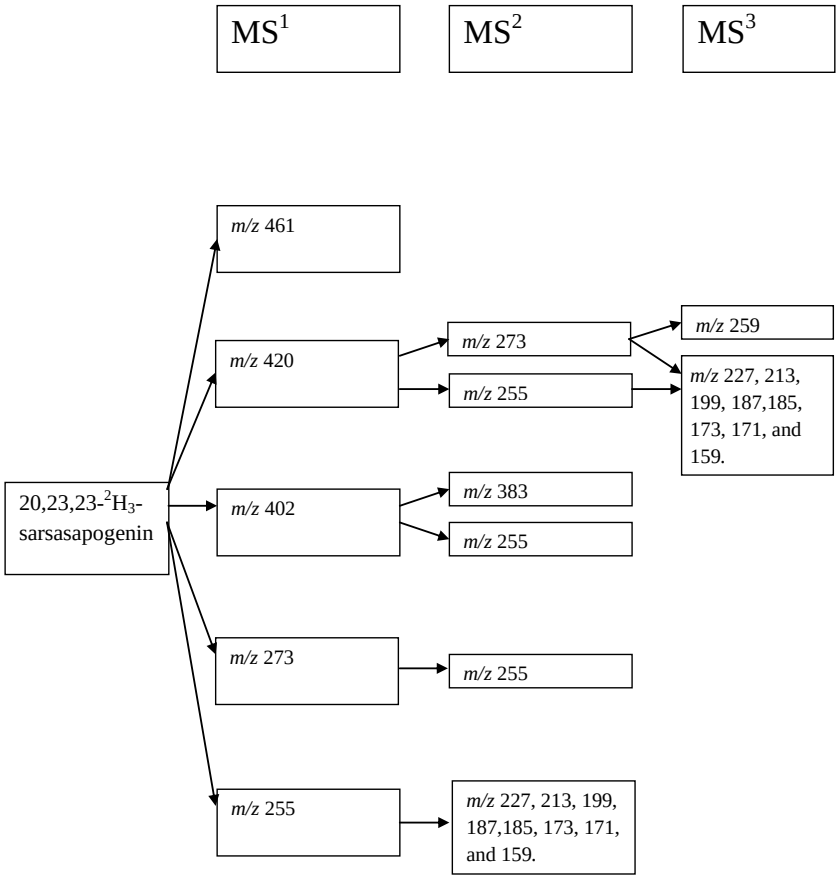

Figure 4.10. ESI fragmentation tree of 20,23,23-$^2H_3$-sarsasapogenin

4.4.4 Plausible Structures for Major ESI Fragment Ions of Sarsasapogenin

Plausible structures for the dominant ions seen in the full scan, MS^2 and MS^3 ESI spectra of sarsasapogenin, 20,23,23-$^2H_3$-sarsasapogenin and 2,2,4,4-$^2H_4$-episarsasapogenin/ 2,2,4,4-$^2H_4$-sarsasapogenin are presented below. For each of these compounds protonation of any of three oxygen atoms would afford the pseudo-molecular ions as illustrated in Figure 4.11 for sarsasapogenin ($[M+H]^+$ at *m/z* **417**). Thereafter loss of a water molecule occurs, either in the ESI interface, or under MS^2 conditions in the ion trap to form an *m/z* 399 ion.

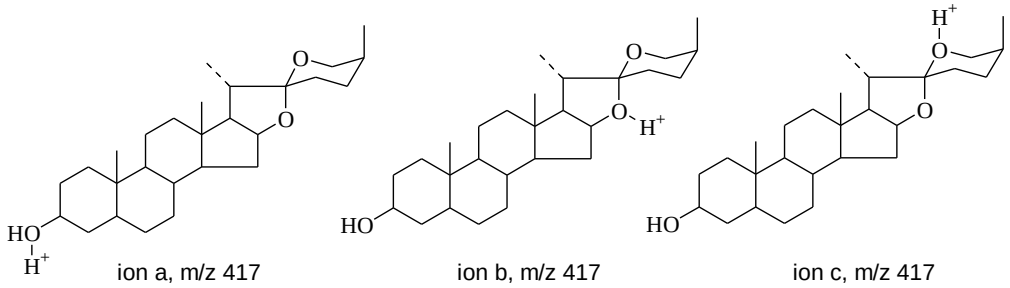

Figure 4.11. Plausible sarsasapogenin pseudo-molecular ion structures

In the ion trap the loss of water was determined, at least in part, to involve the loss of a ring E or F oxygen atom since the dominant fragment in the (*m/z* **417**→ *m/z* 399) MS^3 spectrum was the *m/z* 273 ion. The *m/z* **417**→ *m/z* 399 MS^3 spectrum also included an *m/z* 381 ion, corresponding to the loss of a second water molecule. The proposed *m/z* 273 ion structure (based on that advanced by Blunden et al[26], Figure 4.13) requires the presence of the 3-hydroxyl group.

In contrast to the fragmentation characteristics of the *m/z* 399 ion formed in the ion trap under MS^2 conditions from the full scan *m/z* **417** $[M+H]^+$ ion (Figure 4.11), the full scan *m/z* **399** ion formed in the ESI interface fragmented under MS^2 conditions to afford an *m/z* 255 ion (rather than an *m/z* 273 ion).

Based the foregoing observations it can be inferred that the full scan *m/z* **399** ion formed in the ESI interface arise as a result of dehydration of the C-3 hydroxyl group to form the corresponding 2-ene or 3-ene. (Figure 4.12). The fragmentation process of the plausible structures for major ions observed have been summarised

in Figure 4.13. The proposed formation of the 2-ene or 3-ene analogues upon dehydration at C_3 are consistent with the fragments proposed by Griffiths for the 3-hydroxy-20-keto-steroid oximes[55, 56].

The occurrence of the deuterated variant of the *m/z* 273 and 255 ions observed for sarsasapogenin at *m/z* 277 and *m/z* 259 after water loss in equivalent spectra of 2,2,4,4-$^2H_4$-episarsasapogenin shows (at least in the case of the latter molecule) that none of the C-2 or C-4 deuterium atoms are lost upon dehydration at C-3.

Based upon this observation it can be reasoned for 2,2,4,4- episarsasapogenin, and by implication also sarsasapogenin, dehydration at C-3 procedures either via the loss of the 3-OH group and a more remote proton (eg H-1 or H-5 to afford 1,3- or 3,5-cyclo analogues respectively), or by loss of the 3-OH group and H-3, accompanied by migration of a hydrogen (or deuterium) atom from C-2 to C-3 to afford a 2-ene or from C-4 to C-3 to afford 3-ene structure respectively. Only the latter possibility is depicted in the Figure 4.13. Many plausible structures exist for the various ion fragments observed. For ease of depiction only one option has been shown in the fragmentation sequence proposed for sarsasapogenin.

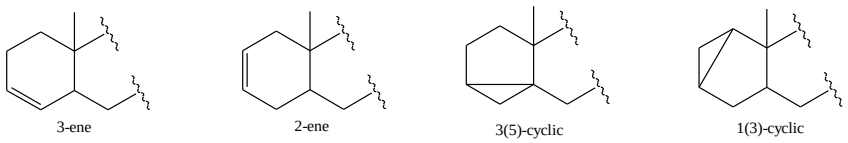

Figure 4.12. Plausible C-3 dehydration structures

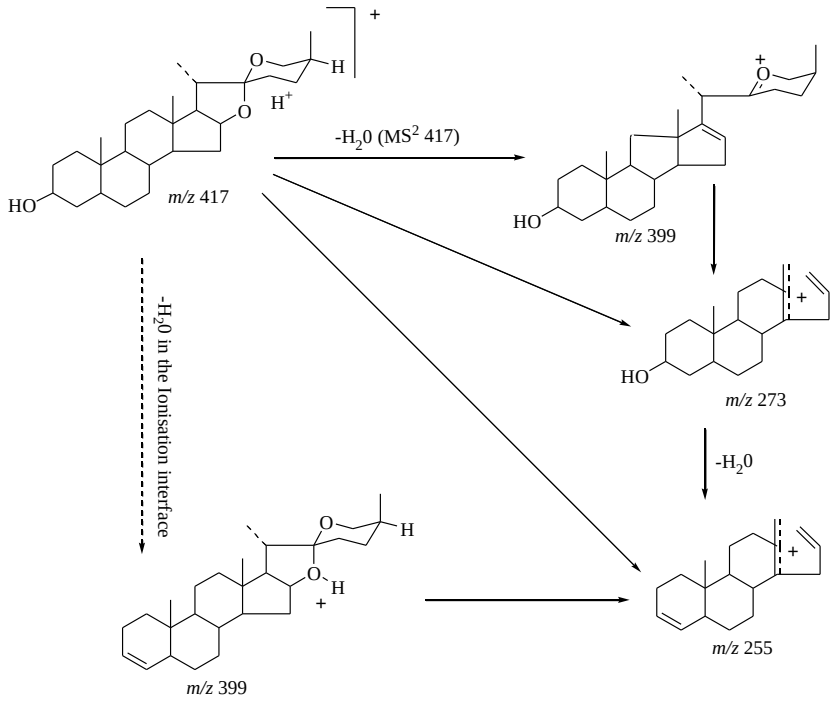

Figure 4.13. Plausible pathways to *m/z* 399, 273 and 255 ions observed for sarsasapogenin

At the MS^2 level the *m/z* **417** → *m/z* 399, *m/z* **417** → 273 or *m/z* **417** → *m/z* 255 ion transitions were the dominant pathways. Provided buffer, ionisation and capillary interface conditions are chosen to optimise the intensity of the *m/z* 417 ion in full scan mode, the foregoing ion transitions are those which would afford the greatest sensitivity in ion trap MS^2 or triple quad SRM analyses.

MS^2 and MS^3 fragmentation data determined for 20,23,23-$^2H_3$ sarsasapogenin and the 80:20 mixture of 2,2,4,4-$^2H_3$- sarsasapogenin and episarsasapogenin (Sections 4.2 and 4.3) were consistent with the structure(s) proposed for the *m/z* 273 ion and its dehydrated *m/z* 255 analogue (Figure 4.13). Specifically the incorporation of four deuterium atoms at the C-2 and C-4 increased the mass to the by four amu so that it occurred at *m/z* 277 and *m/z* 259 respectively, while the incorporation three deuterium atoms at the C-20 and C-23 position did not alter the mass of this ion.

The possibly exists that either or both of these deuterated analogues could be used as internal standards in future SRM based LC-MS^n analysis of sapogenins present in rumen and other extracts. Suitable SRM ion transitions would be *m/z* **417** → *m/z* 399, or *m/z* **417** → *m/z* 273 for natural sapogenins and *m/z* **421** → *m/z* 403 or *m/z* **421** → *m/z* 277 for 2,2,4,4-$^2H_4$-sarsasapogenin or sarsasapogenin as internal

standards. The use 20,23,23-$^{2}H_3$ analogues as internal standards are not considered to be as suitable given the documented tendency of these deuterium atoms to back exchange with hydrogen atoms in aqueous environments[52].

4.4.5 Fragmentation of Sarsasapogenin (APCI)

The APCI MS characteristics of sarsasapogenin were investigated by direct infusion of 0.001 molL^{-1} solution of sarsasapogenin solution into an 1:1 ACN-H_2O eluent flow via a syringe pump. The eluent contained 0.01% formic acid. 30% collision energy was used to obtain MS^2 and MS^3 spectra. The APCI heater and capillary temperature were set to 250° C. Subsequent data showed that these inlet conditions were far from optimal (Section 3.3.4).

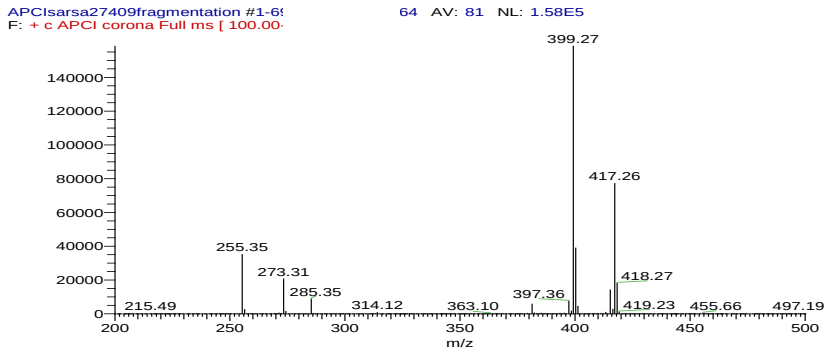

Figure 4.14. Full scan APCI mass spectrum of sarsasapogenin

The full scan APCI mass spectrum showed ions resulting from sarsasapogenin at; *m/z* **417**, **399**, **285**, **273**, and **255**, analogous to ions observed under ESI conditions. Secondary fragmentation of these ions was investigated using MS^2 and MS^3 spectra where ion intensities permitted.

The *m/z* **417** ion is attributed to the pseudo-molecular ion of sarsasapogenin, $[M+H]^+$. Under MS^2 conditions the *m/z* **417** ion fragmented to afford to *m/z* 399 (water loss), 273, and 255 ions. The MS^3 (*m/z* **417** → *m/z* 273) predominantly afforded a *m/z* 255 ion. The MS^2 fragmentation *m/z* 255 ion, which was also observed in the full scan APCI spectrum, afforded *m/z* 213, 199, 173, 159, and 131 ions.

The *m/z* **399** ion is attributed to the mono dehydration product of sarsasapogenin, $[M–H_2O+H]^+$. The MS^2 of the *m/z* **399** ion afforded *m/z* 381, *m/z* 285, and *m/z* 255 ions. The MS^3 fragmentation of the *m/z* **399** →*m/z* 381 ion fragmented predominantly afforded a *m/z* 255 ion and a lesser quantity of a *m/z* 363 (water loss ion). MS^2 fragmentation of the *m/z* **273** ion observed in the full scan APCI spectrum also predominantly afforded an *m/z* 255ion which under MS^3 conditions (*m/z* **273** → *m/z* 255) fragmented to afford ions at *m/z* 199, 173, 159, 147, and 131.

APCI MS^2 and MS^3 fragmentation pathways (Figure 4.8) were generally similar to those observed under ESI conditions (Section 4.4.1).

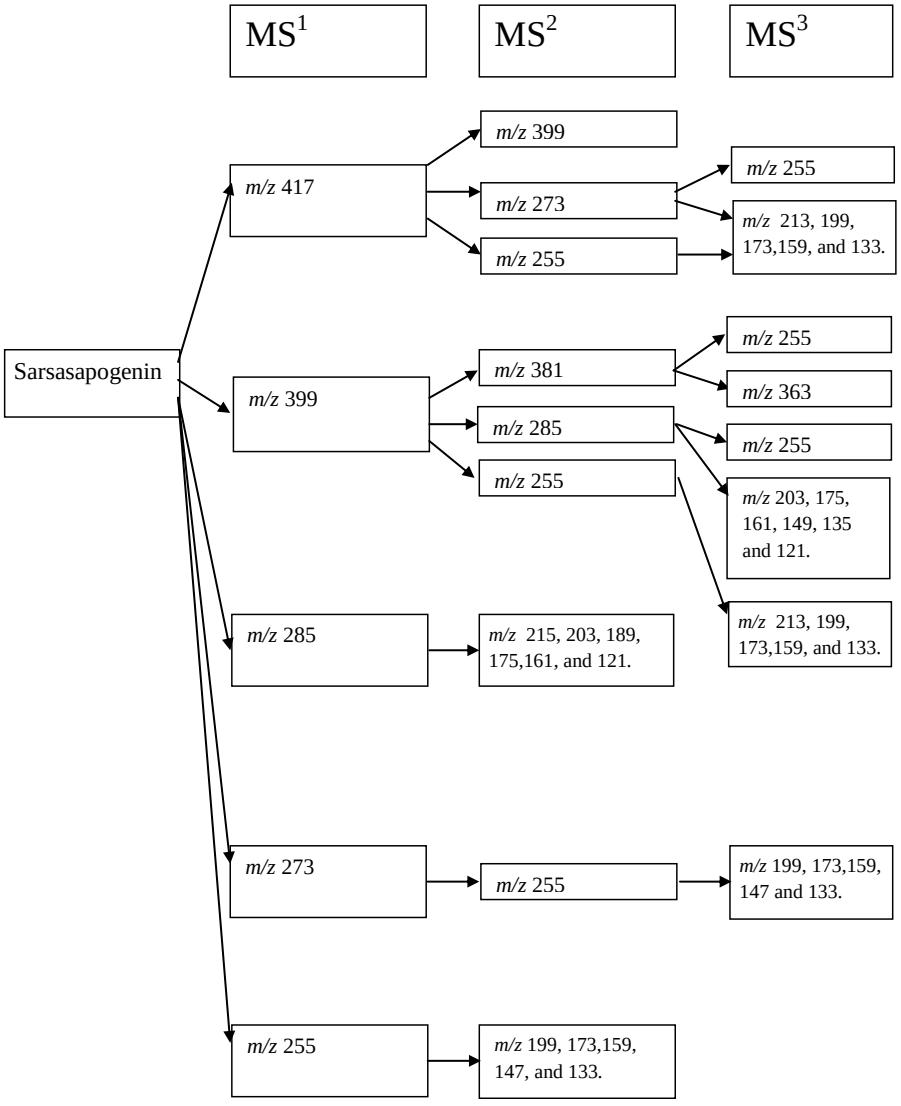

Figure 4.15. APCI fragmentation tree for sarsasapogenin

4.4.6 Fragmentation of 2,2,4,4-$^{2}H_4$-episarsasapogenin (APCI)

Under full scan APCI conditions 2,2,4,4-$^{2}H_4$-episarsasapogenin afforded ions at *m/z* **421**, **403**, **385**, **289**, **277**, and **259**. As all the ion fragments have increased in mass by four amu from the ion fragments seen for sarsasapogenin, it can be reasoned that they included the deuterated ring A portion of molecule.

The *m/z* **421** ion is attributed to the pseudo-molecular ion of 2,2,4,4-$^{2}H_4$-episarsasapogenin, $[M+H]^+$. Under MS^2 conditions the *m/z* **421** ion fragmented to afford *m/z* 403, 277, and 259 ions. These ions are considered to be the deuterated counterparts of the *m/z* 399, 273 and 255 ions observed in both the ESI and APCI spectra of sarsasapogenin (Sections 4.4.1 and 4.4.5).

In general APCI MS^2 and MS^3 fragmentation pathways observed for 2,2,4,4-$^{2}H_4$-episarsasapogenin were similar to those observed under ESI conditions for this compound (Section 4.4.2).

4.4.7 Fragmentation of 20,23,23-$^{2}H_3$-sarsasapogenin (APCI)

The APCI fragmentation of 20,23,23-$^{2}H_3$-sarsasapogenin was investigated under similar conditions to those described for sarsasapogenin and 2,2,4,4-$^{2}H_4$ episarsasapogenin.

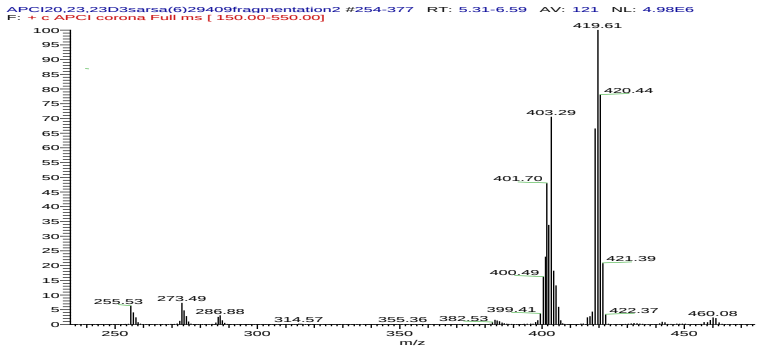

Figure 4.16, Full APCI mass spectrum of 20,23,23-$^{2}H_3$-sarsasapogenin

The full mass spectrum showed ion clusters resulting from 20,23,23-$^{2}H_3$-sarsasapogenin at; *m/z* **459-461**, **420**, **418-421**, **400-403 383-385**, 2**86-287**, **273-275 and 255-257**. Secondary fragmentation of the fragment ions of 20,23,23-$^{2}H_3$-sarsasapogenin was investigated using MS^2 and MS^3 spectra where ion intensities permitted.

The *m/z* **420**, **419**, and **418** ions are attributed to the pseudo-molecular ion of triply, doubly, and singly deuterated sarsasapogenin respectively. This data indicates that some of the deuterium in the 20,23,23-$^{2}H_3$-sarsasapogenin may have been exchanged with protons in the aqueous eluent prior to the sample material entering the mass spectrometer either during passage through the LC column in the presence of water and the formic acid buffer containing eluent, or during the flash vaporisation section of the APCI inlet prior the vaporised material entering the mass spectrometer via its capillary inlet. The ESI inlet does not utilise a flash vaporisation step.

The manner in which the *m/z* **459-461** $[M+ACN+H]^+$, **418-421 [**$M+H]^+$, **400-403** $[M-H_2O+H]^+$ **383-385**, **286-287**, **273-275 and 255-257** ion clusters observed in the full scan MS of 20,23,23-$^{2}H_3$ sarsasapogenin fragmented under MS^2 and subsequently MS^3 conditions were similar to those determined under ESI conditions (Section 4.4.3), taking into the account the apparent loss (back exchange with the protons in the aqueous eluent) during the flash vaporisation stage of the APCI inlet.

4.4.8 Summary of APCI Fragmentation of Sarsasapogenin

By comparing the APCI fragmentation of sarsasapogenin with its deuterated analogues it is possible to assign plausible structures for some of the major ion fragments. Other than an increase in fragmentation in the full mass spectra relative to ESI the fragmentation pathways appeared to be identical to those observed for ESI. Based upon these observations it is proposed the main ion fragments produced for sarsasapogenin using an APCI interface are analogous to those of the ESI interface (Figures 4.11 to 4.13).

4.4.9 Fragmentation of Diosgenin (ESI)

The ESI fragmentation patterns of diosgenin were investigated under similar conditions to those used for the determination of fragmentation patterns for the previous sapogenins.

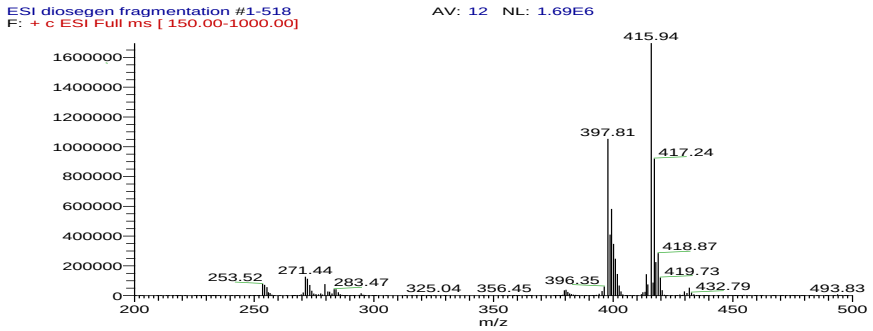

Figure 4.17. Full scan ESI mass spectrum for diosgenin

The mass spectrum showed ions resulting from diosgenin at; *m/z* **431**, **415**, **397**, **379**, **271**, and **253**. Secondary fragmentation of these ions was investigated using MS^2 and MS^3 spectra where ion intensities permitted. Nominal collision energy of 30% was used during obtaining all the MS^2 and MS^3 spectra.

The weak *m/z* **431** ion is probably attributable to $[M+H]^+$ ion of a low level of a hydroxylated analogue of diosgenin, rather than to the formation of $[M+CH_4+H]^+$ or $[M+O+H]^+$ ions.

The *m/z* **415** ion is attributed to the pseudo-molecular ion of diosgenin, $[M+H]^+$. The MS^2 (*m/z* **415**) ion fragmented to ions at *m/z* 397, 379, 283, 271, and 253. The *m/z* **415** → *m/z* 397 is a result of loss of water (dehydration) from the pseudo-molecular ion. The MS^3 (*m/z* **415** → *m/z* 397) fragments gave a spectrum containing predominantly *m/z* 271 ions. Ion intensities were too low to permit spectra of MS^3 (*m/z* **415** → *m/z* 379) MS^3 (*m/z* **415** → *m/z* 283) to be observed. The MS^3 (*m/z* **415** → *m/z* 271) fragmented to predominantly the *m/z* 253 ion as a result of loss of water (dehydration), with smaller ion fragments of low intensities at *m/z* 225, 211, 197, 171, 157, 147, 145, 133, and 121. The MS^3 (*m/z* **415** → *m/z* 253) fragmented to ions consistent with those observed in the MS^2 (*m/z* **253**) spectra, namely *m/z* 225, 211, 197, 183, 171, and 157 ions.

The *m/z* **397** ion is attributed to the mono dehydration product of diosgenin, $[M–H_2O+H]^+$. The MS^2 (*m/z* **397**) fragmented to ions at *m/z* 379, 361, 283, 253, and 215. The MS^3 (*m/z* **397** → *m/z* 379) fragmented predominantly to ions at *m/z* 361 with a lesser quantity of *m/z* 253. The MS^3 (*m/z* **397** → *m/z* 253) fragmented to ions consistent with those observed in the MS^2 (*m/z* **253**) spectrum, with *m/z* 225, 211, 197, 171, 157, 145, 143, and 131 ions. The MS^2 (*m/z* **381**) fragmented to predominantly the ion *m/z* 253, with lesser amounts of the *m/z* 361 ion.

The MS^2 (*m/z* **271**) predominantly gave the ion fragment *m/z* 253 with lesser quantities of smaller fragments at, *m/z* 225, 211, 197, 183, 171, and 157. The loss of 18amu from *m/z* **271** → *m/z* 253 can be attributed to loss of water (dehydration). The MS^3 (*m/z* **271** → *m/z* 253) gave fragment ions at *m/z* 225, 211, 197, 183, 171, and 157 ions.

The ion fragment at *m/z* **253** seems to be a fairly stable ion fragment that most of the ions seen in the full MS eventually can be fragmented to. The MS^2 (*m/z* **253**) resulted in ions at *m/z* 238, 225, 211, 197, 183, 171, 157, 145, and 143. The weak MS^3 (*m/z* **253** → *m/z* 197) spectra suggested the fragments include, *m/z* 182, 169, and 155. The weak MS^3 (*m/z* **253** → *m/z* 171) spectra suggested the fragment *m/z* 143 ions.

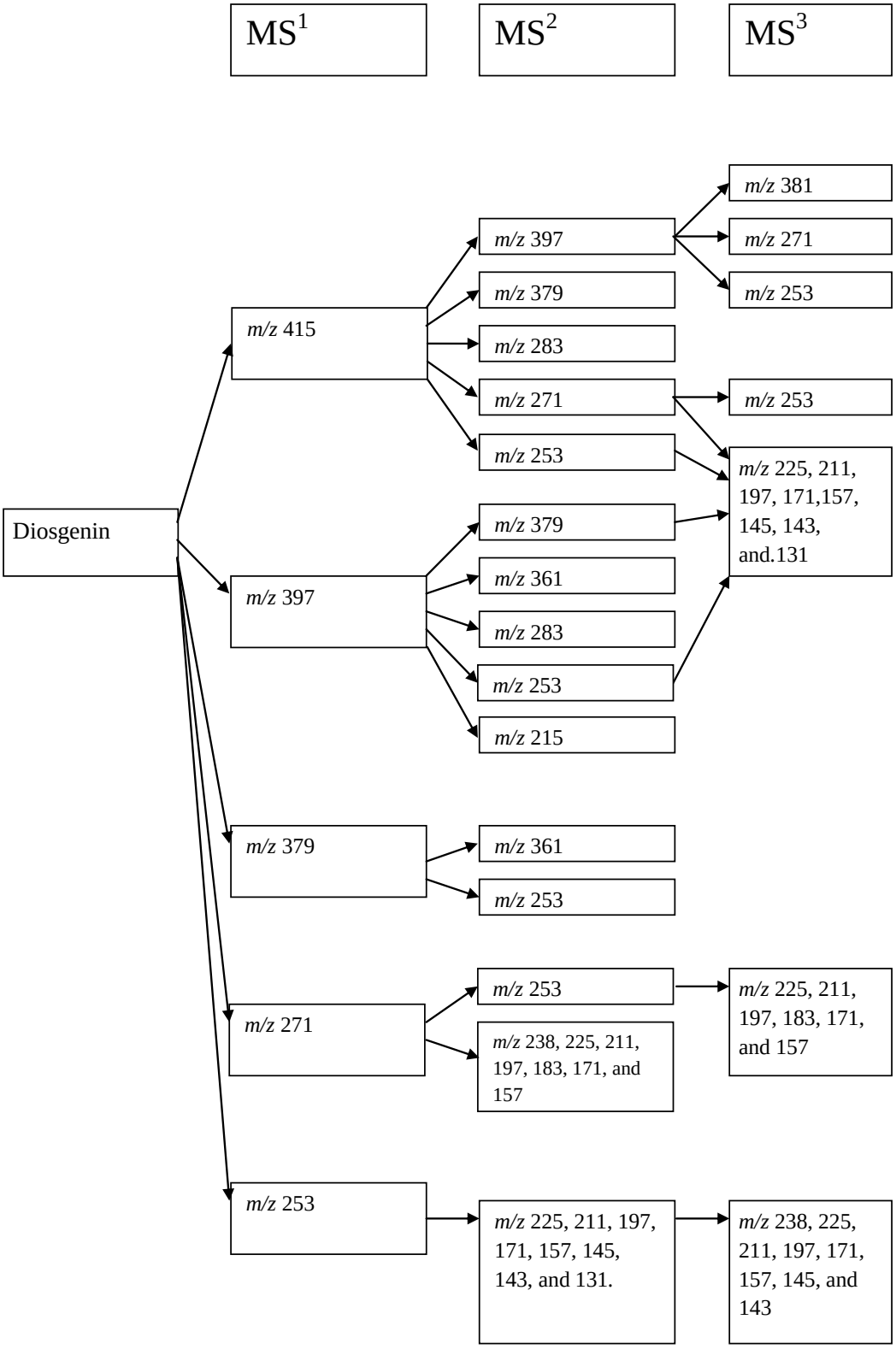

Figure 4.18. ESI fragmentation tree for diosgenin

4.4.10 Fragmentation of Diosgenin (APCI)

Conditions used for the determination of the APCI fragmentation patterns of diosgenin were similar to those used for the determination of APCI fragmentation patterns for the previous sapogenins in this investigation.

The mass spectrum showed ions resulting from diosgenin at; *m/z* **415**, **397**, **379**, and **253**. Secondary fragmentation of these ions was investigated using MS^2 and MS^3 spectra where ion intensities permitted. Nominal collision energy of 30% was used during obtaining all the MS^2 and MS^3 spectra.

The *m/z* **415** ion is attributed to the pseudo-molecular ion of diosgenin, $[M+H]^+$. The MS^2 (*m/z* **415**) ion fragmented primarily to the ion at *m/z* 271 with lesser intensity ions of *m/z* 397, 379, 283, 253, 211, 172, and 157. In the MS^2 (*m/z* **415**), *m/z* 397 is a result of loss of water (dehydration) from the pseudo-molecular ion.. The MS^3 (*m/z* **415** → *m/z* 271) fragmented to give predominantly the *m/z* 253 ion as a result of loss of water (dehydration), with smaller ion fragments of low intensities at *m/z* 225, 213, 211, 197, 171, 159, and 157. The MS^3 (*m/z* **415** → *m/z* 253) fragmented to ions at *m/z* 211, 197, 183, and 155.

The *m/z* **397** ion is attributed to the mono dehydration product of diosgenin, $[M–H_2O+H]^+$. The MS^2 (*m/z* **397**) fragmented predominantly to *m/z* 253 with lesser intensity ion fragments at *m/z* 379, 361, 283, 215, 171, and 157. The MS^3 (*m/z* **397** → *m/z* 253) fragmented to ions consistent with those observed in the MS^2 (*m/z* **253**) spectrum, specifically *m/z* 225, 224, 211, 197, 185, 183, 173, 171, 169, 159, and 157 ions. The MS^2 (*m/z* **379**) gave predominantly the ion fragment *m/z* 253, with lesser amounts of the *m/z* 361 ion.

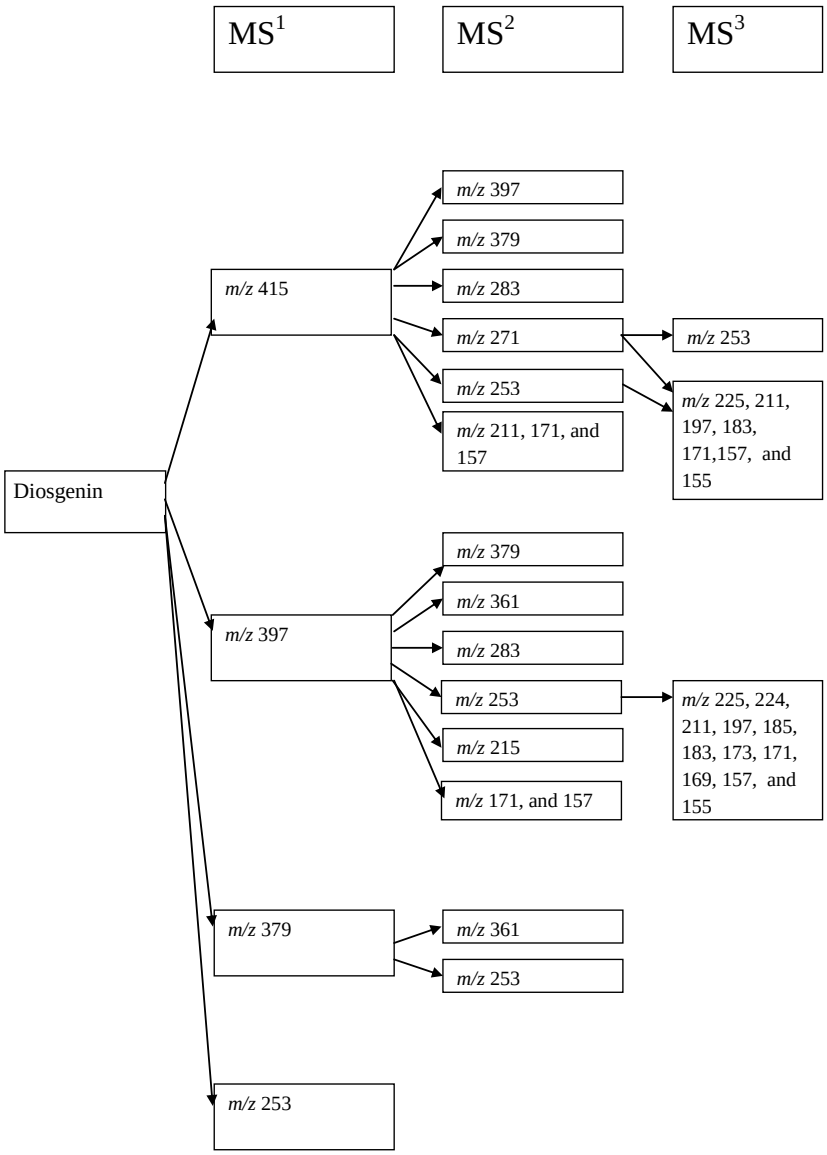

Figure 4.19. APCI fragmentation tree for diosgenin

4.4.11 Summary of Fragmentation of Diosgenin

The fragmentation patterns observed for diosgenin under both ESI and APCI are consistent with the fragmentation patterns observed for sarsasapogenin with the exception of two mass units difference due to the 5-ene in diosgenin. Based upon the fragmentation observed a plausible structural fragmentation sequence for diosgenin was proposed based on those proposed in Section 4.4.4 for sarsasapogenin (Figure 4.20).

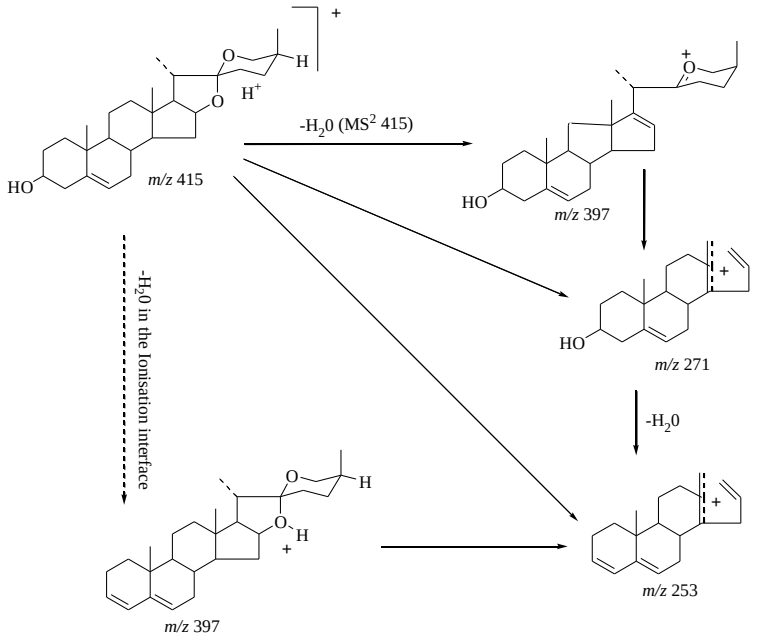

Figure 4.20. Plausible pathways to *m/z* 397, 271 and 253 ions for diosgenin

4.4.12 Fragmentation of Sarsasapogenin-β-D-glucoside (ESI)

The conditions used for the generation of ESI fragmentation patterns data for sarsasapogenin-β-D-glucoside were similar to those used above for the determination of ESI patterns of sapogenins.

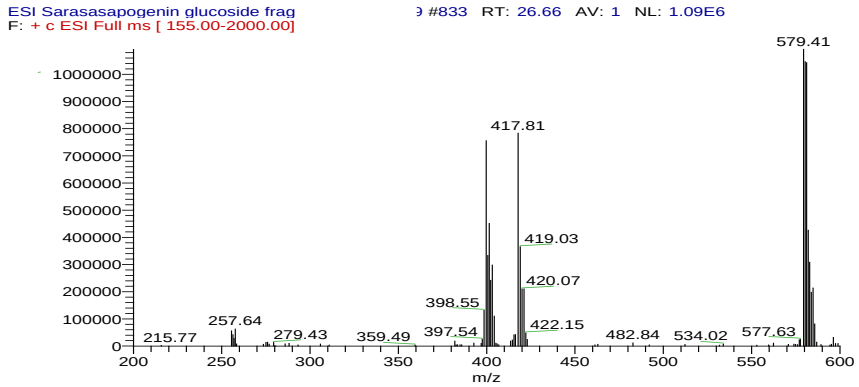

Figure 4.21. Full scan ESI mass spectrum of sarsasapogenin-β-D-glucoside

The mass spectrum showed ions resulting from sarsasapogenin-β-D-glucoside at; *m/z* **579**, **417**, **399**, **273**, and **255**. Fragmentation of these ions was investigated using MS^2 and MS^3 spectra where ion intensities permitted.

The *m/z* **579** ion is attributed to the pseudo-molecular ion of sarsasapogenin-β-D-glucoside $[M+H]^+$. The MS^2 (*m/z* **579)** fragmented to ions at *m/z* 435, 417, 399, 381, 285, 273, 255 and 173. MS^3 (*m/z* **579**→*m/z* 435) resulted in the observation of fragments at *m/z* 273, and 255. The MS^3 (*m/z* **579** → *m/z* 417) fragmented to an ion at *m/z* 273. The MS^3 (*m/z* **579** → *m/z* 399) fragmented to ions at *m/z* 255 and 381. The MS^3 (*m/z* **579** → *m/z* 273) fragmented to ions at *m/z* 255, 147, and 159. The ion fragment of MS^3 (*m/z* **579** → *m/z* 255) fragments to ions consistent with those observed in the MS^2 (*m/z* **255**) of sarsasapogenin, namely *m/z* 227, 213, 199, 187, 185, 173, 159, 147, 145, and 133 ions.

The *m/z* **417** ion is attributed to the pseudo-molecular ion of sarsasapogenin, $[sapogenin+H]^+$, and is a result of the loss of a dehydrated glucose unit (162 amu) from the sarsasapogenin-β-D-glucoside pseudo-molecular ion. The MS^2 (*m/z* **417**) ion fragmented to ion fragments *m/z* 399, 285, 273, and 255. The MS^3 (*m/z* **417** → *m/z* 273) fragmented predominantly to the *m/z* 255 ion with traces of *m/z* 227, 199, 185, 173, 159, 147, 145, 133, and 121 ions observed. The MS^3 (*m/z* **417** → *m/z* 255) fragments to ions consistent with those observed in the spectra of MS^2 (*m/z* **255**) of sarsasapogenin, namely *m/z* 227, 213, 199, 185, 173, 159, 147, 145, 133, and 121 ions.

The *m/z* **399** ion is attributed to the mono dehydration product of sarsasapogenin, $[sapogenin–H_2O+H]^+$, and is the result of the loss of a glucose unit (180 amu) or the loss of a dehydrated glucose unit and the loss of one water molecule, from the sarsasapogenin-β-D-glucoside pseudo-molecular ion. The MS^2 (*m/z* **399)** fragmented to ions at *m/z* 381, 285, 255, and 159. The MS^3 (*m/z* **399** → *m/z* 381) fragmented to *m/z* 255, the ion response observed was weak. The ion fragment MS^3 (*m/z* **399** →*m/z* 255) fragments to ions consistent with those observed in the MS^2 (*m/z* **255**) spectrum of sarsasapogenin, with *m/z* 227, 213,199, 187, 185, 173, 161, 159, 147, 145, 133, 131, 121, and 105 ions. The foregoing fragmentation pathways for the ions of *m/z* 417 or lower were essentially identical to those observed for sarsasapogenin.

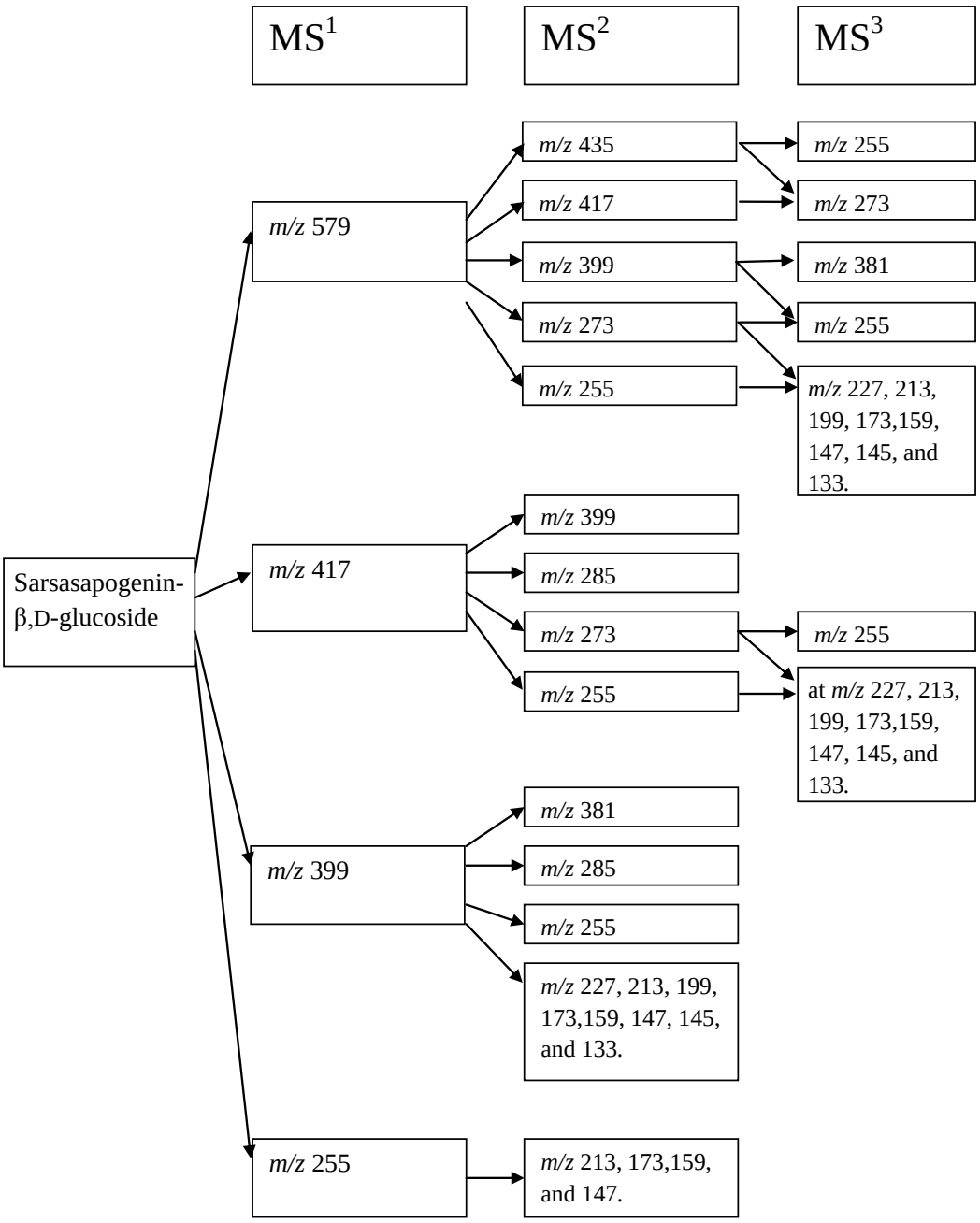

Figure 4.22. ESI fragmentation tree for sarsasapogenin-β-D-glucoside

4.4.13 Fragmentation of Sarsasapogenin-β-D-glucoside (APCI)

The conditions used for the generation of APCI fragmentation patterns data for sarsasapogenin-β-D-glucoside were similar to those used for the determination of APCI fragmentation patterns of sapogenins.

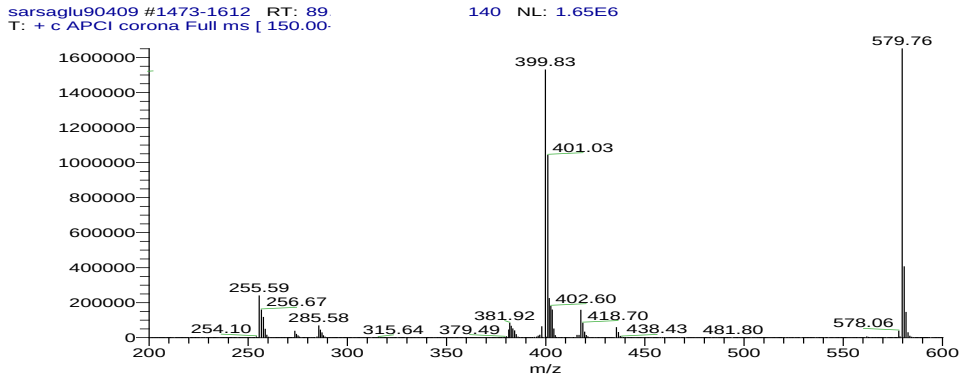

Figure 4.23. Full scan APCI mass spectrum of sarsasapogenin-β-D-glucoside

The mass spectrum showed ions resulting from sarsasapogenin-β-D-glucoside at *m/z* **579**, **458**, **417**, **399**, **386**, **273**, and **255**. Secondary fragmentation of these ions was investigated using MS^2 and MS^3 spectra where ion intensities permitted.

The APCI interface induced a larger degree of fragmentation than ESI resulting in the observation of more ion fragments relative to the pseudo-molecular ion. As with ESI the ion fragments seen at *m/z* 417 and lower are consistent with those ions seen for the saponin component, sarsasapogenin (Section 4.4.5).

The *m/z* **579** ion is attributed to the pseudo-molecular ion of sarsasapogenin-β-D-glucoside $[M+H]^+$. The MS^2 (*m/z* **579**) fragmented to ions at *m/z* 435, 417, 399, 273, and 255. The MS^3 (*m/z* **579** → *m/z* 417) fragmented to an ion at *m/z* 273. The MS^3 (*m/z* **579** → *m/z* 399) predominately fragmented to an ion at *m/z* 255 with lesser intensities of ions at *m/z* 381. The MS^3 (*m/z* **579** → *m/z* 273) fragmented to an ion at *m/z* 255. The MS^3 (*m/z* **579** → *m/z* 255) fragments to ions consistent with those observed in the MS^2 (*m/z* **255**) of sarsasapogenin, ie *m/z* 227, 213, 199, 187, 185, 173, 159, 147, 145, and 133 ions.

The *m/z* **417** ion is attributed to the pseudo-molecular ion of sarsasapogenin, [sapogenin+H^+], and is a result of the loss of a dehydrated glucose unit from sarsasapogenin-β-D-glucoside. The fragmentation characteristics of the *m/z* 417 ion and other lower mass ions (Figure 4.24) were analogous to those observed for sarsasapogenin.

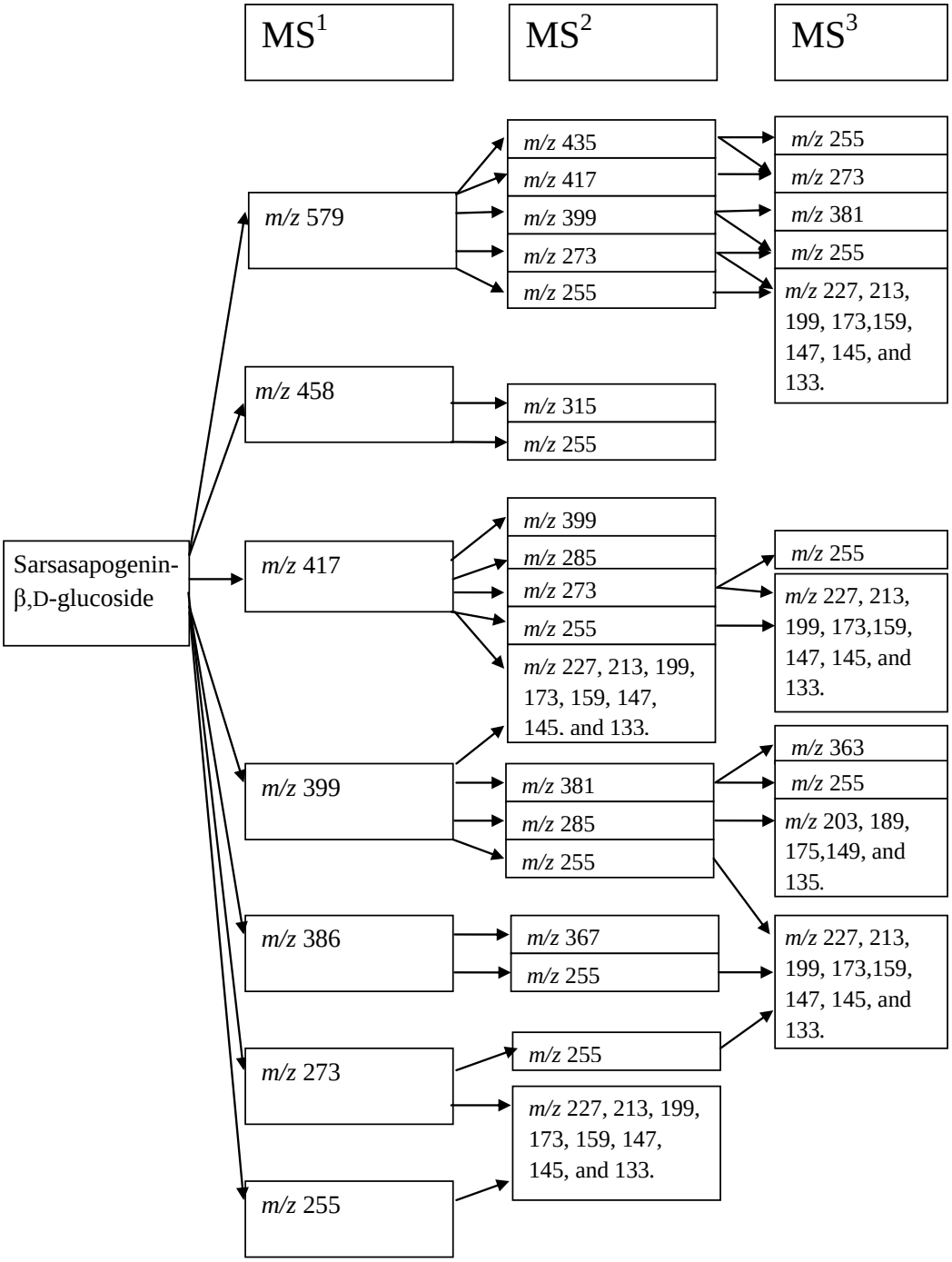

Figure 4.24. APCI fragmentation tree for sarsasapogenin-β-D-glucoside

4.4.14 Fragmentation of Sarsasapogenin-β-D-galactoside (ESI and APCI)

The full scan ESI and APCI mass spectrum of sarsasapogenin-β-D-galactoside showed ions at *m/z* **579**, **433**, **417**, **399**, **273** and **255**. These ions fragmented in an manner analogous to that above for sarsasapogenin-β-D-glucoside

The ESI and APCI fragmentation trees determined for sarsasapogenin-β-D-galactoside are given in Figure 4.25 and 4.26 respectively. It was apparent that this fragmentation data could not be used to identify the structure of the glycoside residue, be it a glucosyl, galacosyl or another six carbon sugar residue.

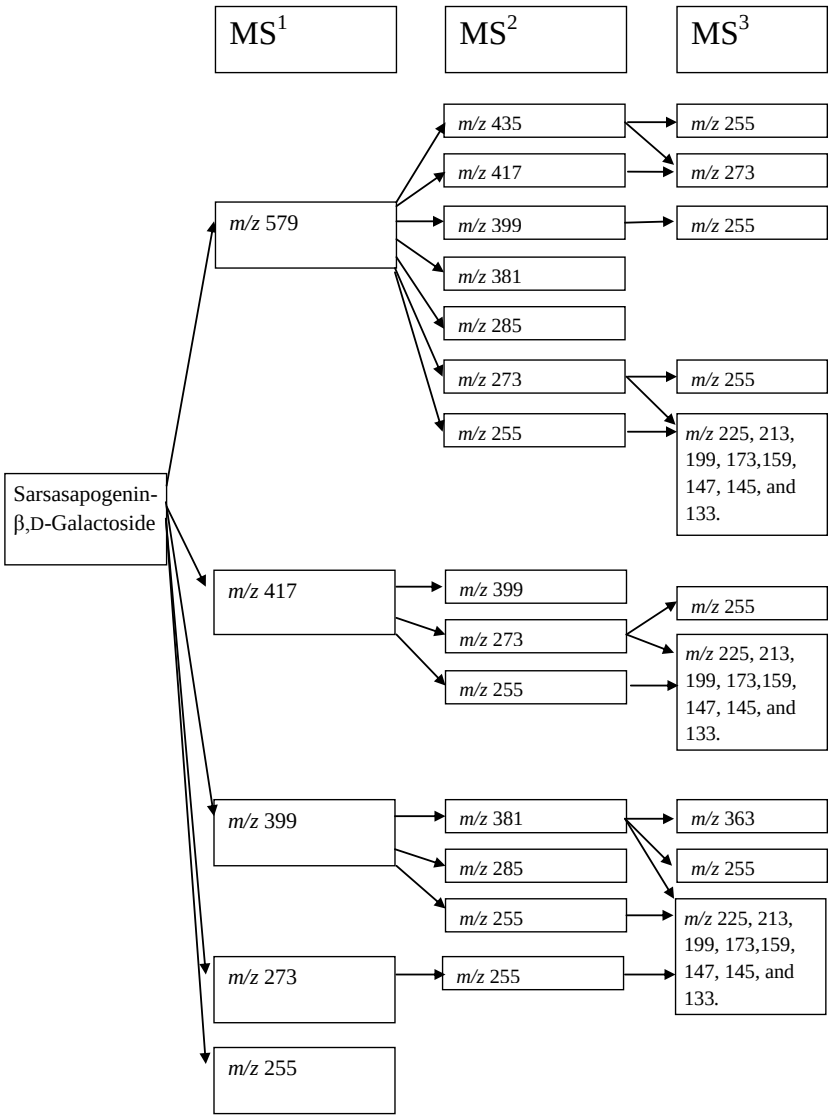

Figure 4.25. ESI fragmentation tree for sarsasapogenin-β-D-galactoside

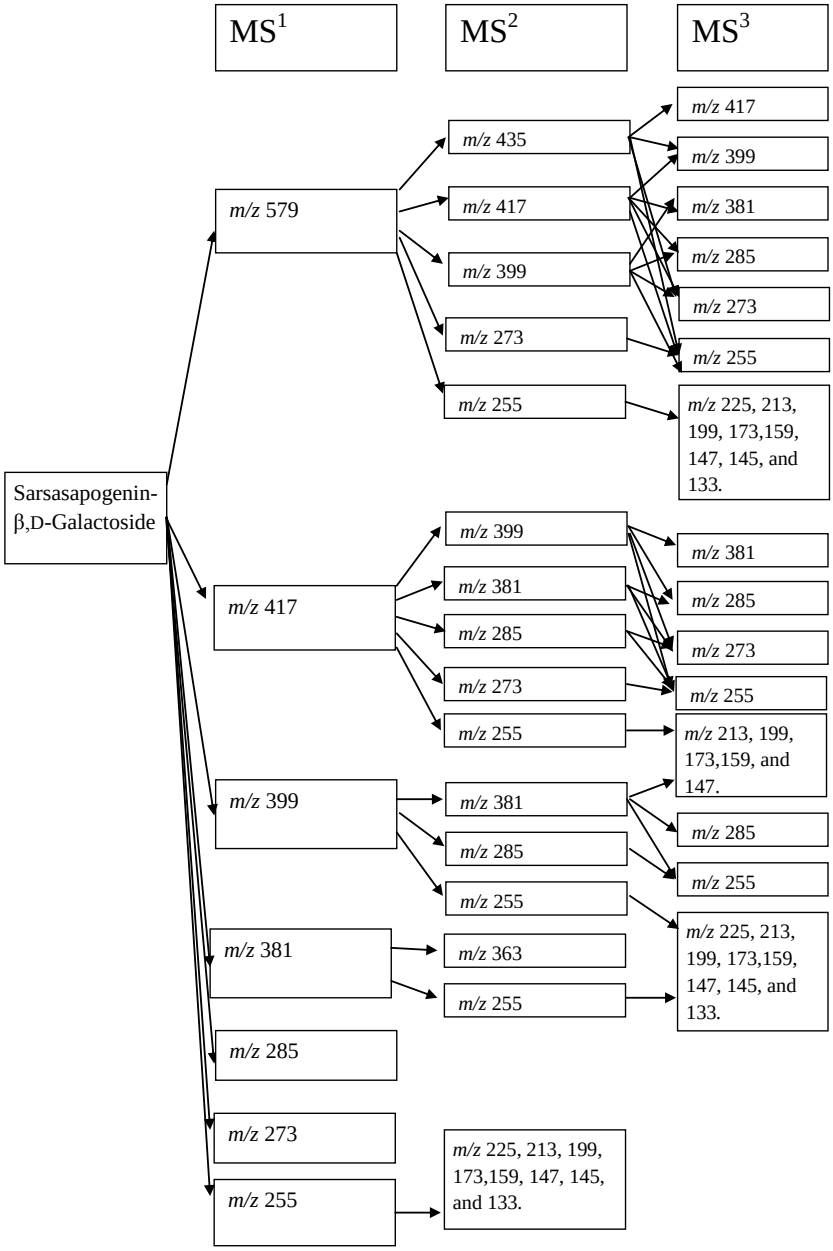

Figure 4.26. APCI fragmentation tree for sarsasapogenin-β-D-galactoside

4.4.15 Fragmentation of Episarsasapogenin, Tigogenin and Smilagenin (ESI and APCI)

The fragmentation patterns of the structural isomers episarsasapogenin, tigogenin and smilagenin were investigated in the same manner as the model compounds previously described for both ESI and APCI interfaces. It was hoped that a difference in fragmentation characteristics may allow the distinction of one or more of episarsasapogenin, tigogenin and smilagenin from sarsasapogenin.

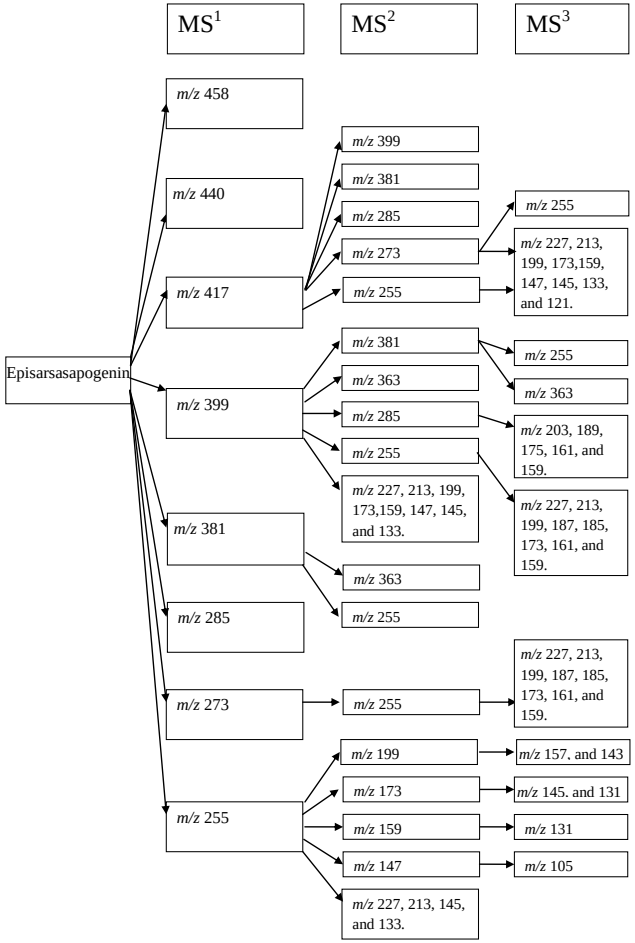

Figure 4.27. ESI fragmentation tree for episarsasapogenin

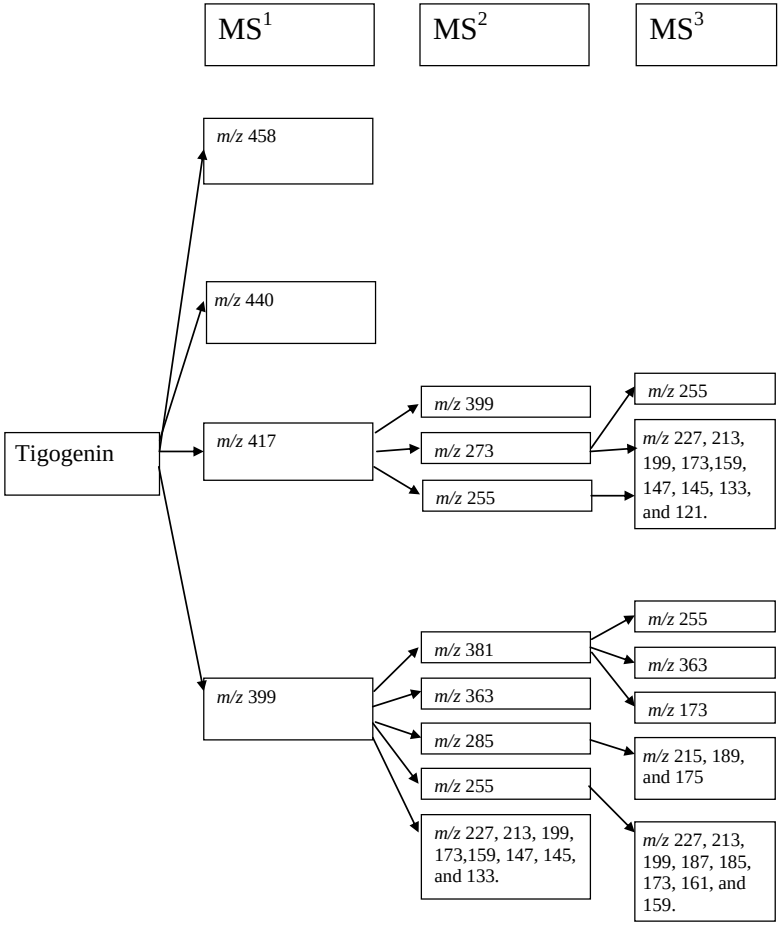

Figure 4.28. ESI fragmentation tree for tigogenin

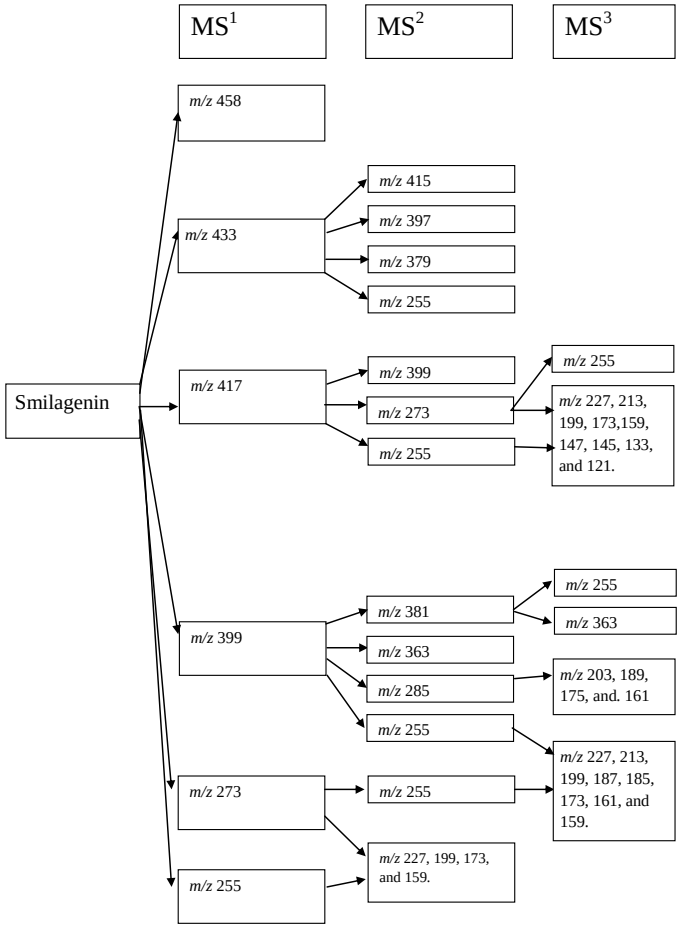

Figure 4.29. ESI fragmentation tree for smilagenin

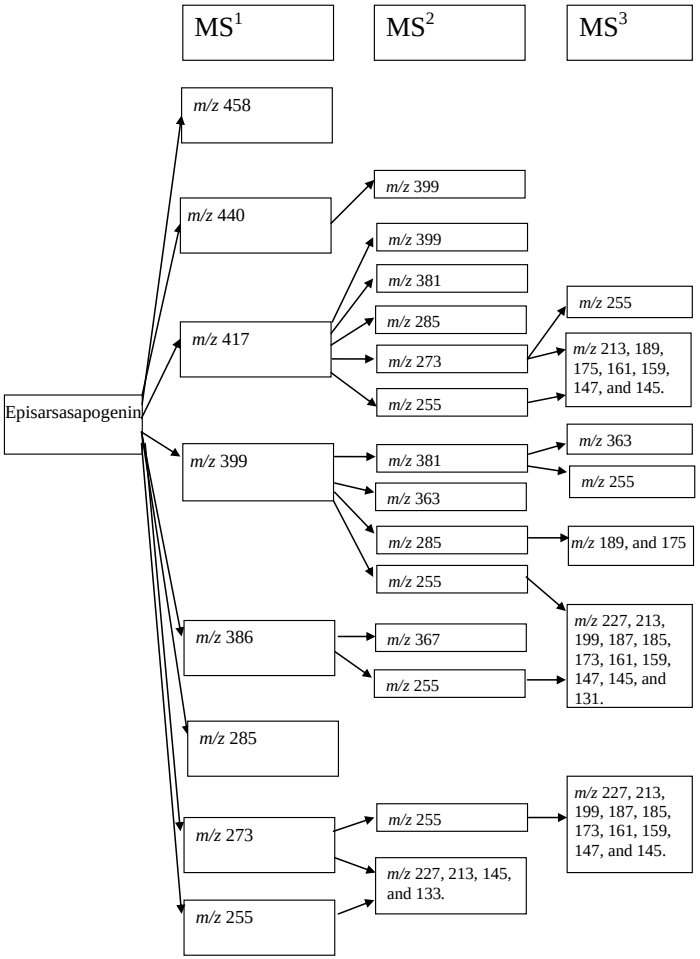

Figure 4.30. APCI fragmentation tree for episarsasapogenin

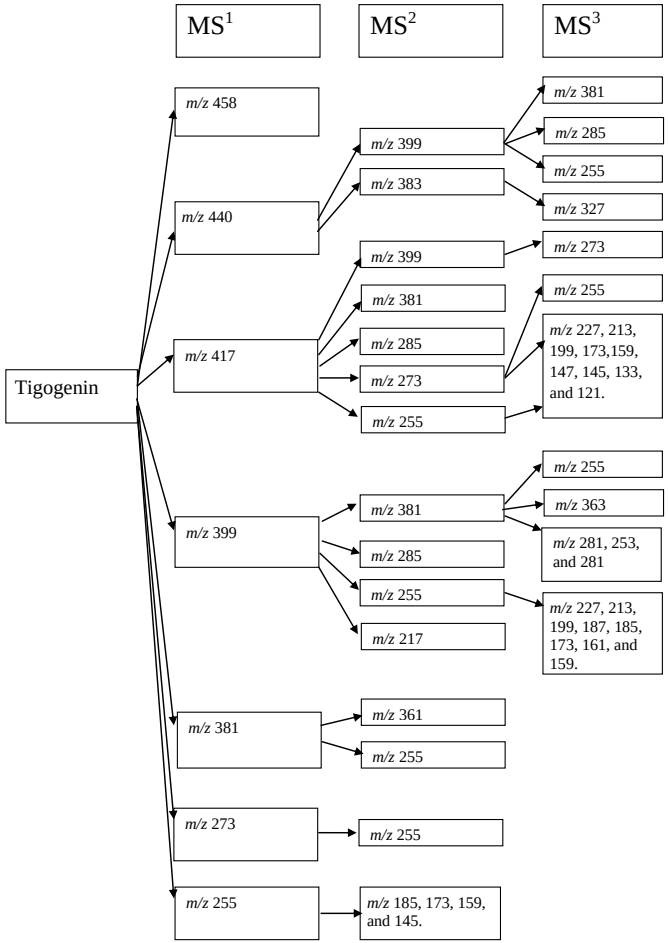

Figure 4.31. APCI fragmentation tree for tigogenin

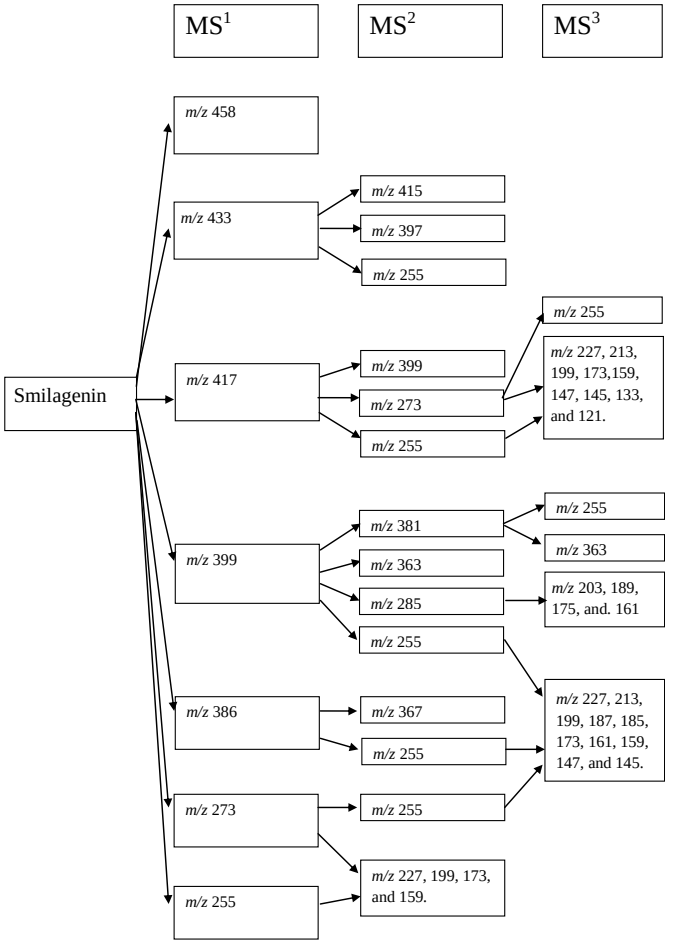

Figure 4.32. APCI fragmentation tree for smilagenin

4.5 Mass Spectral Findings

4.5.1 Established Mass Spectral Techniques for Isomeric Identification of Sapogenins

Using EI- MS Blunden et al[26] have reported that isomeric 3α/3β, 5α/5β, 25(*R/S*)-sapogenin alcohols (smilagenin, sarsasapogenin, etc) can be distinguished by the ratios of three moderate intensity ions and their dehydration, namely the ratio of the *m/z* 302/284, *m/z* 287/269 and *m/z* 273/255 ion pairs observed in the EI mass spectra of parent alcohols[26].

Subsequently Wilkins et al[16] found that isomeric 3α/3β, 5α/5β, 25(*R/S*)-sapogenin acetates could be distinguished in a like manner by consideration of *m/z* 284/344, *m/z* 329/269 and *m/z* 315/255 ion ratios observed for the isomeric acetates. Two advantages the use of acetates rather alcohols were (i) greater values for the ion ratios (especially so in the case of the range of values exhibited by *m/z* 284/344 ratio) and (ii) amenability of the acetates to GC-MS analyses.

A combination of ion ratio and GC capillary column retention time data, such as that reported by Meagher[25] (Table 4.2), readily distinguishes isomeric acetates, and hence the sapogenins the acetates are derived from. The sharpness of the GC-MS peaks (ca 0.1 min or less) enables the distinction of 25*R*- and 25*S*-isomers which typically eluted 0.4-0.5 min apart. 3α and 3β-acetylated sapogenins are also readily distinguished.

Table 4.2. GC-MS of sapogenin acetates

		RT[a]	*m/z* 284	*m/z* 269	*m/z* 255
compound	stereochemistry	(min)	*m/z* 344	*m/z* 329	*m/z* 315
smilagenin acetate	3β,5β,25*R*	16.87	2.92	0.74	0.9
sarsasapogenin acetate	3β,5β,25*S*	17.23	3.13	0.7	0.87
epismilagenin acetate	3α,5β,25*R*	17.19	7.89	0.8	1.3
episarsasapogenin acetate	3α,5β,25*S*	17.55	12.3	0.79	1.39
tigogenin acetate	3β,5α,25*R*	18.38	0.22	0.73	0.41
neotigogen acetate	3β,5α,25*S*	18.83	0.22	0.71	0.41
epitigogenin acetate	3α,5α,25*R*	17.25	0.31	0.76	0.67
epineotigogenin acetate	3α,5α,25*S*	17.64	0.3	0.8	0.64
[a]RT = Retention time (min) on a 25 m x 0.25 mm id HP-1 column.					

Data taken from Meagher (1996)[25].

An objective of the investigations reported in this thesis was to determine if ESI or APCI full scan and MS^2 mass data could, in a manner analogous that described above for EI-GC-MS data, determine the isomeric form of sapogenins. Such specificity would be utilised to distinguish free and conjugated sapogenins of the type expected to be present in rumen and other GI tract samples of animals grazing saponin containing plants implicated in the development of photo-sensitisation diseases.

4.5.2 Mass Spectral Techniques for Isomeric Identification by LC-MS^n

The ESI and APCI LC-MS fragmentation trees were determined for smilagenin, episarsasapogenin, tigogenin and sarsasapogenin-β-D-galactoside under identical conditions to those utilised to determine the ESI and APCI LC-MS fragmentation trees for sarsasapogenin, diosgenin, and sarsasapogenin-β-D-glucoside (Section 4.4). The mass spectral fragmentation characteristics established for the four sapogenin isomers showed no significant variation upon which distinction could be made between isomers or stereo-isomeric configurations. Likewise no

significant variation was observed between the Saponin isomers, sarsasapogenin-β-D-glucoside and sarsasapogenin-β-D-galactoside.

Only one significant ion pair of the type observed by Blunden[26] in EI mass spectra, namely an *m/z* 273 ion and its *m/z* 255 dehydrated partner, was seen in the full scan, MS^2 and/or MS^3 ESI or APCI spectra of all of the sapogenins examined in this study. Due to the unpredictable nature observed for ESI and APCI interfaces in promoting consistent ionisation, monitoring of fragmentation in the ion trap was deemed more likely to give rise to consistent difference in ion ratio. However, for all the isomers investigated the relative intensities of the *m/z* 273/255 ion ratios were similar and it was apparent that this data could not be used to deduce the C3, C-5 or C-25 stereochemistry of the investigated genins by $LC\text{-}MS^n$.

4.6 Chromatographic Properties

4.6.1 The Need for Adequate Chromatographic Separation

Ensuring adequate chromatographic peak separation of compounds/analytes that are indistinguishable from each other via their mass spectral fragmentation characteristics is highly desirable as it may be the only mechanism by which identification and quantification of a specific compound can be achieved.

The GC-MS procedure described in Section 4.5.1 has been found to be capable of distinguishing the eight isomeric sapogenins listed in Table 4.2. Amongst the eight compounds listed in Table 4.2, only glucuronic acid conjugates of two of those compounds have been detected in crystalline biliary material recovered from sheep exhibiting hepatogenous photo-sensitisation disease symptoms. This demonstrates why the ability to distinguish between the isomers of the spirostanols is highly beneficial to the analysis of saponins associated with hepatogenous photo-sensitisation diseases of livestock.

The situation in respect of the chromatographic separation of the conjugated analogues (saponins) is more complicated than that of parent sapogenins in that numerous conjugated forms of a particular genin (eg mono-, di-, or triglycosylated) may exist. To date there is no report of an LC-MS procedure which can be used to distinguish the eight isomeric 3α/3β, 5α/5β, 25(*R/S*)-sapogenins in either free or conjugated forms. Since the full scan MS and MS^n data reported in Section 4.4 cannot be used to distinguish isomeric forms of a selection free and conjugated sapogenin the possibility that retention time data may be able to distinguish between isomers was investigated.

4.6.2 Liquid Chromatographic Separation

The retention times of sarsasapogenin, episarsasapogenin, tigogenin, smilagenin, sarsasapogenin-β-D-glucoside and sarsasapogenin-β-D-galactoside were analysed using a C-18 reverse phase column variety of column flow rates and choice of ACN-H_2O gradient conditions. As noted in Section 3.2.4, the low water content of the ACN- H_2O gradient mixtures required to elute isomeric sapogenins from the C-18 column utilised in the investigations reported in this thesis were not conducive to efficient ionisation of these compounds.

Irrespective of the choice of gradient conditions and flow rates only small differences in retention times were observed for sarsasapogenin, episarsasapogenin, tigogenin, and smilagenin. In general such differences that were observed were less than the peak width of a target substance. Likewise sarsasapogenin-β-D-glucoside and sarsasapogenin-β-D-galactoside were also indistinguishable from each other based upon retention time data.

As noted in above the low water content of the ACN-water gradient mixtures required to elute isomeric sapogenins from the C-18 column utilised in the investigations reported in this thesis were not conducive to efficient ionisation of these compounds, and in some cases retention time data was constrained by sensitivity limitations.

Some concern exists to whether the spirostanol sapogenins undergo structural modification in certain solutions analogus to those observed for furostanols as have been reported by other workers[34]. During the course of the retention time investigations multiple peaks had been observed in some chromatograms of aged solutions of spirostanols that had previously been as checked as isomerically pure by NMR and GC-MS (as described in Sections 4.2. and 4.3). The samples used in the above investigation into chromatographic separation were made up fresh in DCM/ACN to minimise any structural modification.

4.6.3 Summary of LC-MS^n Chromatographic Retention Findings

It was apparent that while full scan and MS^2 or MS^3 LC-MS^n analyses can be used to identify the molecular weight of a conjugated sapogenins, and to demonstrate the sapogenin type nature of the genin component via its MS^n characteristics, LC-MS retention time was not capable of distinguishing between isomeric sapogenins and saponins (at least under the conditions explored in this study).

Accordingly, it can be concluded that where a knowledge of both the molecular weight of conjugated sapogenin constituents of rumen extracts and the structure of the genin component of a particular saponin is required, a combination of GC-MS and LC-MS^n data will be required. The isolation of a sufficient quantity of a target compound will be required to unequivocally identify its structure via detailed one and two-dimensional NMR analyses as neither LC-MS^n nor GC-MS are capable of unequivocal identification of an unknown structure.

Increased LC resolution may enable identification of isomeric sapogenins and saponins. The application of UPLC column technology may improve separation of isomeric peaks for either saponins or sapogenins. UPLC columns possess smaller stationary phase particles (< 2 μm) and generate more effective separation (chromatographic resolution) than traditional HPLC columns utilising 5 μm stationary phase particles.

5 Summary, Conclusions and Recommendations for Further Work

5.1 Overview of the Research

As noted in Chapter 1, one of the principle objectives of the investigations reported in this thesis was to determine if LC-MS methods could be developed to identify free and conjugate sapogenins expected to be present in rumen and other GI tracts of susceptible and non-susceptible populations of sheep grazing saponin containing plants implicated in the development of photo-sensitisation.

Depending on the progress and duration of a breeding programme currently underway in South America, it is envisaged that rumen and other GI tract samples from some sheep culled from the susceptible and non-susceptible groups will be available in 18-30 months. An objective of the collaborative research will be to identify free and conjugate sapogenins performed when the GI extract samples are available. The conjugated sapogenins expected may include glycosyl, glucuronide, sulphate, phosphate, fatty acid ester, or other conjugates. The detection of conjugated sapogenins present in the biological tissue would be beneficial to determining whether or not differences may exist in the absorption and transportation characteristics of specific ruminal metabolites of sapogenins. An example of particular interest is the metabolism of conjugated sapogenins in the liver where, in the case of animals suffering from hepatogenous photo-sensitisation diseases, the deposition of calcium salts of epismilagenin and/or episarsasapogenin-β-D-glucuronides have been found in the bile ducts[12-14].

It is of note that episapogeninn-β-D-glucuronides conjugates have only been identified in liver samples recovered from susceptible sheep. It is not currently known if other conjugate sapogenin 'marker' substances (e.g. sulphate, phosphate, fatty acid, etc conjugates) are present other GI tract regions of affected sheep. LC-MS analyses of the type described above may lead to the identification of such compounds amongst the level of unidentified conjugated sapogenins known to be present in GI tract samples of photo-sensitised livestock.

5.2 Significance of Ionisation Conditions, Eluent Composition and Flow Rate

It is apparent for the investigations reported in this thesis that the sensitivity of LC-MS analyses can be substantially improved by careful attention to ionisation conditions such as;

(i) eluent composition at the point of elution of a target analyte,

(ii) eluent flow rate, and

(iii)capillary temperature.

Specifically it was found that there was a *ca* 2-20 fold increase in both APCI and ESI ion currents when the capillary interface temperature was maintained at 275-300°C compared to than obtained at 200-225°C (Sections 3.2.5 and 3.3.4). It was also found that the water content of the ACN-H_2O (0.01% formic acid) at the point of elution had a large effect upon the measured ion current, in the region of a 1-2 order of magnitude increase from 100% ACN (0.01% formic acid) to the optimal composition of eluent.

While the use of a 150 mm x 2.00 mm 5 µm C-18 column resulted in it being possible to elute sarsasapogenin-β-D-glucoside and its galactoside analogue near optimal ACN-H_2O, this was not the case for free sapogenins. The free sapogenins eluted when the water content of ACN-H_2O (0.01% formic acid) was well below optimal for ionisation. It can be reasoned that the use that the use of shorter hydrocarbon chain length support (e.g. a C-8 rather than a C-18 column) would increase the LC-MS ion current and therefore sensitivity of sapogenin analyses by allowing the sapogenins to elute closer to optimal eluent compositions and flow rates based on the data presented in Section 3.2.4. Moreover it is apparent that the use of a lower flow rate, notwithstanding the any tendency towards broader peaks at lower rates also increases the sensitivity of both conjugated and free genin analyses 3-30 fold (Section 3.2.6). In combination these factors translate to *ca* 100 fold increases in sensitivity relative to conditions that were believed to be appropriate prior to the investigations reported in this thesis.

The significance of choosing elution conditions which maximise ionisation is demonstrated in Figure 5.1 and Figure 5.2 for chromatographic runs of sarsasapogenin-β-D-glucoside at four concentrations using 'optimal' ionisation conditions as defined in this thesis and 'typical' conditions commonly used prior to the investigations reported in this thesis.

The data presented in Figure 5.1 and Figure 5.2 shows that the optimised conditions can detect as little as $2.5*10^{-9}$ mol of sarsasapogenin-β-D-glucoside on the column, whereas the typical conditions did not detect the compound at $1*10^{-8}$ mol.

Figure 5.1 illustrates the dramatic increase in optimised ion currents and sensitivity for both *m/z* 579 $[M+H]^+$ and TIC responses as a function of the nmol of injected sample. By comparison non optimised ion currents were not recognisable or quantifiable above baseline noise when plotted on the same scale (note non optimised *m/z* 579 $[M+H]^+$ and TIC ion are overlapped in Figure 5.1).

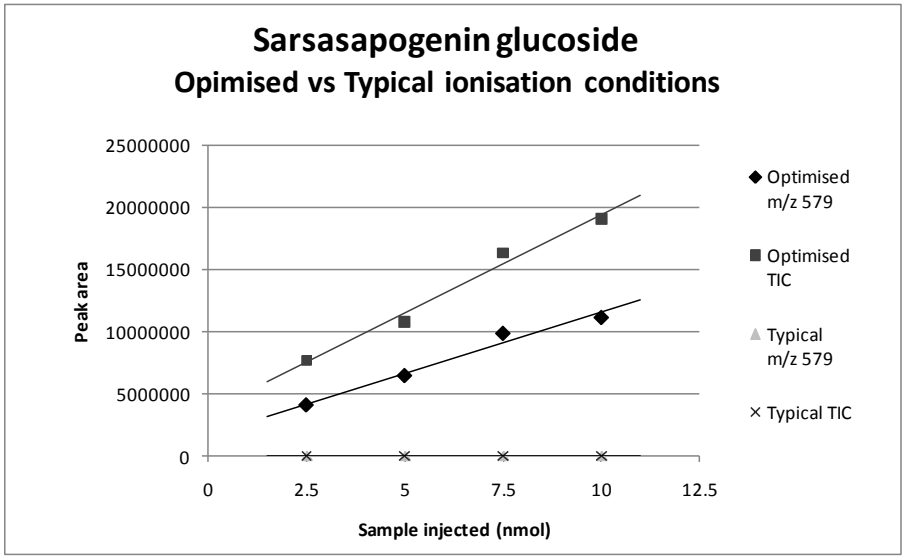

Figure 5.1. Comparison of optimal ionisation conditions and those commonly used prior to this investigation

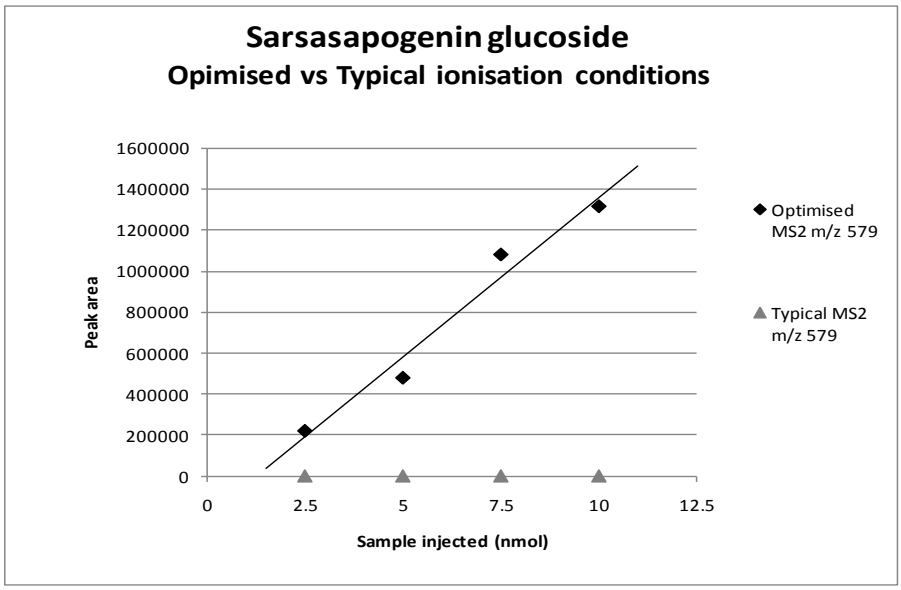

Figure 5.2. Comparison of optimal ionisation conditions and those commonly used prior to this investigation

5.3 Recommendations for Further Work

5.3.1 LC-MS Analysis

As in earlier ovine studies, it is recommended that freeze dried GI tract samples should be sequential extracted with a non-polar solvent such as hexane or dichloromethane, and there after a moderately-polar solvent such as ethanol to afford free and conjugated extracts respectively. Precautions will need to be taken to avoid the use of solute conditions which cause the solute to be reactive towards the analytes.

Since optimal eluent compositions and detector response for saponins and sapogenins differ maximum sensitivity will require the use of two sets of conditions: namely saponin optimised conditions and sapogenin optimised conditions.

Saponins can be eluted during analysis of the sapogenins without causing any ill effects to the sapogenin analysis, however, to elute the sapogenins from the column used for saponins would significantly extend the duration of the chromatographic run and waste solvent. Removal of the saponins from the column between each analysis is desirable for repeatability of retention time data, and removal of possible interfering peaks in future runs. These negative effects are overcome by the application of the two step extraction process recommended above.

Portions of the free and conjugated extracts should analysed by full scan positive ion ESI using C-8 and C-18 columns respectively, with the former likely to give the greatest response and acceptable retention times for sapogenins and the latter for conjugated analogues. LC-MS conditions, capillary temperature, eluent composition, ionisation agent, and flow rate, should be based on the optimised conditions discussed in Section 3.2.

Full scan LC-MS analyses should be supplemented by MS^2 analyses of $[M+H]^+$ ions believed to be attributable to sapogenins and conjugated analogues. Therefore two or three MS^2 events can be programmed per LC-MS while maintaining acceptable sensitivity. If a triple quad MS system is avaliable, MS^2 ion trap analyses should be supplemented by SRM analyses of $[M+H]^+ \rightarrow m/z$ 399, $[M+H]^+ \rightarrow m/z$ 273, and $[M+H]^+ \rightarrow m/z$ 255 transitions for sapogenins, and in addition $[M+H]^+ \rightarrow m/z$ 417 for the saponins. Diosgenin and other spirosten-3-ol analogues would require values 2 amu lower.

5.3.2 Reducing Flow Rates by Application of low flow Columns

Low flow rate, short 50 mm x 2.0 mm, 1.7 µm particle size micro UPLC columns are being used in place of higher flow rate, longer 100-150 mm x 2.4 mm (or even x 4.6 mm) 5 µm particle size conventional HPLC columns. It can be concluded from the data presented in Chapters 3 and 4 that provided column capacity is not a limiting factor, the use in future investigations of a 50 mm C-8 micro UPLC column will result an appreciable gain in sensitivity for sapogenin isomers compared to that which can be obtained using a conventional 150 mm C-18 HPLC column. On the other hand it is likely a C-18 UPLC column would be more suited to glycosylated saponin analyses than a C-8 UPLC column.

A further well documented benefit that would arise from the use of a micro UPLC rather than a micro HPLC column is sharper (narrower peaks). For a given peak area a 2-4 fold reduction in peak width is typically observed, leading to the ability to resolve peaks that may overlap using a conventional HPLC column[50, 51]. The increase in peak height associated with narrower peaks increases detection limits by increasing the concentration of the analytes in the eluent as the analyte peaks pass through the ionisation interface. Peak overlapping was found to be a problem for the saponins sarsasapogenin-β-D-glucoside and sarsasapogenin-β-D-galactoside in this investigation. UPLC columns may give the resolution required to separate these peaks.

Notwithstanding the performance gains that might arise from the use of a C-8 micro UPLC as opposed to a C-18 HPLC column, it is apparent that neither full scan or MS^2/MS^3 ESI or APCI ion ratio data can be used to establish the structures of isomeric free or conjugated sapogenins, in a manner similar to that which that which can be achieved for sapogenin acetates using EI-GC-MS.

5.3.3 SRM Detection

The principle advantage of ESI and APCI LC-MS methods is their ability to identify the molecular weight of a conjugated saponin metabolite, as illustrated in the present investigation for sarsasapogenin-β-D-glucoside and galactoside (Sections 4.4.12-4.4.14). The conjugated portion of such a metabolite can be recognised in full scan ESI or APCI spectra, followed by MS^2 fragmentation (30% collision energy) of the parent $[M+H]^+$ ion to afford ions attributable to *m/z* 417 (protonated genin) and/or *m/z* 399 ions and a number of other distinctive fragment ions, including *m/z* 273 and 255 ions for spirostan-3-ols (Sections 4.4.12-4.4.14).

Rumen and other GI tract samples typically contain complex series of free and conjugated sapogenin and other metabolites, including steroidal plant compounds such as b-sitosterol, stigmasterol, cholesterol, bile acids, and other lipids such as triglycerides, fatty acids, etc. EI-GC-MS methods for the identification of sapogenins have utilised selected ion mode (SIM) detection of the universally present *m/z* 139 ion, aided by the analyses of the ratio of three lower intensity pairs of ions (Section 4.5.1). In the case of ion trap or triple quad based LC-MS analyses selectivity can be achieved using SRM (MS^2) based detection.

In the case of sapogenins (spirostan-3-ol type), suitable SRM parent-daughter ion transitions are *m/z* 417 → *m/z* 399, *m/z* 417 → *m/z* 273, and *m/z* 417 → *m/z* 255, or the corresponding $[M+H]^+$ → *m/z* 417, $[M+H]^+$ → *m/z* 399, $[M+H]^+$ → *m/z* 273, and $[M+H]^+$ → *m/z* 255 transitions in the case of conjugated sapogenins. Substantially greater sensitivity would be observed using a triple quad MS systems as opposed to an ion trap MS since a triple quad system can continuously

monitor specified transitions whereas the sensitivity of an ion trap system is constrained by the time required to load ions generated in the MS source into the trap, expel non target ions, fragment the target ion, expel non target MS^2 ions and record only the target SRM daughter ion.

If required MS^3 fragmentation to either the *m/z* 273 or 255 ions can be used to confirm the origin of these ions are from free or conjugate spirostanol containing precursor molecules (see for example fragmentation trees represented in Sections 4.4 from sarsasapogenin and sarsasapogenin-β-D-glucoside).

5.3.4 Superiority of ESI Detection

The use of an ESI interface was found to be superior to be use of an APCI interface, at least when using the Department's LCQ MS system on standard solutions. Under APCI conditions a greater degree of fragmentation was observed in full scan MS, presumably due to increased thermal fragment during the passage of analytes through the flash vapour stage of the APCI inlet. Full scan APCI ion currents were typically two to tenfold lower than ESI ion currents for the model compounds.

5.3.5 Compensating for Signal Suppression

It is envisaged that signal suppression will be of huge significance for the accurate quantification and even identification of saponins and sapogenins extracted from the GI tract of photo-sensitised sheep. ESI, the preferred ionisation interface for the analysis of saponins, as determined by this investigation, is prone to strong signal suppression by components in the matrix at the time of ionisation. To overcome the restrictions that can be induced by signal suppression careful method development that minimises its effect needs to be conducted. Factors to be investigated include;

(i) Sample extraction processes with preferable methods being those that would extract the analytes without many of the offending signal suppressing compounds.

(ii) The region in which signal suppressing compounds elute, with a view to manipulating LC conditions so they don't co-elute with the analytes.

(iii) Inclusion of appropriate internal standards for quantification of the extent signal suppression excerts upon the analytes.

Prior to LC-MS or GC-MS analyses there may be a requirement to clean up samples, options include using short C-18 or sep-pak or GPC type columns. Sep-pak or GPC type columns can be used to remove earlier eluting highly polar and/or later eluting non polar compounds from sapogenin and saponin containing extracts.

Based upon the fragmentation characteristics of 2,2,4,4-$^{2}H_4$-episarsasapogenin and 2,2,4,4-$^{2}H_4$-sarsasapogenin, introduction of deuterium at the C-2 and C-4 positions, as synthesised by loader et al[46], would be highly suitable choices as internal standards for sapogenin and saponin quantification by LC-MS^{n}. The 20,23,23-$^{2}H_3$-sapogenin/saponin analogues are not considered as suitable due to the tendency to back exchange deuterium with protic solvents[52].

5.3.6 Requirement for Complementary GC-MS analysis

GC-MS methodology has been tried and tested and found to give accurate quantitative data for the analysis of derivatised genins. Any method developed for LC-MS detection of the genins should have the results directly compared to results obtained for the existing GC-MS methodology to ascertain the accuracy using the newly developed LC-MS methodology. The GC-MS analysis should be performed on portions of both the free and hydrolysed conjugate extracts as per the Wilkins et al method[16].

While full scan and SRM ESI/APCI-MS data can be used to define the molecular weight of a parent saponins and its genin component, it does not specificially define the structure of the genin, be it smilagenin, epismilagenin, sarsasapogenin, episarsasapogenin, etc. Some identification can be achieved by comparing chromatographic retention times, but this in itself does not provide unequivocal identification as many isomers may have indistinguisable retention times. To this end there remains a requirement to hydrolyse conjugated saponin containing extracts and analyse a subsample of the acetylated free genins using GC-MS protocols[16]. Once the saponins are partially identified by GC-MS techniques it may be possible to assign the sapogenin content of saponins by comparison of GC-MS and LC-MS spectra.

5.3.7 Requirement for Isolation, and Structural Determination via NMR and HRMS

Since MS data alone cannot be used to identify the gross structure of conjugated sapogenins, there will be a need to isolate sufficient quantities of metabolites which have not been formally characterised using one and two dimensional NMR methods. Molecular weights will need to be established using high resolution MS data, especially if it transpires that susceptible sheep are characterised by the presence of a different series of conjugated metabolites in one or more of the GI tract regions.

5.4 Conclusions

Based on the large increase in ionisation efficiency obtained in this investigation it is anticipated LC-MS^n determination of the saponins implicated in hepatogenous photo-sensitisation of livestock should be achievable on the University of Waikato's LC-MS^n system.

This investigation has also shown some of the limitations in current LC-MS^n analysis including the inability to distinguish many structural isomers. Importantly MS^n data can be used to determine the mass of a saponin, along with the mass of the glycoside and sapogenin portions of the saponin.

Quantification of the saponins should be achievable via LC-MS^n but will require careful and precise method development to minimise the significance of signal suppression effects (matrix effects).

LC-MS^n data should complement the current GC-MS methodology and contribute to an improved understanding of the ruminal metabolism of saponins in animals suffering from hepatogenous photo-sensitisation diseases.

1. Abe, I.; Rohmer, M.; Prestwich, G. D., Enzymatic cyclization of squalene and oxidosqualene to sterols and triterpenes. *Chemical Reviews* **1993,** 93, 2189-2206.

2. Phillips, D. R.; Rasbery, J. M.; Bartel, B.; Matsuda, S. P. T., Biosynthetic diversity in plant triterpene cyclization. *Current Opinion in Plant Biology* **2006,** 9, 305-314.

3. Xu, R.; Fazio, G. C.; Matsuda, S. P. T., On the origins of triterpenoid skeletal diversity. *Phytochemistry* **2004,** 65, 261-291.

4. Miller, W. L., Molecular biology of steroid hormone synthesis. *Endocr Rev* **1988,** 9, 295-318.

5. Parker, K. L.; Schimmer, B. P.; Gerald, L., Transcriptional Regulation of the Genes Encoding the Cytochrome P-450 Steroid Hydroxylases. In *Vitamins & Hormones*, Academic Press: 1995; Vol. Volume 51, pp 339-370.

6. Wina, E.; Muetzel, S.; Becker, K., The impact of saponins or saponin-containing plant materials on ruminant production - a review. *Journal of Agricultural and Food Chemistry* **2005,** 53, 8093-8105.

7. Francis, G.; Kerem, Z.; Makkar, H. P.; Becker, K., The biological action of saponins in animal systems: a review. *Br J Nutr* **2002,** 88, 587-605.

8. Gomes, R.; Meredith, W.; Snape, C.; Sephton, M., Conjugated steroids: analytical approaches and applications. *Analytical and Bioanalytical Chemistry* **2009,** 393, 453-458.

9. Fox, P. A.; Carter, J.; Farrimond, P., Analysis of bacteriohopanepolyols in sediment and bacterial extracts by high performance liquid chromatography/atmospheric pressure chemical ionization mass spectrometry. *Rapid Communications in Mass Spectrometry* **1998,** 12, 609-612.

10. Talbot, H. M.; Watson, D. F.; Murrell, J. C.; Carter, J. F.; Farrimond, P., Analysis of intact bacteriohopanepolyols from methanotrophic bacteria by reversed-phase high-performance liquid chromatography-atmospheric pressure chemical ionisation mass spectrometry. *Journal of Chromatography A* **2001,** 921, 175-185.

11. Huang, X.-F.; Lin, Y.-Y.; Kong, L.-Y., Steroids from the roots of *Asparagus officinalis* and their cytotoxic activity. *Journal of Integrative Plant Biology* **2008,** 50, (6), 717-722.

12. Miles, C. O.; Munday, S. C.; Holland, P. T.; Lancaster, M. J.; Wilkins, A. L., Further analysis of bile crystals from sheep grazing *Panicum schinzii* (sweet grass). *Aust Vet J* **1992,** 69, 34.

13. Miles, C. O.; Wilkins, A. L.; Munday, S. C.; Flaoyen, A.; Holland, P. T.; Smith, B. L., Identification of insoluble salts of the .beta.-D-glucuronides of episarsasapogenin and epismilagenin in the bile of lambs with alveld and examination of *Narthecium ossifragum*, *Tribulus terrestris*, and *Panicum miliaceum* for sapogenins. *Journal of Agricultural and Food Chemistry* **1993,** 41, 914-917.

14. Miles, C. O.; Wilkins, A. L.; Munday, S. C.; Holland, P. T.; Smith, B. L.; Lancaster, M. J.; Embling, P. P., Identification of the calcium salt of epismilagenin .beta.-D-glucuronide in the bile crystals of sheep affected by *Panicum dichotomiflorum* and *Panicum schinzii* toxicoses. *Journal of Agricultural and Food Chemistry* **1992,** 40, 1606-1609.

15. Wisløff, H.; Uhlig, S.; Scheie, E.; Loader, J.; Wilkins, A.; Flåøyen, A., Toxicity testing of saponin-containing *Yucca schidigera* roetzl. juice in relation to hepato- and nephrotoxicity of *Narthecium ossifragum* (L.) huds. *Toxicon* **2008,** 51, 140-150.

16. Wilkins, A. L.; Miles, C. O.; Smith, B. L.; Meagher, L. P.; Ede, R. M., GC-MS method for analysis of steroidal sapogenins in plant and animal samples associated with ovine photosensitisation. In *Plant associated toxins*, Colgate, S. M.; Dorling, P. R., Eds. CAB International: Wallingford, 1994; pp 263-268.

17. al-Alousi, L. M.; Anderson, R. A., A relatively simple and rapid multi-component method for analysis of steroid profiles in blood, fecal and liver samples. *Steroids* **2002,** 67, 269-275.

18. Larner, J. M.; Pahuja, S. L.; Shackleton, C. H.; McMurray, W. J.; Giordano, G.; Hochberg, R. B., The isolation and characterization of estradiol-fatty acid esters in human ovarian follicular fluid. Identification of an endogenous long-lived and potent family of estrogens. *Journal of Biological Chemistry* **1993,** 268, 13893-13899.

19. Lillington, J. M.; Trafford, D. J. H.; Makin, H. L. J., A rapid and simple method for the esterification of fatty acids and steroid carboxylic acids prior to gas-liquid chromatography. *Clinica Chimica Acta* **1981,** 111, 91-98.

20. Watson, J. T.; Spearman, O. D., *Introduction to mass spectrometry, instrumentation, applications and strategies for data interpretation*. Fourth Edition ed.; Wiley: West Sussex, 2007.

21. Ma, Y.-C.; Kim, H.-Y., Determination of steroids by liquid chromatography/mass spectrometry. *Journal of the American Society for Mass Spectrometry* **1997,** 8, 1010-1020.

22. Pozo, O. J.; Van Eenoo, P.; Deventer, K.; Delbeke, F., T. , Ionization of anabolic steroids by adduct formation in liquid chromatography electrospray mass spectrometry. *Journal of Mass Spectrometry* **2007,** 42, 497-516.

23. Hostettmann, K.; Marston, A., *Saponins*. Cambridge University Press: New York, 1995.

24. Ricardo, R., Isolating bioactive compounds from marine organisms. *Journal of Marine Biotechnology* **1997,** 5, 187-193.

25. Meagher, L. P. Aspects of some agricultural myco- and phytotoxins. University of Waikato, Hamilton, 1996.

26. Blunden, G.; Jaffer, J. A.; Jewers, K.; Robinson, J. M., Configurational assignments to spirostan-3-ols by mass spectrometry. *Steroids* **1980,** 36, 299-303.

27. Wisløff, H.; Wilkins, A. L.; Scheie, E.; Flåøyen, A., Accumulation of sapogenin conjugates and histological changes in the liver and kidneys of lambs suffering from alveld, a hepatogenous photosensitization disease of sheep grazing *Narthecium ossifragum*. *Veterinary Research Communications* **2002,** 26, 381-396.

28. Flåøyen, A.; Wilkins, A. L., Metabolism of saponins from *Narthecium ossifragum* - a plant implicated in the aetiology of alveld, a hepatogenous photosensitization of sheep. *Veterinary Research Communications* **1997,** 21, 335-345.

29. Flåøyen, A., A difference in susceptibility of two breeds of sheep to the 'Alveld toxin'. *Veterinary Research Communications* **1991,** 15, 455-457.

30. Morris, C. A.; Amyes, N. C.; Towers, N. R.; Wesselink, C., Correlated responses to selection for or against facial eczema susceptibility in Romney sheep in New Zealand. *New Zealand Journal of Agricultural Research* **1999,** 42, 475-481.

31. Boult, C. H. Development of a method of analysis by gas chromatography-mass spectrometry using selected ion monitoring for the measurement of fish sex steroids in water. The University of Waikato, Hamilton, 2009.

32. Ekman, R.; Silberring, J.; Westman-Brinkmalm, A. M.; Kraj, A., *Mass spectrometry instrumentation, interpretation, and applications*. John Wiley & Sons: Hoboken, 2009.

33. de Hoffmann, E.; Stroobant, V., *Mass spectrometry principles and applications*. Third edition ed.; John Wiley & Sons: Chichester, 2007.

34. Kite, G. C.; Porter, E. A.; Simmonds, M. S. J., Chromatographic behaviour of steroidal saponins studied by high-performance liquid chromatography-mass spectrometry. *Journal of Chromatography A* **2007,** 1148, 177-183.

35. Needham, S. R.; Brown, P. R.; Duff, K.; Bell, D., Optimized stationary phases for the high-performance liquid chromatography-electrospray ionization mass spectrometric analysis of basic pharmaceuticals. *Journal of Chromatography A* **2000,** 869, 159-170.

36. Rogatsky, E.; Stein, D., Evaluation of matrix effect and chromatography efficiency: New parameters for validation of method development. *Journal of the American Society for Mass Spectrometry* **2005,** 16, 1757-1759.

37. King, R.; Bonfiglio, R.; Fernandez-Metzler, C.; Miller-Stein, C.; Olah, T., Mechanistic investigation of ionization suppression in electrospray ionization. *Journal of the American Society for Mass Spectrometry* **2000,** 11, 942-950.

38. Dams, R.; Huestis, M. A.; Lambert, W. E.; Murphy, C. M., Matrix effect in bio-analysis of illicit drugs with LC-MS/MS: influence of ionization type, sample preparation, and biofluid. *Journal of the American Society for Mass Spectrometry* **2003,** 14, 1290-1294.

39. Pozo, O. J.; Deventer, K.; Van Eenoo, P.; Delbeke, F., T., Presence of endogenous interferences in the urinary detection of selected anabolic steroids by liquid chromatography/electrospray tandem mass spectrometry. *Rapid Communications in Mass Spectrometry* **2007,** 21, 2785-2796.

40. Matuszewski, B. K.; Constanzer, M. L.; Chavez-Eng, C. M., Matrix Effect in Quantitative LC/MS/MS Analyses of Biological Fluids: A Method for Determination of Finasteride in Human Plasma at Picogram Per Milliliter Concentrations. *Analytical Chemistry* **1998,** 70, 882-889.

41. Stüber, M.; Reemtsma, T., Evaluation of three calibration methods to compensate matrix effects in environmental analysis with LC-ESI-MS. *Analytical and Bioanalytical Chemistry* **2004,** 378, 910-916.

42. Higashi, T.; Shimada, K., Derivatization of neutral steroids to enhance their detection characteristics in liquid chromatography–mass spectrometry. *Analytical and Bioanalytical Chemistry* **2004,** 378, 875-882.

43. Van Berkel, G. J.; Quirke, J. M. E.; Tigani, R. A.; Dilley, A. S.; Covey, T. R., Derivatization for electrospray ionization mass spectrometry. 3. electrochemically ionizable derivatives. *Analytical Chemistry* **1998,** 70, 1544-1554.

44. Williams, D.; Young, M. K., Analysis of neutral isomeric low molecular weight carbohydrates using ferrocenyl boronate derivatization and tandem electrospray mass spectrometry. *Rapid Communications in Mass Spectrometry* **2000,** 14, 2083-2091.

45. Baronti, C.; Curini, R.; D'Ascenzo, G.; Di Corcia, A.; Gentili, A.; Samperi, R., Monitoring natural and synthetic estrogens at activated sludge sewage treatment plants and in a receiving river water. *Environmental Science & Technology* **2000,** 34, 5059-5066.

46. Loader, J. I.; Wilkins, A. L.; Flaoyen, A.; Ryste, E.; Hove, K., Ovine metabolism of lithogenic sapogenins. synthesis of [2,2,4,4-2H4]sarsasapogenone, [2,2,4,4-2H4]sarsasapogenin, and [2,2,4,4-2H4]episarsasapogenin and evaluation of deuterium retention in a sheep-

dosing trial. *Journal of Agricultural and Food Chemistry* **2003,** 51, 2641-2645.

47. Kellerman, T. S.; Miles, C. O.; Erasmus, G. L.; Wilkins, A. L.; Coetzer, J. A. W., The possible role of steroidal saponins in the pathogenesis of geeldikkop, a major hepatogenous photosensitisation of small stock in South Africa. In *Plant associated toxins*, Colgate, S. M.; Dorling, P. R., Eds. CAB International: Wallingford, 1994; pp 287-292.

48. Rundberget, T.; Wilkins, A. L., Determination of Penicillium mycotoxins in foods and feeds using liquid chromatography-mass spectrometry. *Journal of Chromatography A* **2002,** 964, 189-197.

49. Taylor, W. G.; Zaman, M. S.; Mir, Z.; Mir, P. S.; Acharya, S. N.; Mears, G. J.; Elder, J. L., Analysis of steroidal sapogenins from amber fenugreek (*Trigonella foenum-graecum*) by capillary gas chromatography and combined gas chromatography/mass spectrometry. *Journal of Agricultural and Food Chemistry* **1997,** 45, 753-759.

50. Churchwell, M. I.; Twaddle, N. C.; Meeker, L. R.; Doerge, D. R., Improving LC-MS sensitivity through increases in chromatographic performance: Comparisons of UPLC-ES/MS/MS to HPLC-ES/MS/MS. *Journal of Chromatography B* **2005,** 825, 134-143.

51. Johnson, K. A.; Plumb, R., Investigating the human metabolism of acetaminophen using UPLC and exact mass oa-TOF MS. *Journal of Pharmaceutical and Biomedical Analysis* **2005,** 39, 805-810.

52. Deng, D. Chemical aspects of some ovine hepatogenous photosensitization diseases. University of Waikato, Hamilton, 1999.

53. Agrawal, P. K.; Bunsawansong, P.; Morris, G. A., Dependence of the 1H NMR chemical shifts of ring F resonances on the orientation of the 27-methyl group of spirostane-type steroidal sapogenins. *Phytochemistry* **1998,** 47, 255-257.

54. Agrawal, P., K.; Bunsawansong, P.; Morris, G., A., Complete assignment of the ^{1}H and ^{13}C NMR spectra of steroidal sapogenins: smilagenin and sarsasapogenin. *Magnetic Resonance in Chemistry* **1997,** 35, 441-446.

55. Griffiths, W. J., Tandem mass spectrometry in the study of fatty acids, bile acids, and steroids. *Mass Spectrometry Reviews* **2003,** 22, 81-152.

56. Liu, S.; Sjövall, J.; Griffiths, W. J., Analysis of oxosteroids by nano-electrospray mass spectrometry of their oximes. *Rapid Communications in Mass Spectrometry* **2000,** 14, 390-400.